1.0

1.1

1.25 1.4 1.6

2.8 2.5

3.2 2.2

3.6

4.0 2.0

1.8

MICROCOPY RESOLUTION TEST CHART
NATIONAL BUREAU OF STANDARDS 1963 A

School of

OCEANOGRAPHY

AD A107954

OSU

DTIC
ELECTE
DEC 1 1981
S   D
D

Compilation of Reprints
No. 18,
Office of Naval Research

Contracts
N00014-76-C-0067
and
N00014-75-C-0210
and
N00014-75-C-0271
N00014-75-C-0067
N00014-75-C-0004

C O N T E N T S

SECURITY CLASSIFICATION OF THIS PAGE (When Data Entered)

REPORT DOCUMENTATION PAGE	READ INSTRUCTIONS BEFORE COMPLETING FORM

1. REPORT NUMBER / - 80-25	2. GOVT ACCESSION NO. AD-A107 954	3. RECIPIENT'S CATALOG NUMBER

4. TITLE (and Subtitle) ASPECTS OF REPRODUCTION OF LIPARID FISHES FROM THE CONTINENTAL SLOPE AND ABYSSAL PLAIN OFF OREGON, WITH NOTES ON GROWTH	5. TYPE OF REPORT & PERIOD COVERED Reprint
	6. PERFORMING ORG. REPORT NUMBER

7. AUTHOR(s) David L. Stein	8. CONTRACT OR GRANT NUMBER(s) N00014-76-C-0067

9. PERFORMING ORGANIZATION NAME AND ADDRESS School of Oceanography Oregon State University Corvallis, Oregon 97330	10. PROGRAM ELEMENT. PROJECT, TASK AREA & WORK UNIT NUMBERS NR 083-102

11. CONTROLLING OFFICE NAME AND ADDRESS Office of Naval Research Ocean Science & Technology Division Arlington, Virginia 22217	12. REPORT DATE 1980
	13. NUMBER OF PAGES 13

14. MONITORING AGENCY NAME & ADDRESS(if different from Controlling Office)	15. SECURITY CLASS. (of this report) Unclassified
	15a. DECLASSIFICATION/DOWNGRADING SCHEDULE

16. DISTRIBUTION STATEMENT (of this Report)

Approved for public release; distribution unlimited

17. DISTRIBUTION STATEMENT (of the abstract entered in Block 20, if different from Report)

19. KEY WORDS (Continue on reverse side if necessary and identify by block number)

20. ABSTRACT (Continue on reverse side if necessary and identify by block number)

Reproduction of 13 species of bathyal and abyssal benthic liparids (*Osteodiscus cascadiae, Acantholiparis opercularis, Paraliparis latifrons, P. rosaceus, P. megalopus, P. mento, P. cephalus, Careproctus melanurus, C. microstomus, C. oregonensis, C. ovigerum, C. longifilis,* and *C. filamentosus*) off the coast of Oregon was studied. Information on fecundity, reproductive periodicity, size at maturity and length-weight relationships were obtained from all but *P. cephalus* and *C. filamentosus*. These species can be

DD FORM 1 JAN 73 1473   EDITION OF 1 NOV 65 IS OBSOLETE
S/N 0102-014-6601

divided into three groups on the basis of fecundity relationships, and into two groups based on whether they appear to spawn throughout the year or periodically. Characterization of species as continuous or periodic spawners was based upon presence of ripe eggs throughout the year, presence of ripe eggs seasonally, or size distributions of ovarian eggs in ripe females.

Species which spawn throughout the year are all primarily abyssal (>2,100 m). Those spawning at relatively long intervals (the durations and frequencies of which are generally unknown) are bathyal and abyssal. All ripe females had large (2.5-8.0 mm diameter) eggs. Maximum fecundities of the species ranged from six to 1,277.

Based upon previously published information and the new data, a possible life history for abyssal liparids is constructed.

REPORT DOCUMENTATION PAGE		READ INSTRUCTIONS BEFORE COMPLETING FORM
1. REPORT NUMBER - 80-26	2. GOVT ACCESSION NO.	3. RECIPIENT'S CATALOG NUMBER
4. TITLE (and Subtitle) SURFACE SEDIMENTS OF THE PERU-CHILE CONTINENTAL MARGIN AND THE NAZCA PLATE		5. TYPE OF REPORT & PERIOD COVERED Reprint
		6. PERFORMING ORG. REPORT NUMBER
7. AUTHOR(s) Lawrence A. Krissek Kenneth F. Scheidegger LaVerne D. Kulm		8. CONTRACT OR GRANT NUMBER(s) N00014-75-C-0210 N00014-76-C-0067
9. PERFORMING ORGANIZATION NAME AND ADDRESS School of Oceanography Oregon State University Corvallis, Oregon 97330		10. PROGRAM ELEMENT, PROJECT, TASK AREA & WORK UNIT NUMBERS
11. CONTROLLING OFFICE NAME AND ADDRESS Office of Naval Research Ocean Science & Technology Division Arlington, Virginia 22217		12. REPORT DATE June 1980
		13. NUMBER OF PAGES 11
14. MONITORING AGENCY NAME & ADDRESS(if different from Controlling Office)		15. SECURITY CLASS. (of this report) Unclassified
		15a. DECLASSIFICATION/DOWNGRADING SCHEDULE

16. DISTRIBUTION STATEMENT (of this Report)

Approved for public release; distribution unlimited

17. DISTRIBUTION STATEMENT (of the abstract entered in Block 20, if different from Report)

18. SUPPLEMENTARY NOTES

19. KEY WORDS (Continue on reverse side if necessary and identify by block number)

20. ABSTRACT (Continue on reverse side if necessary and identify by block number)

Surface sediment samples from 86 locations on the Peru-Chile continental margin and the Nazca plate have been analyzed for bulk chemistry and texture to evaluate the factors influencing sediment formation on continental slope and adjacent abyssal plain depositional environments. Sand-sized calcareous microfossils are abundant above the carbonate compensation depth (CCD), but their removal by dissolution leaves fine-grained deposits in the deeper basins. Terrigenous silts are found seaward of the Peru-Chile Trench, (cont.)

DD FORM 1473 EDITION OF 1 NOV 65 IS OBSOLETE
1 JAN 73
S/N 0102-014-6601

especially south of 7°S, and may be transported there by wind, mid-water turbid layers, or bottom waters flowing north through the deep ocean basins. Sediments become finer grained away from shore as coarse terrigenous particles settle out. The more humid climate of northern Peru produces finer fluvial sediments there than to the south. This textural change also appears in adjacent marine sediments. In the Peru Basin, bottom nepheloid layers are found where clay-sized terrigenous material dominates the sediments. On the adjacent Galapagos Rise, however, nepheloid layers are absent, and eolian-derived sedimentary components in the <5µ size range may exceed those transported to the area by currents.

R-mode factor analysis has outlined sediment constituents from the geochemical data. Terrigenous components dominate the slowly accumulating clay-sized sediments of the Peru and Chile Basins, and the coarser, more rapidly forming margin deposits south of 14°S. Biogenic deposits form at intermediate rates on topographic highs on the Nazca plate. Very slow hydrogenous sedimentation occurs in the seaward portions of the deep basins. Sediments rich in organic components are concentrated in rapidly forming deposits along the margin north of 14°S, beneath centers of strong coastal upwelling.

Several distinct sediment accumulations have been mapped on the continental shelf and upper slope. An upper-slope deposit is anomalously fine grained and organic rich; it lies between 10.5°S and 13.6°S, in the region of most intense upwelling. Preservation of this body is enhanced by the inclusion of fine inorganic material in biogenic fecal pellets, and by the impingement of the shallow-water oxygen minimum layer on the slope at the same level.

REPORT DOCUMENTATION PAGE		READ INSTRUCTIONS BEFORE COMPLETING FORM
1. REPORT NUMBER 80-27	2. GOVT ACCESSION NO.	3. RECIPIENT'S CATALOG NUMBER
4. TITLE (and Subtitle) ON THE INTERMEDIATE PARTICLE MAXIMA ASSOCIATED WITH OXYGEN-POOR WATER OFF WESTERN SOUTH AMERICA		5. TYPE OF REPORT & PERIOD COVERED Reprint
		6. PERFORMING ORG. REPORT NUMBER
7. AUTHOR(s) Hasong Pak L. A. Codispoti J. Ronald V. Zaneveld		8. CONTRACT OR GRANT NUMBER(s) N00014-76-C-0271 N00014-76-0067
9. PERFORMING ORGANIZATION NAME AND ADDRESS School of Oceanography Oregon State University Corvallis, Oregon 97330		10. PROGRAM ELEMENT, PROJECT, TASK AREA & WORK UNIT NUMBERS NR 083-102
11. CONTROLLING OFFICE NAME AND ADDRESS Office of Naval Research Ocean Science & Technology Division Arlington, Virginia 22217		12. REPORT DATE 1980
		13. NUMBER OF PAGES 15
14. MONITORING AGENCY NAME & ADDRESS(if different from Controlling Office)		15. SECURITY CLASS. (of this report) Unclassified
		15a. DECLASSIFICATION/DOWNGRADING SCHEDULE

16. DISTRIBUTION STATEMENT (of this Report)

Approved for public release; distribution unlimited

17. DISTRIBUTION STATEMENT (of the abstract entered in Block 20, if different from Report)

19. KEY WORDS (Continue on reverse side if necessary and identify by block number)

20. ABSTRACT (Continue on reverse side if necessary and identify by block number)

The distribution of suspended particulate matter was measured during 21 May and 18 June 1977 between 4 and 23°S from the coast of South America to about 500 nautical miles offshore. A well-defined maximum was observed over the continental margins at depths of about 200 m between ≈9 and 23°S. At 4°S, the main particle maximum was at approximately 400 m, but in the nearshore zone the maximum extended upwards to ≈200 m. A comparison of the particle and chemical data shows that the particle maxima are usually at approximately

DD FORM 1473 , 1 JAN 73 EDITION OF 1 NOV 65 IS OBSOLETE
S/N 0102-014-6601 |

the core depth of the oxygen minimum layer. A nitrite maximum and a nitrate minimum were also observed at or near the particle maximum core depth south of ≈9°S. Near 4°S, a weak nitrite maximum was observed within the oxygen minimum layer at some stations. The protein distribution near 15°S suggests that the material in the particle maximum contains significant amounts of organic matter.

The distribution of the particle maximum layer between 9 and 23°S and its relations to the density field and the cross-shelf flow suggest that most of the particles could originate in the bottom waters over the outer continental shelf and be transported offshore in a quasi-horizontal path.

Offshore particle transport near the equator is probably supported by a westward current off northern Peru between and under the eastward extension of the Equatorial Undercurrent and the Subsurface South Equatorial Countercurrent. However, the source of the particles in this ≈400-m maximum has not been determined.

REPORT DOCUMENTATION PAGE	READ INSTRUCTIONS BEFORE COMPLETING FORM

1. REPORT NUMBER 80-28	2. GOVT ACCESSION NO.	3. RECIPIENT'S CATALOG NUMBER

4. TITLE (and Subtitle) DESCRIPTION AND OCCURRENCE OF MACROURID LARVAE AND JUVENILES IN THE NORTHEAST PACIFIC OCEAN OFF OREGON, U.S.A.	5. TYPE OF REPORT & PERIOD COVERED Reprint
	6. PERFORMING ORG. REPORT NUMBER

7. AUTHOR(s) David L. Stein	8. CONTRACT OR GRANT NUMBER(s) N00014-79-C-0004

9. PERFORMING ORGANIZATION NAME AND ADDRESS School of Oceanography Oregon State University Corvallis, Oregon 97330	10. PROGRAM ELEMENT, PROJECT, TASK AREA & WORK UNIT NUMBERS

11. CONTROLLING OFFICE NAME AND ADDRESS Office of Naval Research Ocean Science & Technology Division Arlington, Virginia 22217	12. REPORT DATE 1980
	13. NUMBER OF PAGES 12

14. MONITORING AGENCY NAME & ADDRESS(if different from Controlling Office)	15. SECURITY CLASS. (of this report) Unclassified
	15a. DECLASSIFICATION: DOWNGRADING SCHEDULE

16. DISTRIBUTION STATEMENT (of this Report)

Approved for public release; distribution unlimited

17. DISTRIBUTION STATEMENT (of the abstract entered in Block 20, if different from Report)

18. SUPPLEMENTARY NOTES

19. KEY WORDS (Continue on reverse side if necessary and identify by block number)

20. ABSTRACT (Continue on reverse side if necessary and identify by block number)

Although there are over 100 species of North Pacific macrourids, few of their larvae have previously been identified to species. Descriptions of postlarvae and juveniles of Coryphaenoides acrolepis, C. filifer, and C. leptolepis are given, with a provisional key to the identification of most species known from off Oregon. Vertical distribution of the larvae and juveniles of C. acrolepis apparently changes with ontogenetic development,

DD FORM 1473 EDITION OF 1 NOV 65 IS OBSOLETE
S/N 0102-014-6601 |

the smallest individuals occurring shallowest. Macrourid eggs have not yet been identified from Oregon waters.

SECURITY CLASSIFICATION OF THIS PAGE *(When Data Entered)*

REPORT DOCUMENTATION PAGE		READ INSTRUCTIONS BEFORE COMPLETING FORM
1 REPORT NUMBER 80-29	2. GOVT ACCESSION NO.	3. RECIPIENT'S CATALOG NUMBER
4 TITLE *(and Subtitle)* REPLY		5. TYPE OF REPORT & PERIOD COVERED Reprint
		6. PERFORMING ORG. REPORT NUMBER
7. AUTHOR(s) James J. Simpson Clayton A. Paulson		8. CONTRACT OR GRANT NUMBER(s) N00014-79-C-0004
9. PERFORMING ORGANIZATION NAME AND ADDRESS School of Oceanography Oregon State University Corvallis, Oregon 97330		10. PROGRAM ELEMENT, PROJECT, TASK AREA & WORK UNIT NUMBERS NR 083-102
11. CONTROLLING OFFICE NAME AND ADDRESS Office of Naval Research Ocean Science & Technology Division Arlington, Virginia 22217		12. REPORT DATE 1980
		13. NUMBER OF PAGES 2
14. MONITORING AGENCY NAME & ADDRESS*(If different from Controlling Office)*		15. SECURITY CLASS. *(of this report)* Unclassified
		15a. DECLASSIFICATION/DOWNGRADING SCHEDULE

16. DISTRIBUTION STATEMENT *(of this Report)*

Approved for public release; distribution unlimited

17. DISTRIBUTION STATEMENT *(of the abstract entered in Block 20, If different from Report)*

19. KEY WORDS *(Continue on reverse side if necessary and identify by block number)*

20. ABSTRACT *(Continue on reverse side if necessary and identify by block number)*

DD FORM 1473 EDITION OF 1 NOV 65 IS OBSOLETE
1 JAN 73
S/N 0102-014-6601

SECURITY CLASSIFICATION OF THIS PAGE *(When Data Entered)*

REPORT DOCUMENTATION PAGE		READ INSTRUCTIONS BEFORE COMPLETING FORM
1 REPORT NUMBER 80-30	2. GOVT ACCESSION NO.	3. RECIPIENT'S CATALOG NUMBER
4. TITLE (and Subtitle) PARTICULATE ORGANIC CARBON FLUX IN THE OCEANS -- SURFACE PRODUCTIVITY AND OXYGEN UTILIZATION		5. TYPE OF REPORT & PERIOD COVERED Reprint
		6. PERFORMING ORG. REPORT NUMBER
7. AUTHOR(s) Erwin Suess		8. CONTRACT OR GRANT NUMBER(s) N00014-79-C-0004
9. PERFORMING ORGANIZATION NAME AND ADDRESS School of Oceanography Oregon State University Corvallis, Oregon 97330		10. PROGRAM ELEMENT, PROJECT, TASK AREA & WORK UNIT NUMBERS NR083-1026
11. CONTROLLING OFFICE NAME AND ADDRESS Office of Naval Research Ocean Science & Technology Division Arlington, Virginia 22217		12. REPORT DATE 1980
		13. NUMBER OF PAGES 3
14. MONITORING AGENCY NAME & ADDRESS(if different from Controlling Office)		15. SECURITY CLASS. (of this report) Unclassified
		15a. DECLASSIFICATION DOWNGRADING SCHEDULE

16. DISTRIBUTION STATEMENT (of this Report)

Approved for public release; distribution unlimited

17. DISTRIBUTION STATEMENT (of the abstract entered in Block 20, if different from Report)

18. SUPPLEMENTARY NOTES

19. KEY WORDS (Continue on reverse side if necessary and identify by block number)

20. ABSTRACT (Continue on reverse side if necessary and identify by block number)

Organic detritus passing from the sea surface through the water column to the sea floor controls nutrient regeneration, fules benthic life and affects burial of organic carbon in the sediment record[1-3]. Particle trap systems have enabled the first quantification of this important process. The results suggest that the dominant mechanism of vertical transport is by rapid settling of rare large particles, most likely of faecal pellets or marine snow of the order of >200 µm in diameter, whereas the more

frequent small particles have an insignificant role in vertical mass flux.[4-6]   The ultimate source of organic detritus is biological production in surface waters of the oceans. I determine here an empirical relationship that predicts organic carbon flux at any depth in the oceans below the base of the euphotic zone as a function of the mean net primary production rate at the surface and depth-dependent consumption. Such a relationship aids in estimating rates of decay of organic matter in the water column, benthic and water column respiration of oxygen in the deep sea and burial of organic carbon in the sediment record.

REPORT DOCUMENTATION PAGE		READ INSTRUCTIONS BEFORE COMPLETING FORM
1. REPORT NUMBER 80-31	2. GOVT ACCESSION NO.	3. RECIPIENT'S CATALOG NUMBER
4. TITLE (and Subtitle) PRODUCTIVITY, SEDIMENTATION RATE AND SEDIMENTARY ORGANIC MATTER IN THE OCEANS II. -- ELEMENTAL FRACTIONATION		5. TYPE OF REPORT & PERIOD COVERED Reprint
		6. PERFORMING ORG. REPORT NUMBER
7. AUTHOR(s) Erwin Suess Peter J. Müller		8. CONTRACT OR GRANT NUMBER(s) N00014-76-C-0067
9. PERFORMING ORGANIZATION NAME AND ADDRESS School of Oceanography Oregon State University Corvallis, Oregon 97330		10. PROGRAM ELEMENT, PROJECT, TASK AREA & WORK UNIT NUMBERS NR 083-102
11. CONTROLLING OFFICE NAME AND ADDRESS Office of Naval Research Ocean Science & Technology Division Arlington, Virginia 22217		12. REPORT DATE 1980
		13. NUMBER OF PAGES 10
14. MONITORING AGENCY NAME & ADDRESS(if different from Controlling Office)		15. SECURITY CLASS. (of this report) Unclassified
		15a. DECLASSIFICATION/DOWNGRADING SCHEDULE

16. DISTRIBUTION STATEMENT (of this Report)

Approved for public release; distribution unlimited

17. DISTRIBUTION STATEMENT (of the abstract entered in Block 20, if different from Report)

18. SUPPLEMENTARY NOTES

19. KEY WORDS (Continue on reverse side if necessary and identify by block number)

20. ABSTRACT (Continue on reverse side if necessary and identify by block number)

The vertical flux of biogenous organic matter to the sediment surface is a function of water depth and primary productivity; this relationship can be expressed empirically as:

(1) $\text{org-C}_{flux} = 5.9 \cdot \text{depth}^{-0.616} \cdot \text{productivity}$

Upon descent through the water column and prior to burial, biogenous *detrital organic matter* undergoes strong elemental fractionation by preferential removal of nitrogenous and P-containing organic compounds. At the water-

sediment interface, a portion of the detritus is converted into *biomass* by benthic organisms, which concentrate nitrogen and phosphorus relative to carbon. These two processes are reflected in the elemental composition of sedimentary organic matter. A third process concentrates organic matter in sediments by sorption onto clays. This *sorbed material* is high in organic-N and devoid of organic-P; its relative abundance is highly only in pelagic clays. The concentrations of each of the three forms of organic matter - detrital, biomass, and sorbed - can be calculated from the following expressions:

$$(2) \quad \text{org-C}_{sorb} = 0.005 \cdot Al_2O_3$$

$$(3) \quad \text{org-C}_{detr} = \frac{\text{org-C}_{total} - \text{org-C}_{sorb} - e \cdot \text{org-N}_{total}}{(1 - e/f)}$$

$$(4) \quad \text{org-C}_{biom.} = \text{org-C}_{total} - \text{org-C}_{detr.} - \text{org-C}_{sorb}$$

where *e* and *f* are the C/N elemental weight ratios of biomass and detritus respectively.

Aspects of Reproduction of Liparid Fishes from the Continental Slope and Abyssal Plain off Oregon, with Notes on Growth

David L. Stein

Reproduction of 13 species of bathyal and abyssal benthic liparids (*Osteodiscus cascadiae, Acantholiparis opercularis, Paraliparis latifrons, P. rosaceus, P. megalopus, P. mento, P. cephalus, Careproctus melanurus, C. microstomus, C. oregonensis, C. ovigerum, C. longifilis,* and *C. filamentosus*) off the coast of Oregon was studied. Information on fecundity, reproductive periodicity, size at maturity and length-weight relationships were obtained from all but *P. cephalus* and *C. filamentosus.* These species can be divided into three groups on the basis of fecundity relationships, and into two groups based on whether they appear to spawn throughout the year or periodically. Characterization of species as continuous or periodic spawners was based upon presence of ripe eggs throughout the year, presence of ripe eggs seasonally, or size distributions of ovarian eggs in ripe females.

Species which spawn throughout the year are all primarily abyssal (>2,100 m). Those spawning at relatively long intervals (the durations and frequencies of which are generally unknown) are bathyal and abyssal. All ripe females had large (2.5–8.0 mm diameter) eggs. Maximum fecundities of the species ranged from six to 1,277.

Based upon previously published information and the new data, a possible life history for abyssal liparids is constructed.

THE Liparidae contains several hundred species, occurs in all the oceans of the world and is distributed from the intertidal to the hadal zones. Despite this, little is known about liparid reproduction.

Knowledge about liparid reproduction is of interest and importance. First, because the family is one of the few with an extremely broad depth distribution, it allows comparison of reproductive habits of relatively closely related shallow and deep water species. Second, such knowledge can help decide whether or not deep sea animals reproduce periodically or continuously.

Most knowledge of liparid reproduction concerns shallow water species. Able and Musick (1976: *Liparis inquilinus*) and Detwyler (1963: *Liparis atlanticus*) described egg sizes, spawning periods and growth of the two species. There have been many miscellaneous observations of egg size, development or time of spawning in various species (McIntosh, 1885; Collett, 1909; Schmidt, 1916; Aoyama, 1959; Johnson, 1969; Hart, 1973; DeMartini, 1978).

Much less is known about reproduction of deep water species. Since the review of reproduction in deep water liparids included in Mead et al. (1964), little knowledge has been added. Cohen (1968) mentioned egg sizes of

Paraliparis calidus. Wenner (1979) described the occurrence of *Paraliparis garmani, P. copei, P. calidus,* sizes of ovarian eggs, testes and feeding habits, and speculated about possible mouth brooding by *P. garmani* males. Some species of *Careproctus* are known to lay eggs in lithodid crabs (Hunter, 1969; Parrish, 1972; Peden and Corbett, 1973).

This paper describes the results of a study of the eggs, fecundity, reproductive periodicity, size at maturity and length-weight relationships of 13 species of liparids in four genera. These species occur between 200 and 3,585 m off the coast of Oregon, and were described or redescribed by Stein (1978). They are *Careproctus longifilis* Garman, *C. microstomus* Stein, *C. filamentosus* Stein, *C. oregonensis* Stein, *C. ovigerum* (Gilbert), *C. melanurus* Gilbert, *Osteodiscus cascadiae* Stein, *Acantholiparis opercularis* Gilbert and Burke, *Paraliparis rosaceus* Gilbert, *P. megalopus* Stein, *P. cephalus* Gilbert, *P. latifrons* Garman, and *P. mento* Gilbert.

MATERIALS AND METHODS

All but 11 of the specimens examined were obtained from the bottom trawl collections described by Stein (1978) and made over a period of about 14 years. Eleven specimens of *C. me-*

TABLE 1. SPECIES EXAMINED, THE DEPTHS FROM WHICH THEY CAME, NUMBERS EXAMINED AND THE MONTHS IN WHICH THEY WERE COLLECTED. Months were not sampled equally. Numbers of specimens do not represent relative abundances of individuals within or among species.

Species	Depth (m)	N	Jan	Feb	Mar	April	May	June	July	Aug	Sept	Oct	Nov	Dec
A. opercularis	1,900–2,997	61		10	35			3	7	2	2		2	
C. filamentosus	2,850	1		1										
C. longifilis	2,803–2,816	3		1	1								1	
C. melanurus	190–1,600	26	2		3	3		8	4	1	2	2	1	
C. microstomus	2,740–3,585	3		1	1							1		
C. oregonensis	1,900–2,760	2					1		1					
C. ovigerum	2,510	1									1			
O. cascadiae	1,900–2,997	130	6	28	26		6	14	17	6		12	15	
P. cephalus	580–960	12	1		3	1		2	4	1				
P. latifrons	2,225–2,763	38			14				8		14	2		
P. megalopus	2,825–3,585	5	1					1		1		2		
P. mento	800–960	2	2											
P. rosaceus	2,540–2,809	5	1		4									

lanurus were borrowed from the fish collection of the Department of Fisheries and Wildlife, Oregon State University. All specimens were initially fixed in 10% formalin solution and later transferred to 45% isopropanol. Standard lengths of all individuals were measured to the nearest millimeter. Specimens were weighed to the nearest 0.1 g. When possible, both ovaries of females were removed, lightly blotted with absorbent paper, and weighed to the nearest 0.001 g. Such accuracy was necessary because ovaries and testes of immature individuals often weighed less than 0.001 g. Both testes of male *Acantholiparis opercularis*, *Paraliparis latifrons* and testes of selected males of other species were removed, blotted and weighed as above.

Eggs were measured to the nearest 0.17 mm using an ocular micrometer and a binocular dissecting microscope. All measurements are of greatest diameter of preserved eggs. Johnsen (1921) found that 5.0–5.5 mm fresh eggs could shrink 0.3–1.0 mm in preservation. Because all specimens were preserved similarly, it was assumed that egg sizes, ovary weights, standard lengths and fish weights were comparable. When <50 ripe eggs/ovary were present, all eggs (from both ovaries) with a largest diameter greater than or equal to 0.37 mm (the size below which egg measurement and enumeration was too difficult) were measured and counted. With the exception of the eggs of *C. ovigerum*, if >50 ripe eggs/ovary were present a representative subsample (ca. 50 ripe eggs plus a proportionate number of unripe eggs) was removed after ascertaining the intra-ovarian distribution of eggs of different sizes. The subsample was weighed and the eggs in it measured and counted. The number of eggs of different sizes contained in the whole ovary and both ovaries were then estimated by proportion. In *C. ovigerum*, because of the size of the ovaries and difficulties involved in adequately subsampling the eggs, only eggs from the right ovary >2.87 mm were counted and measured. Fecundity was estimated as the total number of ripe eggs present in each female.

Mature (ripe) eggs were comparatively very large, yolk-filled, barely translucent, with a hard, tough chorionic membrane, almost completely free of ovarian tissues within the ovary (i.e. nearly ovulated). Maturing (ripening) eggs were large, yolky, with a tough chorionic membrane, firmly held in ovarian tissue. Immature eggs were relatively small, transparent, yolk-free, very firmly embedded in ovarian tissues.

Females considered ready to spawn or spawning (ripe) had ovaries containing mature eggs. Spawning females had ovaries with ripe eggs and "large empty spaces" (usually clearly the size and shape of individual ripe eggs). Spent females had flaccid ovaries with no ripe eggs present. All females longer than the shortest female of that species having ripe eggs were considered mature, whereas all females shorter than the shortest female with ripe eggs were considered immature. Minimum length at female maturity was that of the shortest female with ripe eggs of that species.

Ripe males had swollen, translucent, white, reticulated testes. Unripe males had thin,

opaque, cream-colored, usually short testes. Minimum length at male maturity was that of the shortest male with ripe testes of that species.

Conclusions concerning continuity of spawning were based on times of occurrence of ripe females and on size distributions of ovarian eggs in ripe females. Species were considered to be "continuous" spawners if ripe females were captured throughout the year or if ovarian egg sizes in ripe females were widely distributed ("long spawning period" of Hickling and Rutenberg, 1936). Species were considered to be "periodic" spawners if ripe females were present part of the year or if size distributions of ovarian eggs in ripe females were narrowly distributed ("short and definite spawning period" of Hickling and Rutenberg, 1936).

Length-weight relationships were described using a regression equation of the general form $W = aSL^b$, where W = whole body weight in grams, SL = standard length in mm, and a and b are constants.

RESULTS

Osteodiscus cascadiae: One hundred thirty individuals (69 females, 30–81 mm; 61 males, 33–71 mm) captured during nine months of the year (Table 1) were examined. All males with large testes had a prominent genital papilla.

Maximum egg diameter was 5.29 mm. Eggs were not segregated by size within the ovaries; the largest eggs occupied most of the space, with smaller eggs filling the interstices. Those >2.00 mm occurred in distinct size groups composed of few eggs (Fig. 1). Three females had eggs >5.00 mm, 18 females had eggs between 4.00 and 4.99 mm and 9 had eggs between 3.00 and 3.99 mm. The total number of ripe eggs (>4.00 mm)/female ranged from 1 to 7, the mean was 4.05 and the mode was 3 (6 females). There was no clear relationship between fecundity and length. Females mature by ca. 65 mm (Fig. 2).

Ripe females occurred in January, February, March, May, June, July and October. Females which appeared to have spawned recently occurred in March, June and July (Fig. 3). Adult females with maturing eggs, ready to spawn or spent occurred simultaneously (Fig. 1). Ripe males were found in February, March, May, June, July and October. Spawning probably takes place all year, eggs being laid in small clutches or (perhaps) singly.

Length-weight relationships of females and
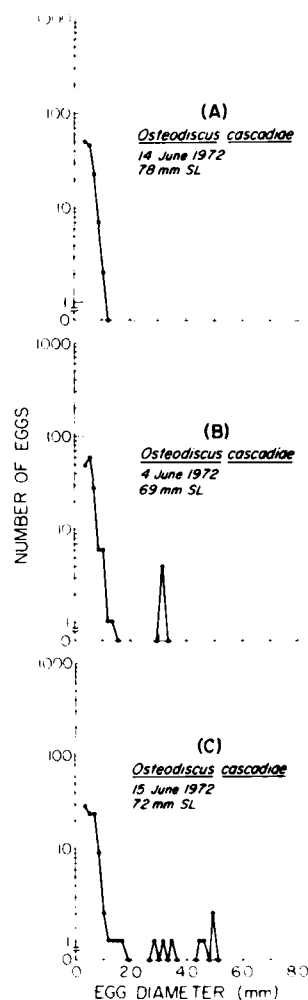
Fig. 1. Size distributions of ovarian eggs in three mature females (A) spent, B) with maturing eggs, C) ready to spawn) of *Osteodiscus cascadiae* captured within two weeks.

males are described by $W = 3.303 \times 10^{-6}SL^{3.13}$, and $W = 1.294 \times 10^{-5}SL^{2.70}$ respectively. Length-weight relationships for all individuals are described by $W = 5.268SL^{3.00}$. Large variations in adult female weights result from the highly variable number of large eggs present.

Acantholiparis opercularis: Sixty-one individuals (36 females, 34–75 mm; 25 males, 32–58 mm) were examined. They were captured during
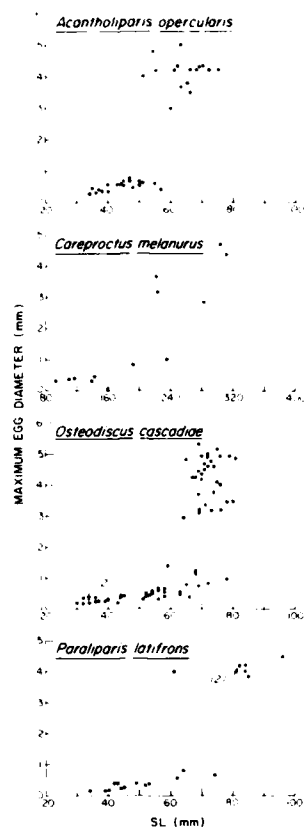
Fig. 2. Standard lengths at sexual maturity of female *Acantholiparis opercularis*, *Careproctus melanurus*, *Osteodiscus cascadiae* and *Paraliparis latifrons*.

Fig. 3. Maximum size of ovarian eggs present in mature individuals of *Acantholiparis opercularis*, *Careproctus melanurus*, *Osteodiscus cascadiae* and *Paraliparis latifrons* at date of capture. o = spent or spawning individual.

seven months of the year (Table 1). No distinct external sexual dimorphism was evident.

Maximum egg diameter was 4.96 mm, but the one egg of this size may have been distorted; the next largest egg was 4.80 mm. Egg distribution in the ovaries was similar to that in *O. cascadiae*. Eggs occurred in distinct size groups, each of which contained relatively few eggs except for those less than 1.00 mm (Fig. 4). Twelve females, SL 51–75 mm, had ripe eggs (>4.00 mm). No female less than 51 mm had eggs >0.74 mm. The number of ripe eggs per female ranged from 1 to 6; the mean number of ripe eggs was 3.2, although the mode was 1. Only females 65 mm or longer contained 4 or ... ripe eggs. One 51 mm female had a ripe ... the right ovary and none over 0.50 mm ... ft.

Females mature by ca. 51 mm SL (Fig. 2). Length of males at maturity could not be determined from the specimens available.

Ripe females occurred in February, March, June, July, September and possibly November. Possibly spent females occurred in February and March (Fig. 3). Males which appeared ripe occurred in March, July and August. Spawning probably takes place throughout the year, few eggs being laid at any one time.

Length-weight relationships of females and males are about the same, $W = 8.136 \times 10^{-7} SL^{3.46}$ and $W = 9.423 \times 10^{-7} SL^{3.41}$, respectively. The combined relationship is $W = 8.05 \times 10^{-7} SL^{3.45}$.

Paraliparis latifrons: Thirty-eight specimens (22 females, 34–96 mm; 16 males, 31–88 mm), captured during four months of the year (Table 1), were examined. Males with ripe testes had a well developed genital papilla.

Maximum egg diameter was 4.47 mm. Egg distribution within the ovaries was similar to that of *O. cascadiae*. Eggs formed distinct size groups; groups of eggs >1.35 mm contained relatively few eggs (Fig. 4). Six females, 61–96 mm, had 2 to 8 ripe eggs (>4.00 mm); the mean was 3.7, the mode was 2. Although the 96 mm female had the most ripe eggs, there was no clear relationship between length and number
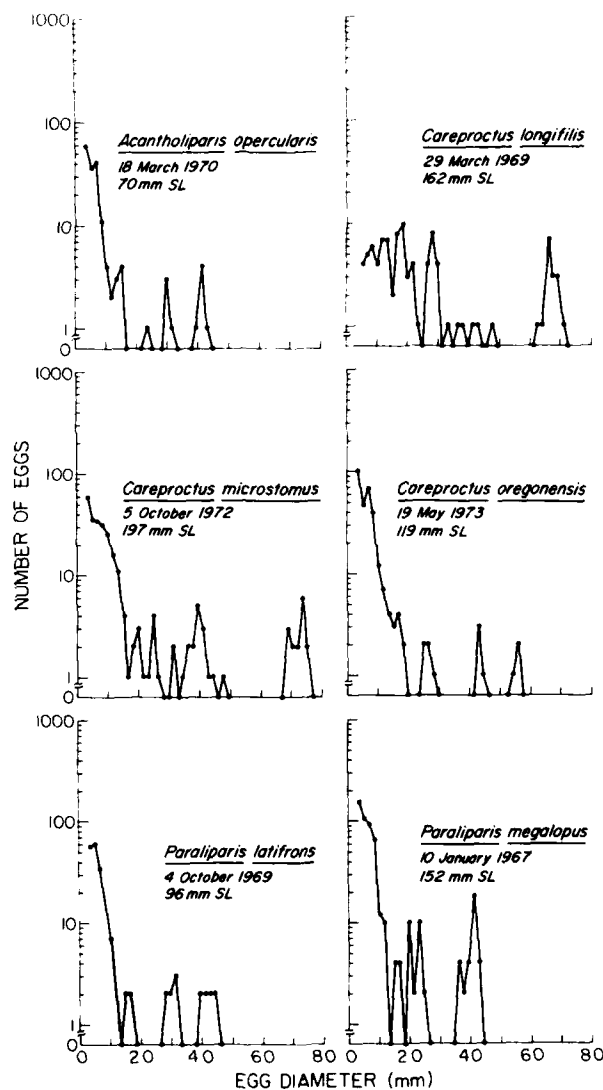
Fig. 4. Size distributions of ovarian eggs in individual mature females of *Acantholiparis opercularis*, *Careproctus longifilis*, *C. microstomus*, *C. oregonensis*, *Paraliparis latifrons* and *P. megalopus*, with dates of captures and SL.

of ripe eggs. Females mature at about 61 mm (Fig. 2).

Ripe females were captured in March, July, September and October (Fig. 3). Apparently ripe males were collected in March and September. Spawning in this species probably occurs throughout the year.

The length-weight relationship for both sexes combined is described by $W = 6.56 \times 10^{-7} SL^{3.47}$. The length-weight relationship of females is described by $W = 5.19 \times 10^{-6} SL^{2.99}$. Insufficient numbers of males were examined to determine a separate L/W curve.

Careproctus melanurus: Twenty-six specimens (15 females, 92–312 mm; 11 males, 126–278
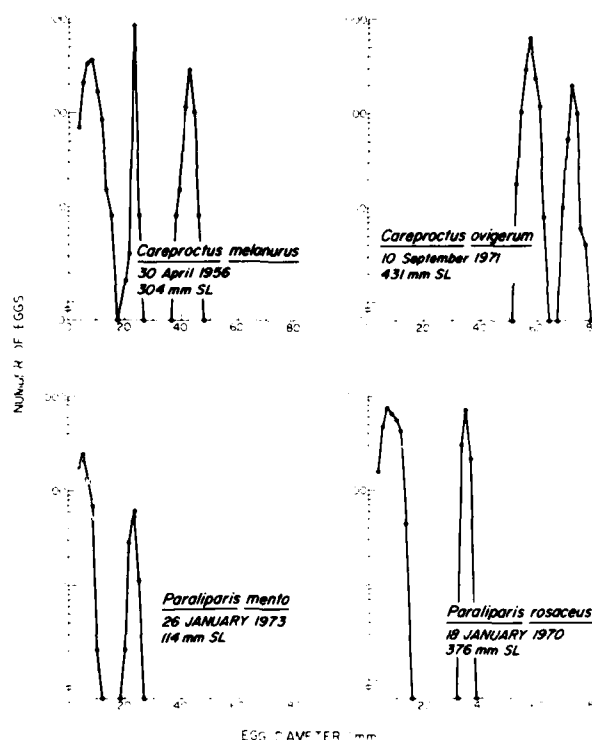
Fig. 5. Size distributions of ovarian eggs in individual mature females of *Careproctus melanurus, C. ovigerum, Paraliparis mento* and *P. rosaceus,* with dates of capture and SL. Eggs of *C. ovigerum* smaller than 2.87 mm were not counted.

mm) captured during nine months of the year (Table 1) were examined. Mature males are externally distinguishable from females by possession of a genital papilla up to 7 mm long.

Maximum egg diameter was 4.63 mm; these eggs were completely free within the lumen of the ovary. Ripe eggs (>3.84 mm) filled the anterior half of the ovary and distinctly smaller unripe eggs filled the posterior half. Maximum observed fecundity was 534. Ripe eggs composed up to 73% of ovarian weight. The ripe eggs form a group widely separated from the smaller eggs (Fig. 5).

Length of female *C. melanurus* at maturity could not be precisely determined because of small sample size and highly variable egg size, but it appears to be between 200 and 220 mm (Fig. 2). Sample size was too small to conclude that the sexes have different maximum sizes.

Spawning may be seasonal; the only females with eggs over 4.0 mm were captured in April and June (Fig. 3) although large females were collected in March, April, June and October. Males with the largest testes were collected in June (0.85% total weight) and in September (0.93% total weight). Ripe or maturing females were collected at 200, 265, 274–430 and 1,300 m depth.

The length-weight relationship for both sexes combined is described by $W = 8.160 \times 10^{-6} SL^{3.09}$; for females, by $W = 7.617 \times 10^{-6} SL^{3.10}$. Insufficient numbers of males were examined to determine a separate L/W curve.

Careproctus microstomus: Three females (178, 183, 197 mm) captured in February, March and October, respectively, were examined.

Maximum egg diameters were 6.60 mm, 6.11 mm and 7.58 mm, respectively. The ovaries of the longest female contained 15 ripe eggs (≥7.00 mm); the next largest eggs present were 4.76 mm (Fig. 4). Ovaries of the other females

contained no eggs as large as 7 mm but did have 11 (left ovary only) and 19 (both ovaries) eggs >6.00 mm. The largest eggs of the 178 mm female each contained a distinct, large oil droplet.

Size distributions of ovarian eggs of three ripe females suggest that members of this species may spawn continuously.

Paraliparis rosaceus: Five females (288–361 mm) captured in January and March, were examined.

The largest egg was 3.65 mm. A number of distinct size groups were present in two specimens. The ovaries of a female (ca. 350 mm) ready to spawn captured in January were swollen and contained two groups of eggs; 3.32–3.65 mm, and <1.35 mm (Fig. 5). Estimated number of ripe eggs was 1,277. The ovaries of another female (333 mm SL) captured in March, did not contain any eggs larger than 1.68 mm.

P. rosaceus appears to spawn at least in the winter. The 333 mm female discussed above could have spawned earlier. A third female (March; 361 mm) had a group of relatively small developing eggs, perhaps indicating recovery from a much earlier spawning.

Careproctus oregonensis: Two females (119, 153 mm) captured in May and July, were examined. Largest eggs were 5.62 mm and 5.29 mm respectively. The ovary of the larger female contained five eggs ⩾5.00 mm and five eggs between 4.51–4.99 mm. The ovary of the smaller contained three eggs ⩾5 mm and four eggs between 4.26 mm and 5.00 mm diameter (Fig. 4). Size distributions of ovarian eggs of the ripe females suggest that this species may have prolonged or continuous spawning.

Careproctus ovigerum: One female, 431 mm, captured in September, was examined. Maximum egg diameter was 7.75 mm. The right ovary contained 936 eggs >5.25 mm, grouped in two distinct size modes close together but widely separated from the next largest eggs (2.87 mm) (Fig. 5). Estimated number of ripe eggs (6.93–7.75 mm) in both ovaries of the specimen was 756. These eggs were free in the lumen of the ovary; immature eggs were peripheral to them. Size distribution of ovarian eggs in this female suggests spawning periods separated by long intervals.

Paraliparis megalopus: Five specimens (three females, 137, 150, 152 mm; two males, 114, 132 mm) captured during four months of the year (Table 1), were examined.

There was no obvious sexual dimorphism. Only one female (152 mm, collected in January) had large eggs, of which the largest was 4.31 mm. Egg size groups were not quite as distinct as those of many of the other species studied, although the pattern was similar to those of the continuous spawners (Fig. 4). There were 32 ripe (>3.62 mm) eggs present with many groups of smaller eggs also present. The males, captured during October, were apparently ripe. Size distribution of ovarian eggs in this female possibly suggest prolonged or continuous spawning.

Careproctus longifilis: Three female specimens, 146, 162, 162 mm, captured in February, March and November, respectively, were examined. The female collected in November had eggs up to 7.09 mm diameter (Fig. 4). There were 16 ripe (>6.31 mm) eggs present. The 146 mm specimen contained eggs up to 1.52 mm; the 162 mm female collected in March had only eggs <0.86 mm. Size distribution of ovarian eggs in a ripe female possibly suggests prolonged or continuous spawning.

Paraliparis mento: Two specimens (female, 114 mm; male, 95 mm), captured in January (Table 1), were examined. There was no obvious sexual dimorphism. The largest egg was 2.50 mm. Eggs of different sizes were evenly distributed throughout the ovaries. There were two groups of different size eggs; (ripe) 2.00–2.50 mm (101 eggs) and <1.00 mm (Fig. 5). The male appeared to be ripe. Size distribution of ovarian eggs in the ripe female suggests possible periodic spawning.

Paraliparis cephalus: Twelve specimens (six females, 37–83 mm; six males, 58–82 mm) captured during six months of the year (Table 1) were examined. There was no obvious sexual dimorphism. Maximum egg diameter was 0.86 mm. No females had mature eggs. One male (82 mm) captured in January had well developed testes and seemed to be ready to spawn. No conclusions were made about reproduction of this species.

Careproctus filamentosus: One female (180 mm) captured in February was examined. The larg-

est eggs were 0.70 mm; they were obviously im-
mature, with no obvious yolk, and a thin outer
membrane. The ovaries were relatively small.
There were no signs of recent spawning. No
conclusions were made about reproduction of
this species.

DISCUSSION

The question of whether seasonal reproduc-
tion exists at abyssal depths has been discussed
at least since Orton (1920) proposed that ani-
mals living in stenothermal environments (po-
lar seas, great depths, tropics) reproduce con-
tinuously. Although the evidence is not
abundant, recent studies have shown that at
least some endemic Antarctic benthic fishes have
distinctly seasonal reproduction (Hureau, 1970)
and that tropical reef fishes may either have
spawning peaks (Munro et al., 1973) or pro-
longed but distinct seasonal reproductive pe-
riods (Russell et al., 1977). Until now there has
been little evidence for or against the existence
of seasonal spawning of fishes in the abyss.

Menzies et al. (1973) reviewed the evidence
for seasonal and continuous spawning of abys-
sal fishes and invertebrates. Based on their own
studies of isopods and on those of other groups
by other authors, Menzies et al. concluded that
"the fauna ... tends to show definite repro-
ductive periodism" but were unable to dem-
onstrate an environmental cue for it. Rokop
(1974) found year round asynchronous repro-
duction in bathyal brittle stars and crustaceans,
continuous reproduction in bivalves and a poly-
chaete, and seasonal reproduction in a bathyal
brachiopod and scaphopod. The last two were
species from the continental shelf whose distri-
butions extended into bathyal depths. He con-
cluded that "year-round reproduction is the
common pattern in the deep-sea benthos."

There is substantial evidence to show that
bathyal fish species (primarily macrourids) ex-
hibit either seasonal or continuous reproduc-
tion. Novikov (1970), Savvatimskii (1969), Hae-
drich and Polloni (1976), S.I.O. (1975) and
Rannou (1976) showed that a number of dif-
ferent macrourid species which live on the con-
tinental slope have definite seasonal spawning.
Nielsen (1969) concluded that an aphyonid,
also from the continental slope, has continuous
spawning. Mead et al. (1964) suggested that
abyssal benthic fishes would spawn continu-
ously, perhaps show parental care, and would
have low fecundity with large eggs. Rannou

(1975) proposed that at least some abyssal fishes
spawn periodically, based on the presence of
"growth checks" (similar to those in otoliths of
shallow water fishes) in the otoliths of *Cory-
phaenoides guentheri* (Macrouridae, 1,800–3,000
m), *Bathysaurus mollis* (Bathysauridae, 4,240 m),
Histiobranchus bathybius (Synaphobranchidae,
4,700 m), *Antimora rostrata* (Moridae, 1,909 m),
Coryphaenoides leptolepis (Macrouridae, 4,256 m)
and *C. armatus* (Macrouridae, 4,256 and 2,750
m), and on the presence of a single group of
larvae in the ovaries of *Cataetyx laticeps*, a vivi-
parous brotulid from 1,889 m. Rannou himself
pointed out that he did not know the length of
the periods which he felt were represented by
the "checks."

The conclusions reached here are that con-
tinuous spawning, and possibly periodic spawn-
ing (deposition of eggs at relatively long inter-
vals), exist in abyssal benthic liparids, and that
at least some slope liparids probably spawn sea-
sonally. The species examined here can be ten-
tatively divided into two classes: continuous
spawners and periodic (at least some of which
are probably seasonal) spawners. Species were
assigned to a group based upon capture of ripe
females throughout the year (*O. cascadiae, P.
latifrons, A. opercularis*), capture of ripe females
during part of the year (*C. melanurus*), and egg
size distributions in ripe females (all other
species).

Following the logic of Hickling and Ruten-
berg (1936), de Vlaming (1974) and Rannou
(1975), the presence of only one size group or
two similar size groups of ripe (yolked) eggs,
absence of intermediate size eggs, and presence
of a group of immature (yolkless) eggs indicates
that a species probably spawns only at relatively
long intervals. Conversely, presence of many
egg size groups indicate prolonged or contin-
uous spawning. Based on these criteria, contin-
uous spawners probably include *Careproctus
longifilis, C. microstomus, C. oregonensis, Osteodis-
cus cascadiae, Acantholiparis opercularis, Paralipa-
ris megalopus* and *P. latifrons*. The periodic
group probably includes *Careproctus melanurus,
C. ovigerum, Paraliparis mento* and *P. rosaceus*.
Rates of oogenesis are unknown for any abyssal
fishes. Rates of egg development in the above
species could be very slow, individual females
spawning at long intervals, but asynchronously
with most conspecifics. Although it is evident
that spawning is asynchronous in *O. cascadiae,
A. opercularis* and *P. latifrons*, it seems unlikely
that females spawn only at long intervals. Al-

TABLE 2. Species Maximum Fecundity Groups, Maximum Fecundity/Female, Maximum Egg Diameters, SL, and Maximum Percent Total Body Weight Represented by the Ovaries. C = continuous, P = periodic spawning.

Group	Species	Fecundity	Max egg diam (mm)	Max SL	% ovary wt	Spawning
I	*A. opercularis*	6	4.96	75	16.95	C
	C. oregonensis	10?	5.62	153	9.98	C
	O. cascadiae	7	5.29	81	8.33	C
	P. latifrons	8	4.47	96	9.21	C
II	*C. longifilis*	16	7.09	162	6.99	C
	P. megalopus	32	4.31	152	7.60	C
	C. microstomus	15	7.58	197	5.80	C
III	*P. mento*	101	2.50	114	10.32	P
	C. melanurus	534	4.63	312	4.43	P
	C. ovigerum	756	7.75	431	1.23	P
	P. rosaceus	1,277	3.65	361	6.66	P

most all adult females had ripe eggs. If spawning occurs at long intervals and egg development is slow, many adult females without ripe eggs should have been captured. Fecundity is extremely low in many species, which, if spawning occurred at long intervals, would result in few offspring. Very few spent *O. cascadiae* and *A. opercularis* and no spent *P. latifrons* were captured. Furthermore, the presence of distinct groups of ripening (intermediate size) eggs may be evidence for relatively frequent replacement of spawned eggs. It seems most likely that spawning is not only asynchronous but that females spawn relatively frequently throughout the year.

The continuous spawning group includes three species which are known to spawn throughout the year: *O. cascadiae*, *A. opercularis* and *P. latifrons*. Ripe females of the first two species were captured during all seasons, and the last during three seasons of the year. Adults of all of these species are less than 200 mm long, and have similar size distributions and numbers of eggs. They have few (often very few) ripe eggs present at one time; the largest eggs are distinctly but not necessarily widely separated from the next largest size mode of eggs; and there is usually at least one group of intermediate sized eggs between the smallest, least mature eggs and the largest, most mature ones. All the species in this group are abyssal; the shallowest occurring species are *C. longifilis* and *A. opercularis*, which reach 1,900 m, the base of the continental slope. Mature female *O. cascadiae* captured in the same month were

found with ripe eggs present in various numbers; spent, with no large eggs and no intermediate (maturing) eggs; and with maturing eggs (Fig. 1). Males of these species appear to be ripe throughout the year. *Careproctus longifilis*, *C. microstomus*, *C. oregonensis* and *P. megalopus* were included on the basis of egg size distributions and occurrence of ripe males.

Evidence is strongest for "periodic" spawning of *C. melanurus*, which possibly spawns in spring and summer. The only running ripe female found was captured at the end of April. Peden and Corbett (1973) found eggs off British Columbia in June, which they concluded (based on meristic characters of larvae and size of egg masses) were probably from *C. melanurus*. Parrish (1972) reported larvae and hatching eggs off Monterey, California in mid-October, although he did not describe how they were identified. These occurrences are widely separated geographically, and may have been from waters of different temperatures. *C. melanurus* may have a prolonged spawning season from early spring to late summer (depending on presently unknown factors).

Why *C. ovigerum* and *P. rosaceus*, the two largest (of ten) abyssal species, would have periodic reproduction is unclear. Stein (1978) suggested that *C. ovigerum*, which displays few of the morphological characteristics of "typical" abyssal liparids, represents a more recent invasion of deep water by liparids. Periodic spawning of this species could be a relict behavior. Shallow water liparids spawn seasonally, although spawning periods may be prolonged (Detwyler,
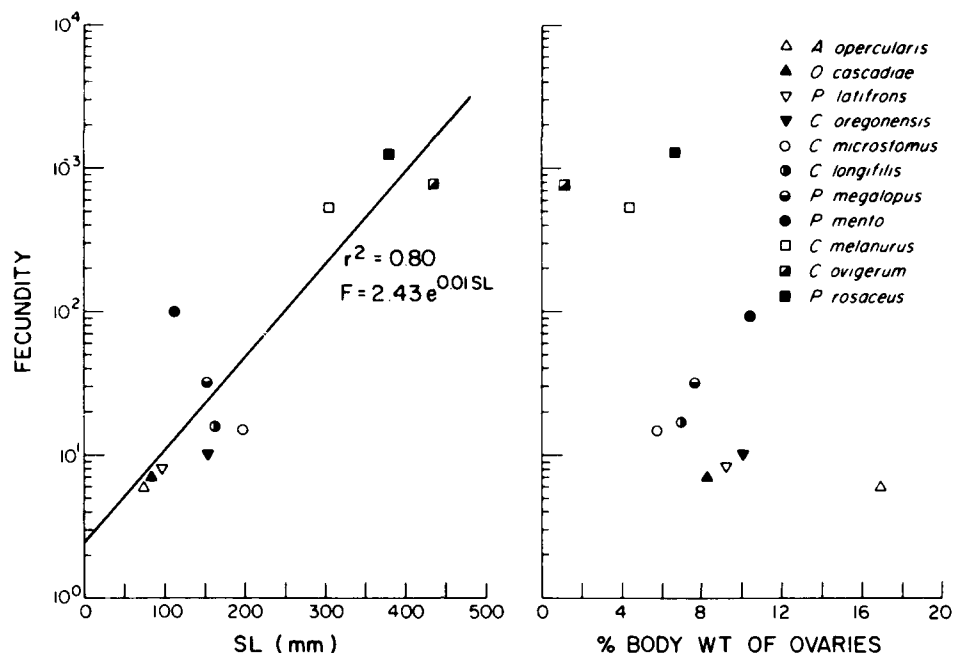
Fig. 6. Relationship of maximum fecundity vs. maximum SL and maximum % body weight of ovaries for 11 species of liparids.

1963; Breder and Rosen, 1966; Able and Musick, 1976). However, *Paraliparis rosaceus* is a typical abyssal liparid in all respects except, perhaps, its size. It has a relatively wide depth distribution (1,799–3,358 m) (Stein, 1978), which extends up onto the lower contintal slope, where it could be affected by seasonally occurring environmental events.

These liparid species can also be divided into three groups based upon maximum fecundity (Table 2). These groups are: Group I, species producing fewer than ten ripe eggs at one time; Group II, species with 10–100 ripe eggs; Group III, species producing more than 100 ripe eggs at once. These groups also generally divide the species by length. *Paraliparis mento* is the only species which falls between groups (II/III); its fecundity is barely high enough to place it in Group III, but its length places it in Group II. A plot of species maximum length against maximum fecundity demonstrates a significant relationship (Fig. 6), demonstrating a close relationship between maximum size of species and fecundity. Fecundity differences between species seem to reflect continuous spawning (few ripe eggs present at once) versus periodic spawning (many ripe eggs present at once).

Great differences in numbers of ripe eggs present per female may not reflect actual yearly spawning effort. If the rate of egg development and deposition in Group I is high (i.e., on the order of two eggs per week) the total number of eggs spawned over a long period (for example, a year) could approach that of some of the periodic spawners. If a female *O. cascadiae* produces 100 eggs a year, and if a female *P. mento* spawns once a year, their yearly egg number would be similar. Thus, egg production of many species might be approximately the same, although the energy devoted to it would not necessarily be equal.

Maximum gonad weights (expressed as a percentage of total body weight) do not show differences as great as egg numbers, and are inversely related to fecundity (Fig. 7). The gonads of the "continuous" spawners are relatively larger than those of the "periodic" species. The liparids all produce large eggs; yet the large species invest relatively less energy (i.e., have relatively lower gonad:body weights) in

reproductive products. This may be an energy saving adaptation, the result of differences in parental care, or the result of other factors differently affecting survival of offspring of large vs. small species. The abyssal benthic environment is considered to be extremely constant (Sanders, 1968; Rokop, 1974) and the benthic community is probably a stable one which is not perturbed very often. If recruitment and loss of offspring are relatively constant, extra offspring would represent an unnecessary energy loss to the adults.

Intertidal or shallow subtidal liparid species may have shorter life spans, higher fecundity and much smaller eggs than the deeper living species. Able (1973) and Able and Musick (1976) described the life history of *Liparis inquilinus*, a small (<71 mm TL), short lived (2 years) shallow water (5–97 m depth) species which probably has only one (prolonged) spawning period in its life. The mean number of large (1.0–1.3 mm) eggs present was 342 for females collected at sea (laboratory raised females had a mean of 447 eggs). Because spawning may be repetitive the total number of eggs laid by each female was unclear. Detwyler (1963) estimated that *L. atlanticus* (<97 mm SL) deposit 1,400–3,000 eggs (average size 1.1 mm) per female per season. Johnson (1969) found that *L. pulchellus* (<170 mm SL) had eggs up to 1.48 mm, but did not estimate number of ripe eggs. Eggs of other shallow water liparids are small. Aoyama (1959) found developing eggs of *L. tanakae* to be 1.7–1.8 mm. Breder and Rosen (1966) stated that eggs of *L. montagui* are about 1.1 mm and those of *L. liparis* are about 1.5 mm. De Martini (1978) stated that fertilized eggs of *L. fucensis* are about 1.0 mm.

A probable life history for deep water liparids can be constructed using new and published data. Eggs are probably laid in a protected location (such as under a rock), or in or on an invertebrate with a hard exoskeleton. Such behavior occurs in shallower living species (Able and Musick, 1976; Hunter, 1969; Parrish, 1972; Peden and Corbett, 1973). Parental care seems likely in species which lay a comparatively large number of eggs at a time, but unlikely in species laying few eggs at a time over long periods; the latter would be required to devote virtually the whole year to protecting the eggs. At least one shallow water liparid species shows parental care (Detwyler, 1963; DeMartini, 1978). Gilbert (1896) concluded that *C. ovigerum* is a mouth brooder because the holotype, a

male, held developing 4.5 mm eggs in its mouth when captured. However, ripe eggs of the species are almost 8 mm, so the holotype almost certainly ate the eggs of another species. Wenner (1979) found that the stomachs of four sexually mature male *P. garmani* contained from three to 17 undeveloped eggs of sizes similar to those occurring in possibly mature females of the same species. A male *P. calidus* was found to have eleven eggs in its stomach. Wenner suggested that *P. garmani* males may be mouth brooders, and that the eggs could have been swallowed "during ascent of the trawl." It seems more likely (if the eggs were from conspecific females) that the males were guarding the eggs. Many fishes which care for their eggs do not feed while doing so. At least one cichlid (*Pterophyllum scalare*) removes unfertilized eggs from the egg mass while caring for the eggs (Breder and Rosen, 1966). Virtual absence of stomach contents other than eggs in the above males of *P. garmani* and *P. calidus* suggests that these species may behave similarly. Egg development is probably slow because larvae from large eggs are generally very well developed at hatching. Kyûshin (1975) found that hatching *Aptocyclus ventricosus* (Cyclopteridae) had no yolk sac, and illustrations of newly hatched larvae of *Careproctus* spp. in Hunter (1969) and Parrish (1972) do not show prominent yolk sacs. If length of young at hatching is proportional to egg diameter, hatchling *C. ovigerum* (7–8 mm eggs) could be >20 mm; Kyûshin (1975) found that average length of *A. ventricosus* larvae hatched from 2.32–2.42 mm eggs was 6.7 mm, and Parrish (1972) found newly hatched *C. melanurus* to be 9–12 mm long (eggs ca. 4.5 mm). Marshall (1953) pointed out that newly hatched *Paraliparis gracilis* are well developed, and suggested that "certain species may have no pelagic stages." The young probably take up benthic residence and habits very soon or immediately after hatching. Sexual maturation may begin comparatively early, although it might take a relatively long time. All females, even those 30 mm long, examined in this study had eggs easily recognizable at 6× magnification.

This pattern of life history may be characteristic of deep sea liparids. Nielsen (1964) found that egg sizes in *Careproctus kermadecensis* (6,660–6,770 m) were distributed similarly to those of the continuous spawners discussed here. One female had about 16 eggs of 8 mm, while another had about seven 6.5 mm eggs

and a continuum of smaller egg sizes. Nielsen also examined a female *C. reinhardti* from about 250 m depth off Greenland. He found that it contained "eggs of almost equal size . . ." which is the pattern in periodic spawners. Johnsen (1921) found that *Rhodichthys regina* from 1,738 m in the North Atlantic had about 70 eggs 3.2–4.0 mm "surrounded by many quite small eggs with a diameter up to 1 mm." Wenner (1979) captured apparently ripe male *Paraliparis garmani* in the northwest Atlantic at undisclosed depths in January, June, August and November, and female conspecifics with 3.3 mm eggs in September and January. Numbers of ripe eggs were not given. Presence of ripe males throughout the year, and presence of ripe females at widely separated times of the year may indicate continuous spawning. Abyssal and many bathyal liparid species may be continuous spawners although some bathyal and all shallow water species may reproduce periodically (possibly seasonally).

ACKNOWLEDGMENTS

LITERATURE CITED

ABLE, K. W. 1973. A new cyclopterid fish, *Liparis inquilinus*, associated with the sea scallop, *Placopecten magellanicus*, in the western North Atlantic, with notes on the *Liparis liparis* complex. Copeia 1973:787–794.

———, AND J. A. MUSICK. 1976. Life history, ecology, and behavior of *Liparis inquilinus* (Pisces: Cyclopteridae) associated with the sea scallop, *Placopecten magellanicus*. Fish. Bull. 74:409–421.

AOYAMA, T. 1959. On the egg and larval stages of *Liparis tanakae* (Gilbert et Burke). Bull. Seikai Reg. Fish. Res. Lab., Nagasaki 18:69–73.

BREDER, C. M., AND D. E. ROSEN. 1966. Modes of reproduction in fishes. Nat. Hist. Press, Garden City, NY.

COHEN, D. M. 1968. The cyclopterid genus *Paraliparis*, a senior synonym of *Gymnolycodes* and *Eutelichthys*, with the description of a new species from the Gulf of Mexico. Copeia 1968:384–388.

COLLETT, R. 1909. Fiske indsamlede under "Michael Sars" Togter i Nordhavet, 1900–02. Rep. Norw. Fishery Mar. Invest. Bergen 2(3):1–152.

DEMARTINI, E. D. 1978. Apparent paternal care in *Liparis fucensis* (Pisces: Cyclopteridae). Copeia 1978:537–539.

DETWYLER, R. 1963. Some aspects of the biology of the seasnail, *Liparis atlanticus* (Jordan and Evermann). Unpubl. Ph.D. Diss., Univ. New Hampshire.

DE VLAMING, V. L. 1974. Environmental and endocrine control of teleost reproduction, p. 13–83 *In*: Control of sex in fishes. C. B. Schreck (ed.). Ext. Div., Va. Poly. Inst. St. Univ., Blacksburg, Va.

GILBERT, C. H. 1896. Ichthyological collections of the United States fisheries steamer "Albatross" in southern California in 1904. Proc. U.S. Nat. Mus. 48:305–380.

HAEDRICH, R. L., AND P. T. POLLONI. 1976. A contribution to the life history of a small rattail fish, *Coryphaenoides carapinus*. Bull. So. Calif. Acad. Sci. 75:203–211.

HART, J. L. 1973. Pacific fishes of Canada. Fish. Res. Bd. Canada Bull. 180.

HICKLING, C. F., AND E. RUTENBERG. 1936. The ovary as an indicator of the spawning period in fishes. J. Mar. Biol. Ass. U.K., New Ser., 21:311–316.

HUNTER, C. J. 1969. Confirmation of symbiotic relationship between liparid fishes (*Careproctus* spp.) and male king crab (*Paralithodes camtschatica*). Pac. Sci. 23:546–547.

HUREAU, J.-C. 1970. Biologie comparee de quelques poissons antarctiques (Nototheniidae). Bull. Inst. Oceanogr. Monaco 68(1391):1–244.

JOHNSEN, S. 1921. Ichthyologiske notiser. Bergens Mus. Aarb. 1918–1919 3:1–95.

JOHNSON, C. R. 1969. Contributions to the biology of the showy snailfish, *Liparis pulchellus* (Liparidae). Copeia 1969:830–835.

KYUSHIN, K. 1975. The embryonic and larval development, growth, survival and changes in body form, and the effect of temperature on these characteristics of the smooth lumpsucker, *Aptocyclus ventricosus* (Pallas). Bull. Fac. Fish. Hokkaido Univ. 26:49–72.

MARSHALL, N. B. 1953. Egg size in arctic, antarctic, and deep-sea fishes. Evolution 7:328–341.

MCINTOSH, W. C. 1885. XXXIX. Notes from the St. Andrew's Marine Laboratory (under the Fishery Board for Scotland). Ann. Mag. Nat. Hist. ser. 5, 15:429–437.

MEAD, G. W., E. BERTELSEN AND D. M. COHEN. 1964. Reproduction among deep-sea fishes. Deep-Sea Res. 11:569–596.

MENZIES, R. J., R. Y. GEORGE AND G. T. ROWE. 1973. Abyssal environment and ecology of the world oceans. John Wiley & Sons, New York.

MUNRO, J. L., V. C. GANT, R. THOMPSON AND P. H. REESON. 1973. The spawning seasons of Caribbean reef fishes. J. Fish. Biol. 5:69–84.

NIELSEN, J. G. 1964. Fishes from depths exceeding 6000 meters. Galathea Rept. 7:113-124.

———. 1969. Systematics and biology of the Aphyonidae (Pisces: Ophidioidea). Ibid. 10:7-90.

NOVIKOV, N. P. 1970. Biology of Chalinura pectoralis in the North Pacific, p. 304-331. In: Soviet fisheries investigations in the northeastern Pacific. P. A. Moiseev (ed.). V. Pac. Sci. Res. Inst. Fish. Oceanogr. 72. Israel Progr. Sci. Transl. Ser. 60044 6.

ORTON, J. H. 1920. Sea temperature, breeding and distribution in marine animals. J. Mar. Biol. Ass. U.K., New Ser. 12:339-366.

PARRISH, R. H. 1972. Symbiosis in the blacktail snailfish, Careproctus melanurus, and the box crab, Lopholithodes foraminatus. Calif. Fish and Game 58:239-240.

PEDEN, A. E., AND C. A. CORBETT. 1973. Commensalism between a liparid fish, Careproctus sp., and the lithodid box crab, Lopholithodes foraminatus. Canad. J. Zool. 51:555-556.

RANNOU, M. 1975. Données nouvelles sur l'activité reproductrice cyclique des poissons benthiques bathyaux et abyssaux. C. R. Acad. Sc. Paris 281, ser. D:1023-1025.

———. 1976. Age et croissance d'un poisson bathyal: Nezumin sclerorhynchus (Macrouridae Gadiforme) de la Mer d'Alboran. Cah. Biol. Mar. 17:413-421.

ROKOP, F. J. 1974. Reproductive patterns in the deep-sea benthos. Science 186:743-745.

RUSSELL, B. C., G. R. V. ANDERSON AND F. H. TALBOT. 1977. Seasonality and recruitment of coral reef fishes. Aust. J. Mar. Freshwater Res. 28:521-528.

SANDERS, H. L. 1968. Marine benthic diversity: a comparative study. Amer. Nat. 102:243-282.

SAVVATIMSKII, P. I. 1969. The grenadier of the North Atlantic. Proc. Polar Res. Inst. Mar. Fish. Oceanogr. 1969. Fish Res. Bd. Canada Transl. Ser. 2879:1-86.

SCHMIDT, P. YU. 1916. Ichthyological notes. 2. On a new cyclogasterid fish with a rudimentary ventral disk. Ann. Mus. Zool. Acad. Imp. Sci. Petrograd 20:627-630.

SCRIPPS INSTITUTION OF OCEANOGRAPHY. 1975. Midwater and benthic fish. Report of Marine Life Research Group, Scripps Institution of Oceanography. Calif. Coop. Fish. Inv. 17:15.

STEIN, D. L. 1978. A review of the deepwater Liparidae (Pisces) from the coast of Oregon and adjacent waters. Occ. Pap. Calif. Acad. Sci. 127.

WENNER, C. A. 1979. Notes on fishes of the genus Paraliparis (Cyclopteridae) on the middle Atlantic continental slope. Copeia 1979:145-146.

SCHOOL OF OCEANOGRAPHY, OREGON STATE UNIVERSITY, CORVALLIS, OREGON 97331. Accepted 18 Oct. 1979.

Surface sediments of the
Peru-Chile continental margin and the Nazca plate

LAWRENCE A. KRISSEK
KENNETH F. SCHEIDEGGER   *School of Oceanography, Oregon State University, Corvallis, Oregon 97331*
LAVERNE D. KULM

ABSTRACT

Surface sediment samples from 86 locations on the Peru-Chile continental margin and the Nazca plate have been analyzed for bulk chemistry and texture to evaluate the factors influencing sediment formation on continental slope and adjacent abyssal plain depositional environments. Sand-sized calcareous microfossils are abundant above the carbonate compensation depth (CCD), but their removal by dissolution leaves fine-grained deposits in the deeper basins. Terrigenous silts are found seaward of the Peru-Chile Trench, especially south of 7°S, and may be transported there by wind, mid-water turbid layers, or bottom waters flowing north through the deep ocean basins. Sediments become finer grained away from shore as coarse terrigenous particles settle out. The more humid climate of northern Peru produces finer fluvial sediments there than to the south. This textural change also appears in adjacent marine sediments. In the Peru Basin, bottom nepheloid layers are found where clay-sized terrigenous material dominates the sediments. On the adjacent Galapagos Rise, however, nepheloid layers are absent, and eolian-derived sedimentary components in the <5 μ size range may exceed those transported to the area by currents.

R-mode factor analysis has outlined sediment constituents from the geochemical data. Terrigenous components dominate the slowly accumulating clay-sized sediments of the Peru and Chile Basins, and the coarser, more rapidly forming margin deposits south of 14°S. Biogenic deposits form at intermediate rates on topographic highs on the Nazca plate. Very slow hydrogenous sedimentation occurs in the seaward portions of the deep basins. Sediments rich in organic components are concentrated in rapidly forming deposits along the margin north of 14°S, beneath centers of strong coastal upwelling.

Several distinct sediment accumulations have been mapped on the continental shelf and upper slope. An upper-slope deposit is anomalously fine grained and organic rich; it lies between 10.5°S and 13.6°S, in the region of most intense upwelling. Preservation of this body is enhanced by the inclusion of fine inorganic material in biogenic fecal pellets, and by the impingement of the shallow-water oxygen minimum layer on the slope at the same level.

INTRODUCTION

The Marine Geology group of the Oregon State University's School of Oceanography began a comprehensive interdisciplinary study of the Peruvian continental margin and adjacent Nazca plate sedimentary environments in May of 1977. This program was designed to compare the processes controlling hemipelagic sediment formation beneath the coastal upwelling and nonupwelling regions of the equatorial east Pacific with those influencing sediments in the adjacent pelagic regimes. The study area is shown in Figure 1.

The region was considered ideal for this study, because in a relatively restricted geographical area, many of the factors which could influence the accumulation of such fine-grained deposits are found. These include: (1) a well-defined continental sediment source which is influenced by latitudinally varying rainfall and river runoff patterns (Johnson, 1976); (2) extreme local variability of the biological productivity within the water column (Zuta and Guillen, 1970); (3) the prominent Peru-Chile Trench which serves as a barrier to the seaward transport of sediment by turbidity currents (Schweller and Kulm, 1978); (4) topographic highs and deep basins of the adjacent abyssal regions of the eastern Nazca plate; and (5) well-defined surface currents and wind patterns (summarized by Molina-Cruz, 1978). This paper discusses the results of textural and chemical analyses of surface sediments recovered from the Peruvian continental margin and the eastern Nazca plate. A major goal of our project has been the recognition of the processes and factors which control the deposition of principally fine grained terrigenous sediments adjacent to a continental landmass.

SAMPLING AND ANALYTICAL TECHNIQUES

Chemical and textural data were obtained from 86 surface sediment samples taken on the Peru-Chile continental margin and the Nazca plate (Fig. 1). Most of the samples were taken with gravity, Reineck box, and Kasten corers.

The gross textural composition (sand, silt, and clay percentages) of the samples was determined with standard techniques, and grain-size frequency analysis of the silt fraction (4 to 63 μ) was made (Thiede and others, 1976).

Surface sediment samples were analyzed for Si, Al, Fe, Mg, Ca, Na, K, Ti, Mn, Ba, organic C, Cu, Ni, An, Sr, PO_4 (soluble), PO_4 (particulate), and $CaCO_3$. Silicon and phosphate measurements were made by standard colorimetric techniques. Other major and transition element analyses were made by AA spectrophotometry. Organic C and $CaCO_3$ abundances were determined with a Leco model WR-12 Automatic Carbon Determinator.

DISTRIBUTION AND GEOMETRY OF SEDIMENT ACCUMULATIONS IN THE STUDY AREA

Sediment cover along the Peruvian continental margin was mapped from 3.5 kHz records obtained during RV *Wecoma* and RV *Yaquina* cruises. These high-resolution reflection profiles are spaced a maximum of 50 km apart along the margin, and they generally extend from the continental shelf
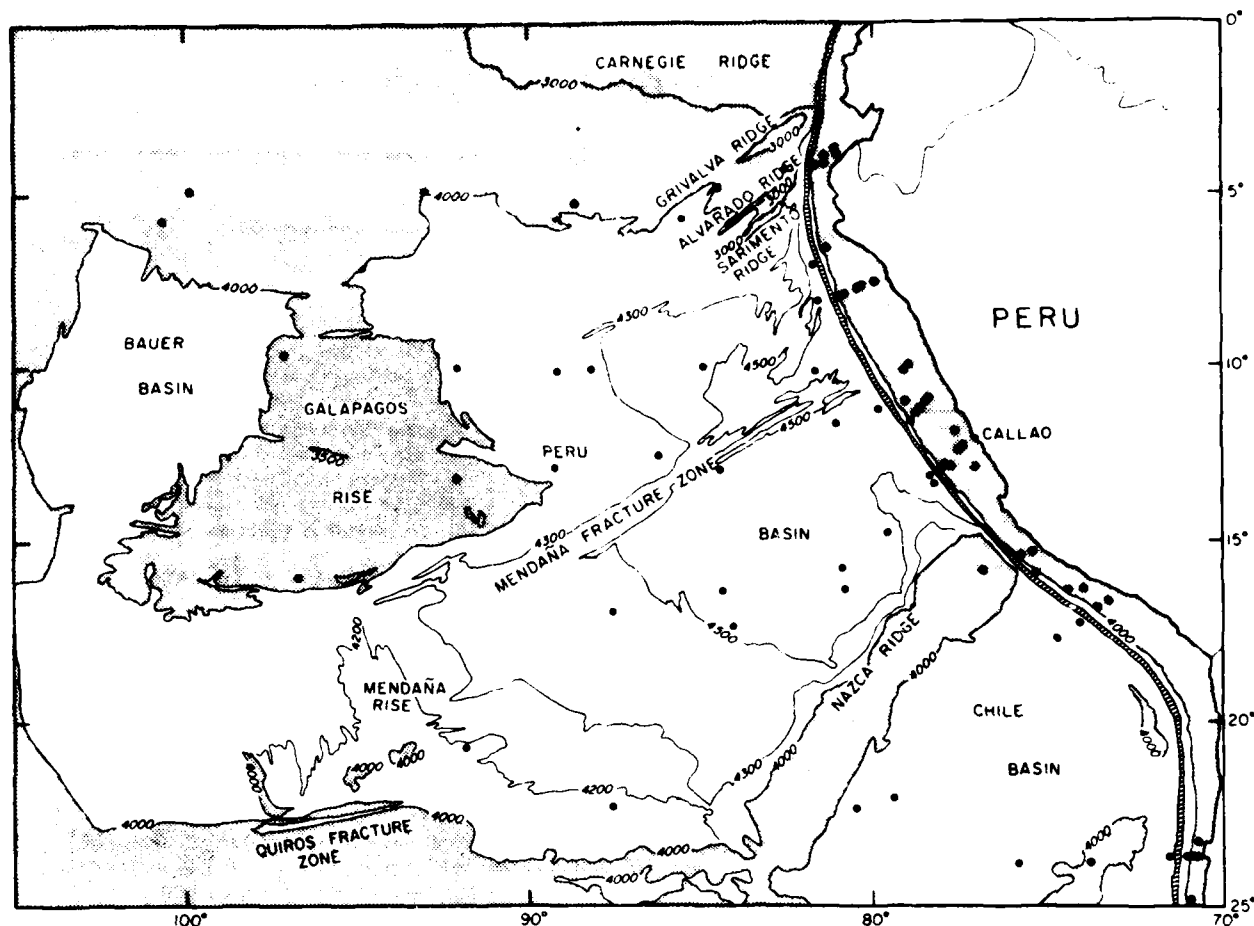
Figure 1. Core locations shown relative to the main physiographic features of the Peru-Chile continental margin and the Nazca plate. Stippled pattern corresponds to topographic features in water depths <4,000 m; line pattern denotes axis of Peru-Chile trench. Modified from Mammerickx and Smith (1978).

out over the slope. Most are of good to excellent quality, and show subbottom penetration of 50 m or less in the mud deposits along the margin.

Three major sediment accumulations have been identified and mapped (Fig. 2). The geometry of one deposit, an upper slope mud lens, is summarized by the representative profiles shown in Figure 3. It is a well-defined and nearly symmetrical body located between 10.5°S and 13.6°S, although it may extend as far south as 15.1°S (see Fig. 2). A structural re-entrant forms a broad, gently sloping upper continental slope in this region. Sediments here are found at water depths from 110 to 683 m, with the depositional axis at depths of 164 to 368 m. A sediment wedge and small ponds of sediment with interspersed barren areas are the typical accumulation

pattern on the upper slope between 6.5°S and 10.5°S and between 16.0°S and 17.2°S. On the adjacent shelf, a mud deposit occurs between 8°S and 10.5°S, widening onto the outer shelf at its southern end. It lies between 40 and 160 m water depth in this area with its depositional axis (maximum sediment thickness) at about 90 m depth in the vicinity of 8°S, and at 135 m at 10.5°S. A similar type of depositional feature extends to the south on the central and outer shelf from 10.5°S to 17.2°S. It reaches seaward to the shelf edge throughout this region.

Published profiles (Prince and Kulm, 1975) show that sediments on the steep lower continental margin are confined to local basins. In the axis of the Peru-Chile Trench, sediment thickness rarely exceeds 850 m, while deposits on the eastern Nazca

plate vary in thickness from 80 to 170 m (Ade-Hall, 1976; Yeats, Hart, and others, 1976; Prince and Kulm, 1975).

TEXTURAL CHARACTERISTICS

The textural characteristics of the Peruvian margin and Nazca plate sediments help to explain the observed variations in occurrence and geometry of the deposits. Figure 4 shows the areal distribution pattern for clay abundance, and the textural data are summarized for each geographic region in Table 1.

Insight into the texture of samples taken seaward of the Peru-Chile Trench can be obtained from a ternary plot of sand, silt, and clay (Fig. 5). Sediments associated with specific physiographic provinces cluster together fairly well. The coarsest studied
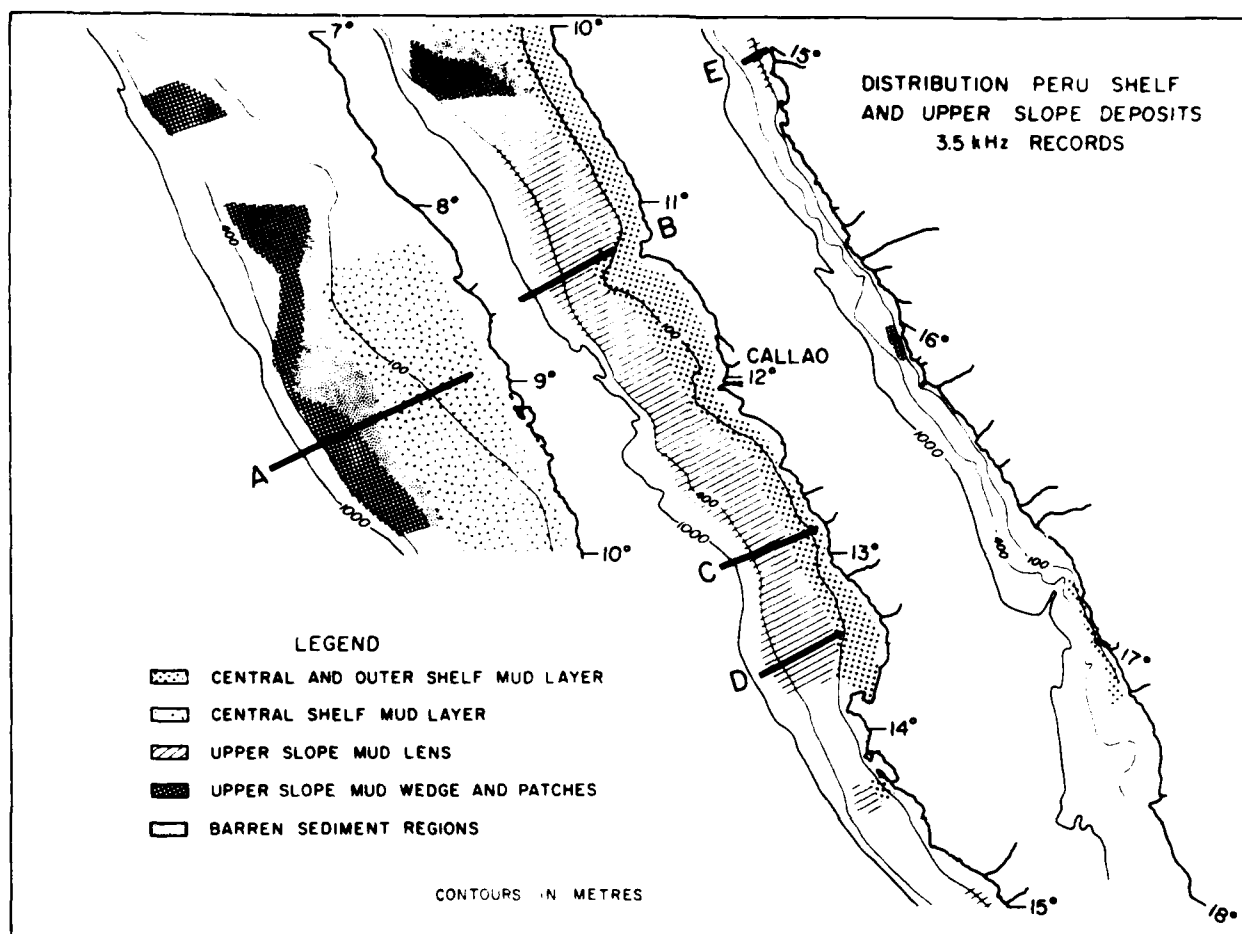
Figure 2. Sediment accumulations determined from 3.5-kHz records on the upper Peruvian continental margin. Profiles shown in Figure 3 are identified by letters.

oceanic sediments are found on the Galapagos Rise above 4,100 m water depth and can be distinguished from sediments in the Peru and Chile Basins by higher sand and silt content. In contrast, Peru and Chile Basin samples are much finer grained but may be distinguished by their silt contents. Chile Basin samples were taken, with one exception, shallower than 4,000 m, and have silt contents of 25% to 30%. Peru Basin sediments, however, were obtained from deeper than 4,200 m, and contain only 10% to 25% silt.

The available data also show both along-and across-margin textural trends. The clay content of samples taken in profiles across the margin at 3°S and 7°S (north), 11°S and 13°S (central), and 22°S (south) are plotted against the sample water depth in Figure 6. Upper-slope samples

(<1,000 m water depth) show no consistent change from south to north. However, at any water depth greater than 1,000 m, clay contents of margin sediments systematically increase from south to north. This figure also illustrates the general trend of sediment fining (increasing clay content) with depth for all profiles, and the anomalously high clay content at the surface of the "middle" profile (13°S profile), which intersects the upper slope mud lens.

Silt grain-size frequency curves illustrate similar but more subtle downslope textural changes. Data from the 7°S transect (Fig. 7) illustrate the normal pattern of seaward fining also observed at 3°S and 22°S. The upper slope curve shows a strong coarse silt signal, with a smaller fine silt mode. The three deeper samples all show very large fine silt modes. In addition, the coarse-silt

tail migrates toward finer grain sizes for samples farther downslope. By comparison, data from the 13°S transect (Fig. 7) show a reversal of the upper- and middle-slope sediment characteristics. Due to the location of the upper-slope sample within the anomalously fine grained upper-slope mud lens, silt size appears to increase downslope.

This reversal may be caused by (1) masking a regional upper slope silt input with an anomalously large local influx of fine silt, or (2) a decrease in the grain size of the regional silt influx in this area only. However, data presented in Table 1 and Figure 6 show a trend of sediment fining from south to north along the entire margin, instead of a pattern restricted to the region 10.5°S to 13.6°S. In addition, strong similarities between the silt curves from the 3°S, 7°S, and 22°S transects and those from the two
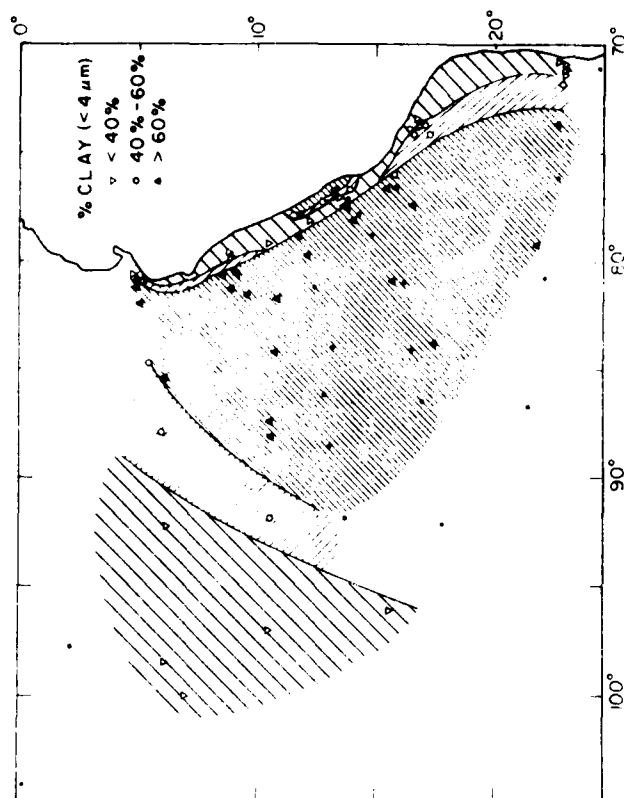
Figure 4. Percentage of clay for surface sediment samples recovered from the study area. Solid dots denote samples which had dried during storage, preventing their disaggregation for grain-size analysis. The relation of core locations to the major physiographic features of the study area is shown in Figure 1. Note the low percentages associated with the northwestern and the southeastern portions of the study area, and the high percentages associated with the upperslope mud lens near 12.5°S.

% CLAY (< 4 μm)
▽ < 40%
○ 40% - 60%
● > 60%

TABLE 1. TEXTURAL CHARACTERISTICS BY REGION

Area	Clay content (%)	Sand content (%)	Sand composition
Continental margin north of 10.5°S	<80	>8	T+B
Upper Slope 10.5°S to 13.6°S	>60	>8	T+B
Continental margin 10.5°S to 13.6°S	<60	>8	T+B
Continental margin south of 13.6°S	<40	>30	T
Peru Basin	>60	<3	T
Chile Basin	>60	<3	T
Galapagos Rise	<40	>30	B

T = terrigenous sands.
B = biogenous sands.
T+B = compositionally mixed sands.

Figure 3. Line drawings of reflection profiles of the Peruvian margin, illustrating the distribution of the sedimentary bodies shown in Figure 2.

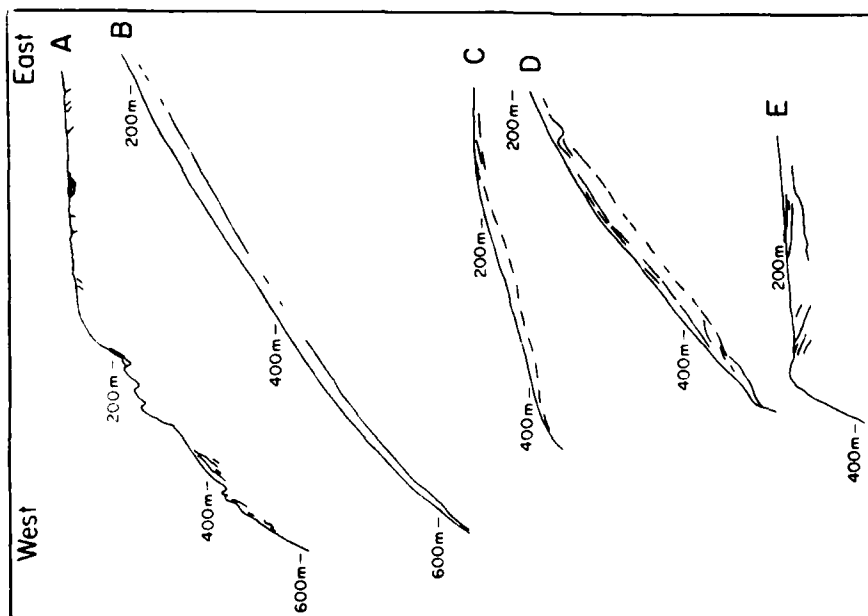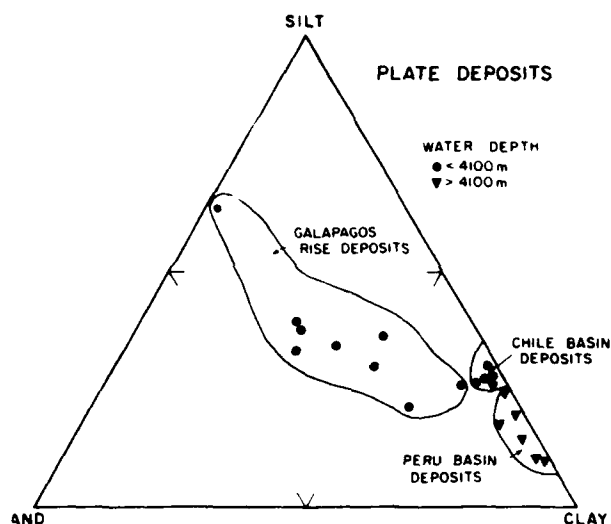**Figure 5.** Ternary plot of sand, silt, and clay for samples recovered from the Peru and Chile Basins and the Galapagos Rise. Samples from the Galapagos Rise typically have significant amounts of biogenous sands and silts, whereas deeper basin deposits consist almost entirely of terrigenous silts and clays. Note the finer grained nature (higher ratio of clay to silt) for the Peru Basin deposits than for the Chile Basin deposits.
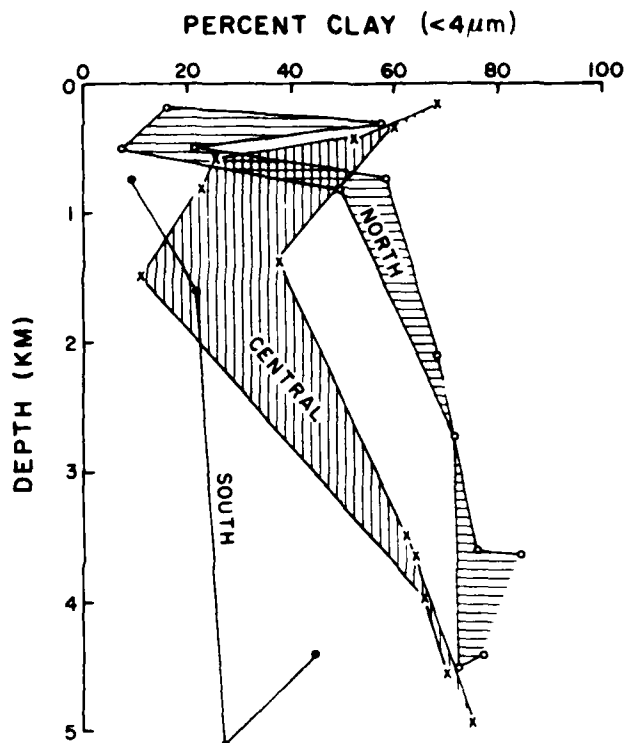
SLOPE - INNER PLATE TRANSECTS

Figure 6. Percentage of clay in surface sediments from transects across the continental slope at 3°S, 7°S, 11°S, 13°S, and 22°S. The lines connect adjoining samples. Note the north-to-south differences in the percentage of clay of the samples, the increasing clay content at greater depth, and the very fine grained upper-slope samples on the middle transect.
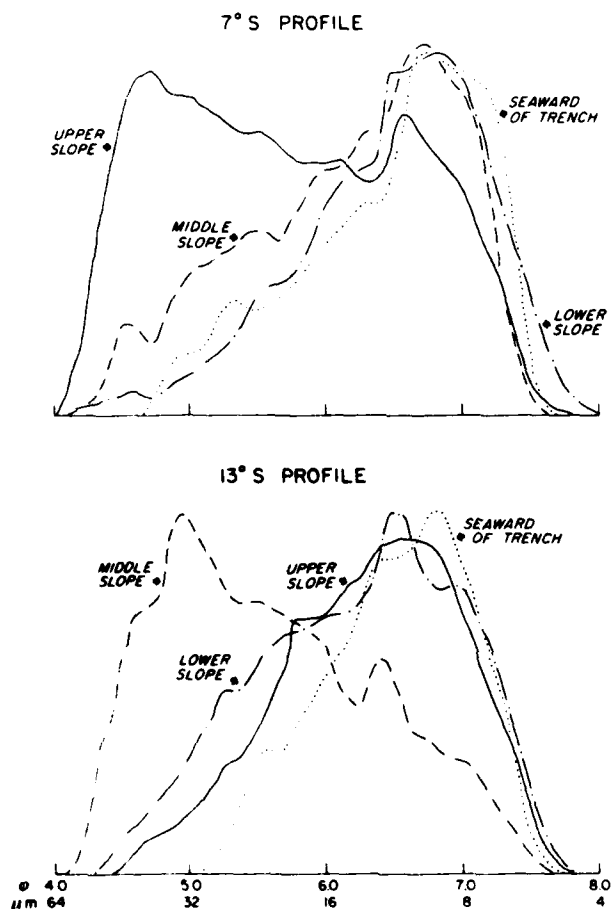
Figure 7. Representative frequency curves for the silt fractions of samples located on the 7°S and 13°S profiles. Note the normal pattern of sediment fining away from the continent in the 7°S profile, the anomalous fine-grained nature of the upper-slope sediment sample in the 13°S profile, and the similar position of the fine silt mode for all samples.

DISTANCE FROM SHORE (km)
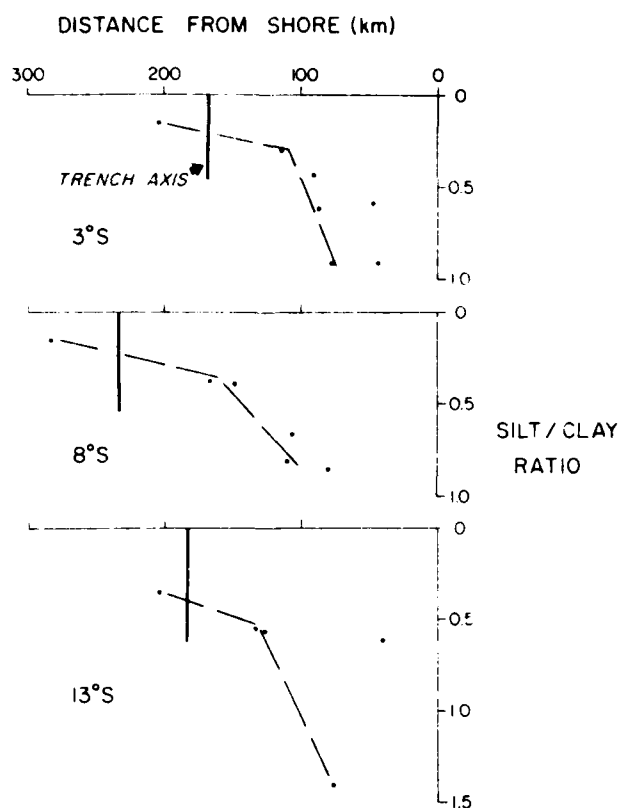
Figure 8. Silt/clay ratios for samples taken on transects at 3°S, 8°S, and 11°S. Only samples below the upper slope were used in drawing the lines shown. Note the change in the rate of fining for samples seaward of the trench axis.

SILT / CLAY
RATIO

deepest samples at 13°S suggest that local influences control the accumulation of anomalously fine grained material on the upper slope in this area. The implications of these observations are discussed further below.

Textural data from transects across the Peru-Chile Trench at 3°S, 7°S, and 13°S have been used to evaluate the role of the trench as a barrier to the seaward transport of terrigenous material. Figure 8 shows the plots of silt/clay ratio versus distance offshore for each profile, as well as the location of the trench axis. Carbonate-free splits of these samples gave similar results. The seaward-fining trend on the margin is illustrated by an approximate best-fit line to data points from below the upper slope on each profile. In each case, the margin fining trend, if extended farther offshore, predicts that the silt/clay ratio should reach zero landward of the trench axis. However, the samples taken seaward of the trench axis all have ratios greater than 0.12. A partial explanation for the anomalously high silt/clay ratios of the abyssal oceanic sediments may involve a greater proportion of coarse biogenous opaline debris. We have found that the opaline (especially radiolarian)

Figure 9. Results of an R-mode factor analysis of all chemical data on surface samples recovered from the study area. Factor score coefficients (F.S.C.) are noted for the chemical variables for each factor.

Figure 9. *(Continued).*

Figure 9. *(Continued).*

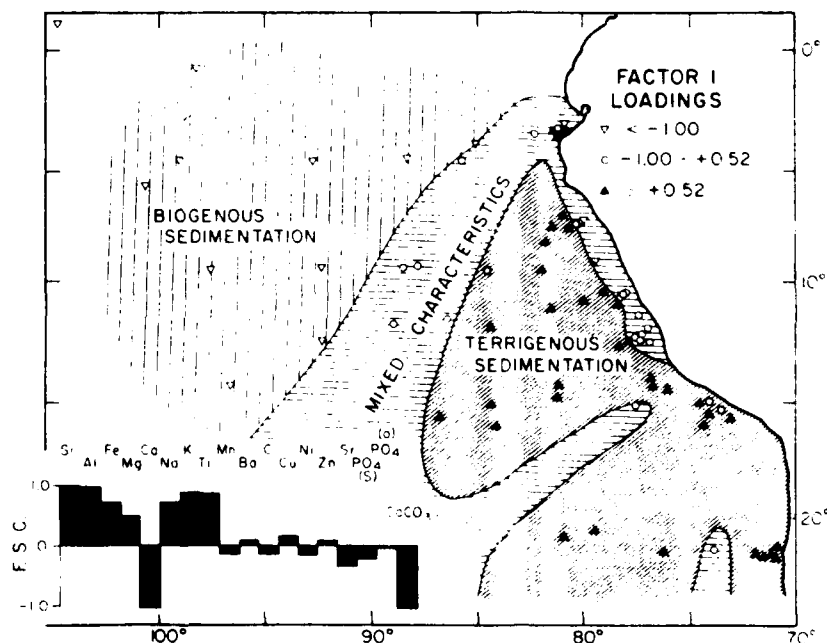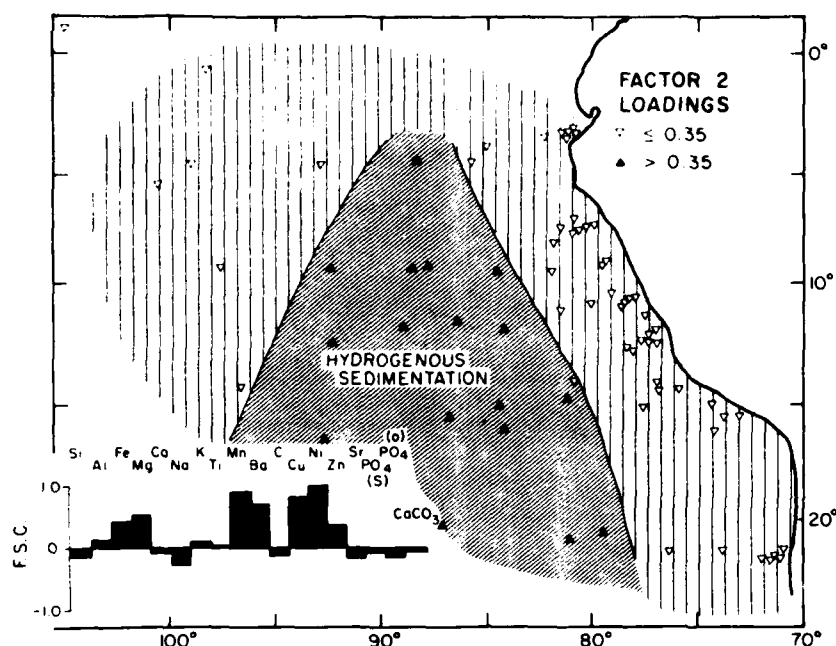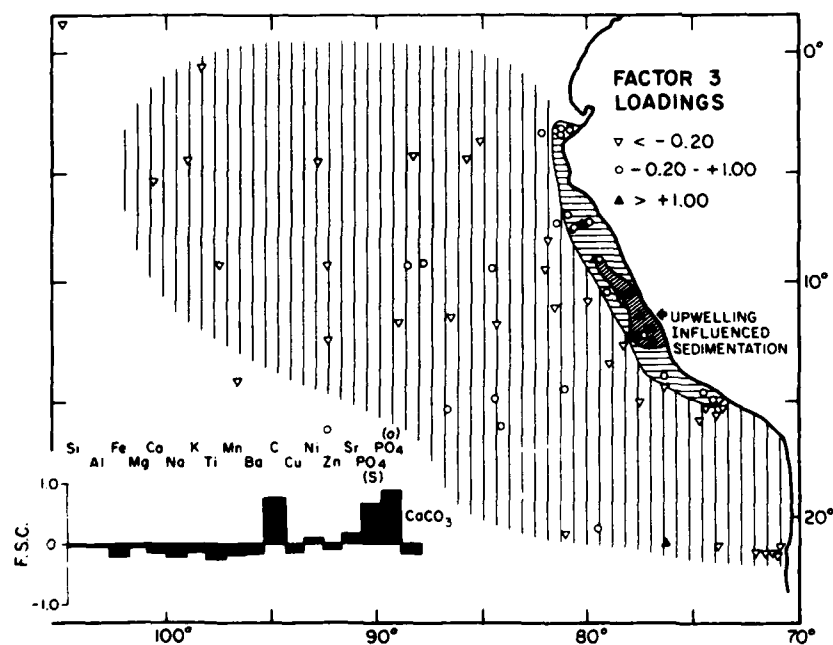content of the silt fraction almost doubles across the trench at 3°S and 7°S. However, at 11°S, the opaline components decrease by a factor of two across the trench, implying that terrigenous particles alone must cause the observed silt content increase. Such terrigenous silts may reach the abyssal plain by eolian transport, transport across the trench within the water column, or transport from the coarser southerly deposits by bottom water flowing north seaward of the trench (Lonsdale, 1976). Unfortunately, our data do not allow distinction between these three possibilities.

BULK SEDIMENT GEOCHEMISTRY

To distinguish and characterize sedimentation types within the study area, 18 chemical species were measured in the surface sediment samples. Complementary data from other areas on the Nazca plate are given in Dymond and Corliss (1980). The results were then subjected to R-mode factor analysis to examine relationships between samples on the basis of all variables. Three major factors accounted for 73.0% of the total date variance, while several minor factors accounted for 2% to 5% each. Figure 9 shows the areal distribution of computed loadings for the three major factors. Although the choice of loading values used to define provinces is arbitrary (not a product of the analysis itself, like a mean or standard deviation), the choice of slightly different values would not significantly alter the provinces defined or the conclusions reached here. To illustrate the actual compositional differences within factors, chemical data for samples with end-member loadings in each factor are given in Table 2.

Terrigenous and Biogenous Sedimentation

Loadings for factor 1, which accounted for 39.9% of the total data variance, are shown in Figure 9A. The factor score coefficients (F.S.C.) show high positive scores for the major elements Si, Al, Fe, Na, K, and Ti, and extremely negative scores for Ca, Sr, and CaCO₃. Accordingly, strong positive loadings in factor 1 indicate samples rich in Si, Al, Fe, Na, K, and Ti, and strong negative loadings indicate an abundance of Ca, Sr, and CaCO₃ (see Table 2). Si, Al, Fe, Na, K, and Ti form six of the nine most abundant oxides in continental crust (Mason, 1966), so that samples with high positive loadings delineate regions dominated by the deposition of land-derived ma-

terial. The major forms of Ca, Sr, and $CaCO_3$ in the marine realm are calcite and aragonite (Mason, 1966) produced by Foraminfera and Coccolithophores (Berger, 1974, and references therein), and so strongly negative loadings indicate a sediment (or an area containing sediments) dominated by biogenic constituents.

Figure 9A shows a strong correlation of the factor 1 loading patterns with the physiography of the study area. High positive loadings occur in the Peru Basin and from the coastline seaward south of about 15°S. Strong negative loadings are found along the broad crest of the Galapagos Rise, while intermediate values occur along the eastern flank of the Galapagos Rise, the continental margin north of about 15°S, the Nazca Ridge, and another topographic high in the southeastern corner of the region.

Hydrogenous Sedimentation

Factor 2 (Fig. 9B) has very strong positive factor score coefficients for the transition elements Mn, Cu, and Ni, as well as Ba. There are no negative score coefficients of equivalent magnitude. Manganese is one of the major elements found in ferromanganese deposits of several types — nodules, micronodules, and crusts. These deposits are enriched in transition metals to some extent, depending on their history of formation and diagenesis. They often contain Ba as an accessory element (Cronan, 1974). Thus, factor 2 characterizes the "hydrogenous" or metal-rich authigenic components of the sediments.

In Figure 9B, factor 2 loadings are highest in a wedge-shaped region, bounded approximately on the west by the Galapagos Rise and on the east somewhat seaward of the Peru-Chile Trench. The northern termination of this province is located in the vicinity of 3°S.

Upwelling-Influenced Sedimentation

Factor 3 is marked by high positive factor score coefficients (F.S.C.) for organic C, PO₄ (soluble), and PO₄ (organic) (Fig. 9C). As a result of the importance of organic compounds in Factor 3, its sample loadings may be taken as an inexact measure of the importance of biological productivity in the overlying water column.

The areal distribution of sample loadings in factor 3 is shown in Figure 9C. Both high positive and intermediate loadings cluster along the Peruvian coast between 3°S and about 16°S, with the high values concen-

trated in a narrow band between 11°S and 14°S. The seaward boundary of the intermediate zone closely follows the axis of the Peru-Chile Trench. The remainder of the study area shows strongly negative loadings for factor 3. This factor has been termed an "upwelling" influence, because a comparison with total primary productivity data (Zuta and Guillen, 1970) shows maxima concentrated landward of the Peru-Chile Trench between 3°S and 15°S. The association of such high productivity with upwelling has been recognized for some time (Smith, 1968), and recent observations indicate that measurable upwelling occurs here (Brink and others, 1978). The fine-grained upper-slope mud lens (see Figs. 2 and 4) is also associated with the zone of high factor 3 loadings, indicating that this depositional environment may be affected by biological activity in the overlying water column.

CONTROLS ON SEDIMENT TEXTURE AND GEOCHEMISTRY

The data presented above have allowed us to define the following factors which influence the textural and geochemical characteristics of hemipelagic and pelagic sediments:

Water Depth at the Site of Deposition

The water depth at a depositional site strongly influences the sediment texture and its terrigenous-biogenous component, as seen in Figures 1, 4, and 9A. Except for the anomalous upper-slope mud lens, margin sediments become finer away from shore (see Figs. 6 and 8; Rosato and others, 1975), because the competence of wave ac-

tion as a transport agent for coarse material decreases as the water depth increases (Komar and Miller, 1973). Finer material is transported by weaker water motions, maintained in suspension (McCave, 1972; Pierce, 1976), and carried farther seaward before deposition occurs. However, the rate of decrease in grain size across the margin is irregular, and it may even be reversed in some areas, such as the upper-slope mud lens (see Figs. 6 and 7; Zen, 1959). Terrigenous components, due to their adjacent source, dominate margin sediments in the absence of upwelling (Fig. 9A). In areas of coastal upwelling, the high input of both terrigenous and biogenous components produces sediments with mixed characteristics.

Seaward of the Peru-Chile Trench, the location of the CCD near 4,000 m (Kulm and others, 1974) maintains the control of water depth on sediment texture and geochemistry. Figures 5 and 9A reveal the association of topographic highs above 4,000 m, high sand contents, and biogenous sedimentation.

Continental Climate and Sediment Supply

The south-to-north fining of margin sediments appears to stem from variations in fluvially introduced material caused by changes in continental climate. The physiography of western Peru is dominated by a coastal plain (which narrows toward the south) and the Andes Mountains. Average rainfall in this region decreases from 14 mm/yr at 9°S to 2.2 mm/yr at 14°S (Johnson, 1976). Studies off Chile (Galli-Olivier, 1969; Scholl and others, 1970) and northwest Africa (Summerhayes and others, 1976) have found that the amount of sedi-

TABLE 2. END-MEMBER CHEMICAL

Sample	Factor	Loading	SiO₂	Al₂O₃	Fe₂O₃	MgO	CaO	Na₂O
W7706-21	1 (Terrigenous)	1.03	54.84	15.98	7.19	3.87	2.18	2.90
W7706-51	1 (Biogenous)	2.36	6.44	0.91	0.26	0.30	52.34	0.32
W7706-66	2 (Hydrogenous)	4.40	54.98	14.12	6.66	2.64	1.50	1.25
W7706-24	2 (Nonhydrogenous)	-.78	63.02	14.11	5.67	2.71	2.89	3.33
W7706-36	3 (Strong upwelling)	5.12	37.72	7.08	1.98	1.63	2.48	0.88
W7706-51	3 (Non upwelling)	-1.18	6.44	0.91	0.26	0.30	52.34	0.32

Note: SiO_2, Al_2O_3, Fe_2O_3, MgO, CaO, Na_2O, K_2O, TiO_2, MnO, C_{org}, and $CaCO_3$ contents are in weight percent. Ba, Cu, Ni, Sr, Zn, PO_4 (soluble), and P_{org} contents are in parts per million.

COMPOSITIONS FOR THE FACTORS SHOWN IN FIGURE 9

K_2O	TiO_2	MnO	Ba	C_{org}	Cu	Ni	Sr	Zn	$CaCO_3$	PO_4	P_{org}
2.87	0.70	1.16	1560	0.15	243	226	317	165	0.04	840	45
0.10	0.41	0.00	330	1.11	29	75	1000	43	86.75	6611	78
2.22	0.93	1.66	9830	0.72	531	592	401	27	0.27	1315	168
2.44	0.81	0.17	400	0.35	794	62	236	80	0.57	1233	109
1.05	2.37	0.03	460	21.16	93	199	191	120	2.01	2879	1120
0.10	0.41	0.00	330	1.11	29	75	1000	43	86.75	6611	78

ment derived from a landmass increases and its grain size decreases (Trask, 1961) as the continental climate becomes more humid. Therefore, the northern Peruvian coastal rivers should carry large amounts of fine material, with a decrease in quantity and an increase in grain size toward the south. In addition, Summerhayes and others (1976) demonstrated the importance of continental physiography in the bypassing of terrigenous detritus to the ocean. The relatively wide coastal plain in northern Peru should effectively trap coarse-grained fluvial sediments before they reach the Pacific Ocean; however, to the south, a greater relative abundance of coarse-grained material should successfully bypass the narrower coastal plain and enter the ocean. The resulting size heterogeneity of land-derived material would explain, at least in part, the south-to-north fining of sediments along the Peruvian margin (see Figs. 4 and 6).

Influence of Biological Processes on the Development of the Upper-Slope Mud Lens

The anomalously fine grained upper-slope mud lens is apparent in all of the margin textural data (see Figs. 4, 6, and 7). Examination of undisaggregated samples with a light microscope, however, showed that small (<200 μm) fecal pellets are abundant in these sediments (W. H. Hutson, 1978, personal commun.). As this deposit occurs beneath the zone of most intense upwelling and biological production, it appears that grazing zooplankton filter fine-grained terrigenous particles out of the water and incorporate them into fecal pellets. These large aggregates settle rapidly to the bottom (Schrader, 1970; Honjo, 1976).

Furthermore, in this area, a shallow oxygen-minimum zone impinges on the upper continental slope (Packard and others, 1978) and would be expected to inhibit the destruction of the organic material encasing the pellets. The high organic carbon content (>20%; see Table 2 and Figure 9C) supports this hypothesis. Thus, the anomalously fine texture of these sediments is, at least in part, a result of our sample treatment. In their natural state, the aggregates in the lens are not anomalous in terms of grain size, and their composition as fecal pellets reflects the local upwelling conditions.

Transport of Material in Suspension

Textural control by bottom-water flow is inferred from unpublished nephelometer data (H. Pak, 1977) obtained during the WELOC-7706 cruise. It shows a well-developed (200-m-thick) bottom nepheloid layer in the clay-rich province of "terrige-

nous sedimentation" in the Peru Basin (see Figs. 4 and 9A). In the Chile Basin, however, where the bottom sediments are relatively coarser (see Figs. 4 and 5) but contain fewer coarse biogenic tests, the bottom nepheloid layer is poorly developed or absent. This suggests that the bottom nepheloid layer is an important mechanism for the transport of clay-sized material away from or along the continental margin (Ewing and others, 1971; Eittreim and Ewing, 1972), or for its redistribution once it has settled near the bottom.

Eolian Transport

Sediment texture can be controlled by the input of continentally derived eolian material. Prospero and Bonatti (1969) collected dust samples in the area 8°N to 17°S and 80°W to 110°W, and found that all samples had maximum mass in the 2 to 5 μm (medium clay to very fine silt) size range. Particles with diameters in the range 20 to 40 μm were common in samples taken within a few hundred kilometres of land. X-ray diffraction profiles of samples taken on the Galapagos Rise above the level of the bottom nepheloid layer are identical to those given by Prospero and Bonatti (1969) for eolian dusts from that region (Scheidegger and Krissek, 1978). This suggests that fine-grained eolian material is the dominant terrigenous component in the sediments to the west of provinces strongly influenced by fluvial input.

Associations of Sediment Texture, Geochemistry, and Sedimentation Rates

A comparison of the textural and geochemical data (Figs. 4 and 9) shows strong spatial correlations between these

TABLE 3. SEDIMENTATION RATES BY PHYSIOGRAPHIC PROVINCE

Province	Average sedimentation (cm/10^3yr)	Number of determinations	Range (cm/10^3yr)	References
Margin north of 15°S	32	4	17-66	DeMaster, 1979
Margin south of 15°S	5.5	4	<5-6	E. Suess, 1979, personal commun.
Peru Basin	0.23	1	..	McMurtry and Burnett, 1975
Nazca Ridge	0.71	3	.61-.84	Molina-Cruz, 1978; Blackman and Somayajulu, 1966
Galapagos Rise	1.67	1	..	CLIMAP, A. Molina-Cruz and T. C. Moore, 1975, personal commun.
Northern plate	3.6	8	2.6-5.5	Ninkovich and Shackleton, 1975; Molina-Cruz, 1978

parameters. The association of the upper-slope mud lens (Fig. 4) with the highest loadings in the geochemical "upwelling factor" (Fig. 9C) is a prime example. Sedimentation rates show a similar spatial correlation. Published rates from the study area have been grouped by physiographic province, and average province values are listed in Table 3. As expected from the rapid input of terrigenous and biogenous detritus, aided by organically produced aggregates, sedimentation rates in the mud lens are the highest in the study area.

The pelagic province of low sand and high clay contents (see Fig. 4) and hydrogenous sediment characteristics (Fig. 9B) have very low sedimentation rates, on the order of 0.5 cm/1,000 yr or less. Such a correlation has been widely noted previously throughout the world ocean (Cronan, 1974).

The association of coarse-grained sediments (Fig. 4) and biogenous sedimentation (Fig. 9A) on topographic highs reflects the effect of deposition above the CCD. This biogenic input increases sedimentation rates in the Galapagos Rise, Nazca Ridge, and northern plate provinces above those found in the Peru Basin.

CONCLUSIONS

Analysis of 3.5-kHz seismic records and of the textural and geochemical characteristics of 86 surface sediment samples from the Peruvian continental margin and the adjacent abyssal ocean floor lead to the following conclusions:

1. Three discrete sediment accumulations exist on the upper continental margin. One, in upper-slope mud lens, has a distinctive geometry.

2. The large-scale textural patterns of sediments in the study area are influenced by water depth, proximity to the continental sediment source, latitudinal changes in terrigenous input, the presence and strength of bottom currents and nepheloid layers, the formation of fecal pellets in highly productive upwelling zones, and eolian addition of fine-grained sediment components.

3. On the continental margin, except in the vicinity of the upper-slope mud lens between 10.5°S and 13.6°S, sediments tend to fine downslope.

4. The Peru-Chile Trench may not act as a physical barrier to the seaward transport of suspended terrigenous silt-sized material south of 7°S, but further study is needed to fully define the textural control exerted by the trench.

5. Margin samples from the upper continental slope < 1,000 m show no coherent pattern of along-margin textural change. However, samples from the middle and lower slope both landward and seaward of the Peru-Chile Trench do show a consistent pattern of south-to-north textural fining. Such along margin changes reflect a south to north fining of the terrigenous constituents added by coastal rivers due to changing continental climates, but they may also indicate south-to-north variations in the current regime along the lower slope.

6. The rapidly accumulating upper slope mud lens, present on the continental margin between 10.5°S and 13.6°S, is related to the high biological activity caused by intense coastal upwelling in that region.

7. R-mode factor analysis of measurements made on 18 chemical species in each sample allows the geochemical definition of sediment provinces. Terrigenous sedimentation is found along the continental margin south of about 14°S and in the Peru and Chile Basins seaward of the Peru-Chile Trench. Biogenous sedimentation is dominant above the CCD on the crest of the Galapagos Rise and other topographic highs. Hydrogenous, or authigenic, sedimentation is found well seaward of the Peru-Chile Trench, but landward of the crest of the Galapagos Rise, in an area below the CCD. Upwelling-influenced sedimentation is located along the continental margin north of about 14°S.

ACKNOWLEDGMENTS

This study has benefitted considerably from informal discussion with colleagues actively involved in the study of other aspects of sedimentation on the Peru-Chile continental margin and the Nazca plate. In this regard, we would like to thank William H. Hutson, George H. Keller, Hans J. Schrader, and Erwin Suess. Suess also read an earlier draft of this manuscript and made helpful suggestions. We would like to acknowledge the valued assistance we received from Mark L. Hower (chemical analyses), Kurt N. Kluttke (textural analyses), Patricia A. Price (analyses for C and CaCO₃), and Carl A. Ungerer (phosphate analyses). Stephen J. Eittreim and Gordon R. Hess made constructive and beneficial reviews of the manuscript.

REFERENCES CITED

Ade-Hall, J. J., 1976, Underway surveys, leg 34, in Yeats, R. S., Hart, S. R., and others, Initial reports of the Deep Sea Drilling Project, Volume 34: Washington, D.C., U.S. Government Printing Office, p. 163–181.

Berger, W. H., 1974, Deep-sea sedimentation, in Burk, C. A., and Drake, C. L., eds., The geology of continental margins: New York, Springer-Verlag, p. 213–241.

Blackman, A., and Somayajulu, B.L.K., 1966, Pacific Pleistocene cores: Faunal analyses and geochronology: Science, v. 154, p. 886–889.

Brink, K. H., Halpern, D., and Smith, R. L., 1978, Circulation in the Peruvian coastal upwelling system near 15°S (abs.): EOS American Geophysical Union Transactions, v. 59, p. 1103.

Cronan, D. S., 1974, Authigenic minerals in deep-sea sediments, in Goldberg, E. D., ed., The sea, Volume 5: New York, John Wiley & Sons, p. 491–525.

DeMaster, D., 1979, The marine budgets of silica and ³²Si [Ph.D. thesis]: New Haven, Connecticut, Yale University, 308 p.

Dymond, J., and Corliss, J. B., 1980, Part II. Chemical composition of Nazca plate surface sediments: Geological Society of America Map and Chart Series MC-34, in press.

Eittreim, S. L., and Ewing, M., 1972, Suspended particulate matter in the deep waters of the North America Basin, in Gordon, A. L., ed., Studies in physical oceanography, Volume 2: New York, Gordon & Breach, p. 123–167.

Ewing, M., and others, 1971, Sediment transport and distribution in the Argentine Basin. Part 2. Nepheloid layer and processes of sedimentation, in Ahrens, L. H., ed., Physics and chemistry of the earth, Volume 8: New York, Pergamon Press, p. 49–78.

Gath, Olivier, G., 1969, Climate: A primary control of sedimentation in the Peru-Chile Trench: Geological Society of America Bulletin, v. 80, p. 1849–1882.

Honjo, S., 1976, Coccoliths: Production, transportation, and sedimentation: Marine Micropaleontology, v. 1, p. 65–79.

Johnson, A. M., 1976, The climate of Peru, Bolivia, and Ecuador, in Schwerdtfeger, W., ed., World survey of climatology: Climates of Central and South America, Volume 12: New York, Elsevier Scientific, p. 147–218.

Komar, P. D., and Miller, M. C., 1973, The threshold of sediment movement under oscillatory water waves: Journal of Sedimentary Petrology, v. 43, p. 1101–1110.

Kulm, L. D., and others, 1974, Transfer of Nazca Ridge pelagic sediments to the Peru continental margin: Geological Society of

America Bulletin, v. 85, p. 769–780.

Lonsdale, P., 1976, Abyssal circulation of the southeastern Pacific and some geological implications: Journal of Geophysical Research, v. 81, p. 1163–1176.

Mammerickx, J., and Smith, S. M., 1978, Bathymetry of the southeast Pacific: Geological Society of America Map and Chart Series MC-26, scale 1:6,442,194 at equator.

Mason, B., 1966, Principles of geochemistry: New York, John Wiley & Sons, 329 p.

McCave, I. N., 1972, Transport and escape of fine-grained sediment from shelf areas, in Swift, D.J.P., Duane, D. B., and Pilkey, O. H., eds., Shelf sediment transport: Stroudsburg, Pennsylvania, Dowden, Hutchinson & Ross, p. 225–248.

McMurtry, G. M., and Burnett, W. C., 1975, Hydrothermal metallogenesis in the Bauer Deep of the southeastern Pacific: Nature, v. 254, p. 42–44.

Molina-Cruz, A., 1978, Late Quaternary oceanic circulation along the Pacific coast of South America [Ph.D. thesis]: Corvallis, Oregon, Oregon State University, 246 p.

Ninkovich, D., and Shackleton, N. J., 1975, Distribution, stratigraphic position and age of ash layer "L," in the Panama Basin region: Earth and Planetary Science Letters, v. 27, p. 20–34.

Packard, T. T., and others, 1978, Nitrate reductase activity in the subsurface waters of the Peru Current: Journal of Marine Research, v. 36, p. 59–76.

Pierce, J. W., 1976, Suspended sediment transport at the shelf break and over the outer margin, in Stanley, D. J., and Swift, D.J.P., eds., Marine sediment transport and environmental management: New York, Wiley-Interscience, p. 437–458.

Prince, R. A., and Kulm, L. D., 1975, Crustal rupture and the initiation of imbricate thrusting in the Peru Trench: Geological Society of America Bulletin, v. 86, p. 1639–1653.

Prospero, J. M., and Bonatti, E., 1969, Continental dust in the atmosphere of the eastern equatorial Pacific: Journal of Geophysical Research, v. 74, p. 3362–3371.

Rosato, V. J., Kulm, L. D., and Derks, P. S., 1975, Surface sediments of the Nazca plate: Pacific Science, v. 29, p. 117–130.

Scheidegger, K. F., and Krissek, L. A., 1978, Distinguishing between fluvial and eolian sediment sources off Peru and Chile [abs.]: EOS (American Geophysical Union Transactions), v. 59, p. 1114.

Scholl, D. W., and others, 1970, Peru-Chile Trench sediments and sea-floor spreading: Geological Society of America Bulletin, v. 81, p. 1339–1360.

Schrader, H. J., 1970, Fecal pellets: Role in sedimentation of pelagic diatom: Science, v. 174, p. 55–57.

Schweller, W. J., and Kulm, L. D., 1978, Depositional patterns and channelized sedimentation in active Eastern Pacific trenches, in Stanley, D. J., and Kelling, G., eds., Sedimentation in submarine canyons, fans, and trenches: Stroudsburg, Pennsylvania, Dowden, Hutchinson & Ross, p. 311–324.

Smith, R. L., 1968, Upwelling: Oceanographic Marine Biology Annual Review, v. 6, p. 11–46.

Summerhayes, C. P., and others, 1976, Northwest African shelf sediments: Influence of climate and sedimentary processes: Journal of Geology, v. 84, p. 277–300.

Thiede, J., and others, 1976, Settling tubes for size analysis of fine and coarse fractions of oceanic sediments: Corvallis, Oregon, School of Oceanography, Oregon State University, Ref. 76-8, 87 p.

Trask, P. D., 1961, Sedimentation in a modern geosyncline off the arid coast of Peru and northern Chile, in Sorgenfrei, T., ed., Report of the 21st session: International Geological Congress (Part 23 of Proceedings of the International Association of Sedimentology, Copenhagen), p. 103–118.

Yeats, R. S., Hart, S. R, and others, 1976, Initial reports of the Deep Sea Drilling Project, Volume 34: Washington, D. C., U.S. Government Printing Office, v. 34, p. 81–153.

Zen, E-An, 1959, Mineralogy and petrography of marine bottom sediment samples off the coast of Peru and Chile: Journal of Sedimentary Petrology, v. 29, p. 513–539.

Zuta, S., and Guillen, O., 1970, Oceanografía de las auguas costeras del Peru [Oceanography of the coastal waters of Peru]: Instituto del Mar del Peru Boletín, v. 2, p. 161–323.

On the intermediate particle maxima associated with
oxygen-poor water off western South America

HASONG PAK*, L. A. CODISPOTI† and J. RONALD V. ZANEVELD*

Abstract The distribution of suspended particulate matter was measured during 21 May and 18 June 1977 between 4 and 23 S from the coast of South America to about 500 nautical miles offshore. A well-defined maximum was observed over the continental margins at depths of about 200 m between ~9 and 23 S. At 4 S, the main particle maximum was at approximately 400 m, but in the nearshore zone the maximum extended upwards to ~200 m. A comparison of the particle and chemical data shows that the particle maxima are usually at approximately the core depth of the oxygen minimum layer. A nitrite maximum and a nitrate minimum were also observed at or near the particle maximum core depth south of ~9 S. Near 4 S, a weak nitrite maximum was observed within the oxygen minimum layer at some stations. The protein distribution near 15 S suggests that the material in the particle maximum contains significant amounts of organic matter.

The distribution of the particle maximum layer between 9 and 23 S and its relations to the density field and the cross-shelf flow suggest that most of the particles could originate in the bottom waters over the outer continental shelf and be transported offshore in a quasi-horizontal path.

Offshore particle transport near the equator is probably supported by a westward current off northern Peru between and under the eastward extension of the Equatorial Undercurrent and the Subsurface South Equatorial Countercurrent. However, the source of the particles in this ~400-m maximum has not been determined.

INTRODUCTION

THE HIGH primary production rates supported by coastal upwelling lead to high subsurface respiration rates in the coastal zone off the west coast of South America (CODISPOTI and PACKARD, 1980), and some of the inflowing subsurface waters are deficient (~ 0.5 ml l^{-1}) in oxygen (BARBER and HUYER, 1979). Consequently, it is not surprising that large bodies of oxygen-poor (< 0.25 ml l^{-1}) waters are found in the region and that within the volumes, there are oxygen-deficient ($O_2 < \sim 0.1$ ml l^{-1}) zones where nitrate reduction and denitrification produce secondary nitrite maxima and nitrate minima (WOOSTER, CHOW and BARRETT, 1965; CODISPOTI and PACKARD, 1980). Despite this knowledge, the exact mechanisms that contribute to the formation and variability of the oxygen-poor regimes are not yet well understood.

The suspended particulate matter in the open ocean is often distributed with maxima in the surface layer and bottom water with clear water in between, but over continental margins, one or more intermediate maxima are frequently encountered. High

---

* School of Oceanography, Oregon State University, Corvallis, OR 97331, U.S.A.
† Bigelow Laboratory for Ocean Sciences, West Boothbay Harbor, ME 04575, U.S.A.

concentrations are usually found throughout the euphotic zone, but a more intense maximum is often observed within the surface layer; it is usually accompanied by high concentrations of chlorophyll and oxygen. The maximum in bottom waters (bottom nepheloid layer) is related to boundary effects because particles may be either resuspended from bottom sediments or maintained in suspension by bottom stresses. On the continental shelf off Oregon, bottom nepheloid layers were highly correlated with bottom mixed layers (PAK and ZANEVELD, 1977).

In the surface layer the particles are organic matter photosynthetically produced in the euphotic zone and terrigenous particles brought into the water by streams and winds. Some of the particles introduced into the surface layer are later found in bottom sediments and in the bottom nepheloid layers. The transfer of the particles from the surface layer to the bottom is not well understood. Mainly because particles in suspension and in sediments are small (0.5 to 40 μm diameter), the settling of single particles is not rapid enough to account for the observed distributions of particle properties in the sediments. Thus, increased settling rates by means of particle aggregation have been proposed by REX and GOLDBERG (1958) and McCAVE (1975), among others, to account for the similarity in species at the surface and in the sediments.

In this paper we describe two intermediate particle maxima that we observed off Peru. and we propose a process for the formation of the ∼ 200-m maximum that we observed between 9 and 23°S. The mechanism is based on spm (suspended particulate matter). oxygen, nitrite, nitrate, protein and hydrographic observations and it suggests that the 'rain' of organic matter from the surface waters is less important than the subsurface horizontal offshore transport of spm from the bottom nepheloid layers over the shelf and upper slope. Our study of the particles and chemical parameters also sheds additional light on the circulation features that influence the horizontal and vertical distributions of the oxygen minima and nitrite maxima.

METHODS

In situ optical instruments measuring either light scattering or beam transmission are the most common devices used for obtaining continuous vertical distributions of suspended particulate matter in the ocean. PETERSON (1977) studied the linear correlation between the beam attenuation coefficient and suspended particulate mass concentrations for waters on the continental shelf off Oregon and obtained a correlation coefficient of 0.91. We used a beam transmissometer during 21 May and 18 June 1977 on R.V. *Wecoma* to measure the vertical distribution of suspended particulate matter off Peru between 4 and 23°S (Fig. 1). The transmissometer was developed by the Optical Oceanography Group at Oregon State University; it uses a light emitting diode with a wavelength of 660 nm as a light source. A porro prism produces a 1-m folded light path. With proper calibration and careful operation the instrument provides data with an error of less than 0.5% transmission. A similar instrument with a 25-cm path length was described in BARTZ, ZANEVELD and PAK (1978). In this paper, our references to the concentration of suspended particulate matter are based solely on light transmissometer data.

The chemical samples we will refer to were collected from the R.V. *Melville* between 4 and 25 May 1977. Nitrate, nitrite, and dissolved oxygen concentrations were determined using the techniques described by HAFFERTY, CODISPOTI and HUYER (1978). A suite of sections from the *Melville* cruise has been published by HAFFERTY, LOWMAN and CODISPOTI (1979).
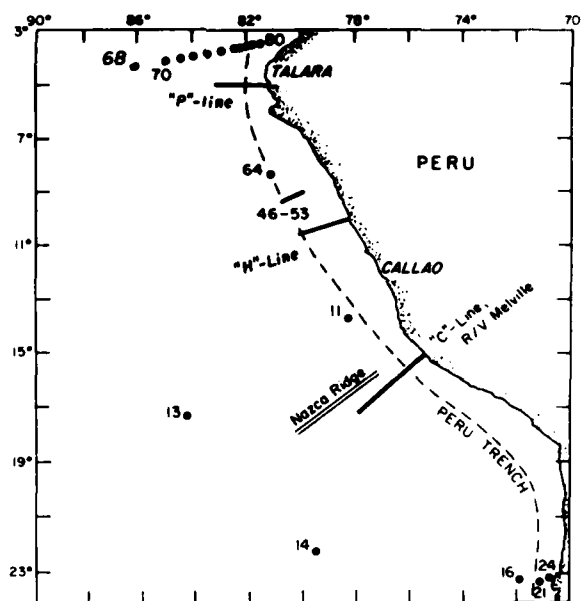
Fig. 1.   Location of the *Weloc* 77 stations where optical measurements were made.

RESULTS

A well-defined particle maximum layer (light transmission minimum) was observed at depths of approximately 200 m at 9 and 23 S. In the section at 9 S (Fig. 2), the particle maximum layer thickness (as defined by the 63% isopleths) decreased in the offshore direction from 175 m on the outer shelf at Sta. 47 to less than 100 m over the offshore side of the coastal trench at Sta. 49. The layer was absent at Stas 13 and 14 in the Peru Basin about 1000 km from the Peruvian Coast (Fig. 1), but it was present in the inshore region near 23 S (Fig. 7). North of Stas 13 and 14 the maximum may extend far offshore because the nitrite maximum with which it is associated (see below) extends out to 90 W near 15 S (WOOSTER *et al.*, 1965).

Along the section near 4 S, the particle maximum layer extended from a depth of approximately 200 m to 500 m near the coast, but it was best developed at approximately 400 m (Fig. 3). The 400-m maximum extended 600 km from the coast to our westernmost station. South of the well-developed 400-m maximum, a weak maximum was found at depths ranging from 350 to 500 m, except at Sta. 34 where it was intense (Fig. 7). Light transmission profiles at Stas 13 and 14 (not shown in this paper), about 1000 km offshore, also showed a weak maximum at about 400 m. Thus, the maximum at about 400 m was present at all of the transmissometer stations, extending to about 1000 km offshore, but its maximum intensity was near the equator.

During the JOINT-II experiment, chemical and biological observations were made in the coastal upwelling area off Peru during R.V. *Melville* Leg IV (4 and 25 May 1977). The measurements were concentrated along sections near 5 S ('P' line), 10 S ('H' line) and 15 S
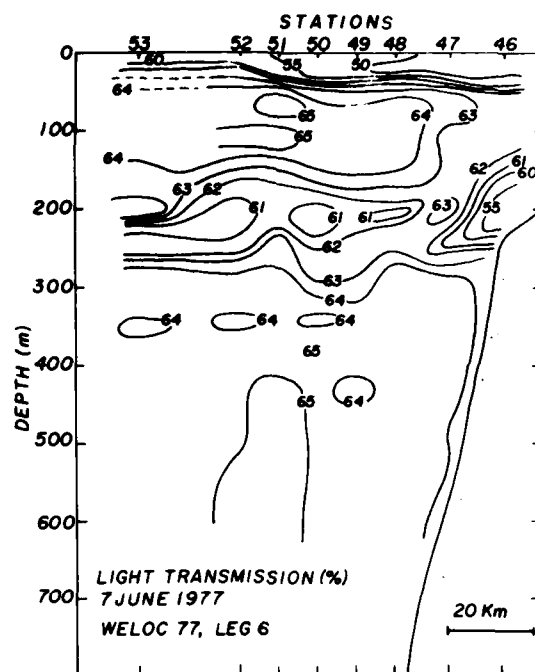
Fig. 2. Distribution of light transmission in a section at approximately 9 S. The section extends from the outer shelf to the axis of the Peru Trench.
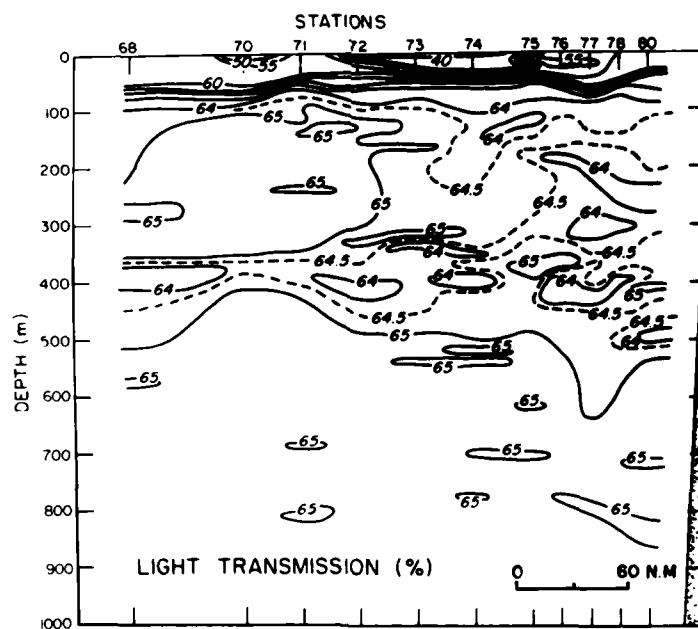

Fig. 3. Distribution of light transmission in a section at approximately 4 S.

('C' line) (Fig. 1). Representative oxygen, nitrate, and nitrite distributions (Figs 4 to 6) show a relation between the 'cores' of the oxygen-poor zones and the suspended particulate matter maxima. As oxygen-poor (<0.2 ml 1^{-1}) water extends more than 2000 km along the west coast of South America and as the layer is 200 to 400 m thick, we can assume that the 'core depths' of the oxygen-poor zones do not change drastically in a month. Measurements along the 'C' line were repeated many times before and during R.V. *Melville* Leg IV, and the results indicate that the assumption is reasonable (HAFFERTY *et al.*, 1979).

The oxygen minimum layer was well defined in all three sections (Figs 4 to 6). During R.V. *Melville* Leg IV, meridional changes in oxygen distribution occurred mainly in the upper 200 m: the concentration of dissolved oxygen in the upper water increase toward the north (Fig. 4). There was an intermediate oxygen maximum at about 150 m on the 'P' line (near 5 S) while the oxygen-poor water was sometimes less than 50 m from the sea surface on the 'C' line.

There was a well-defined nitrite maximum and nitrate minimum approximately at the core depth of the oxygen depleted water on the 'C' line (Fig. 6). Here, the oxygen-depleted water was more than 300 m thick, and its core was not precisely defined. The nitrite maximum and nitrate minimum water on the 'C' line were at about the same depth as the particle maximum (Fig. 7). From the above associations, a significant relation between the distributions of the chemical variables and the particle maximum is expected. Unfortunately, we have both chemical and optical data only near the 'P' and the 'H' lines, not at the 'C' line. However, Dr. Kullenberg of the University of Copenhagen made light
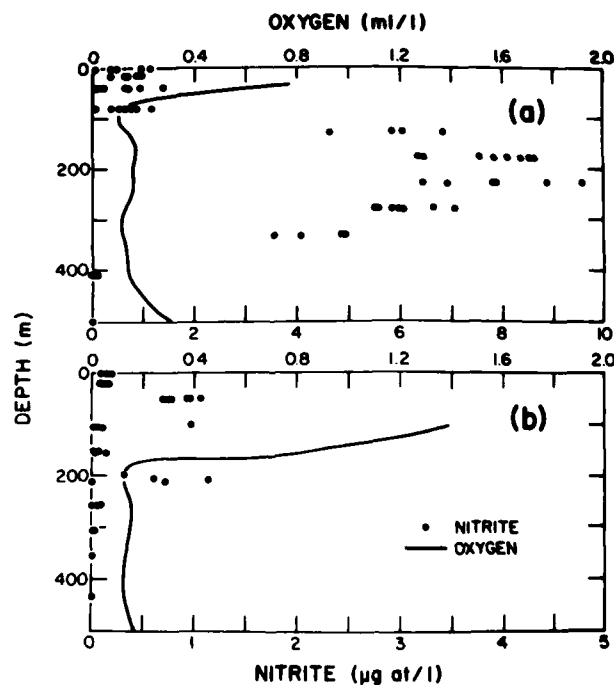
Fig. 4. Oxygen and nitrite in the (a) 'C' line (Fig. 6, near 15 S) and (b) 'H' line (near 10 S). The oxygen profiles are determined by the envelope of all the data in the section.
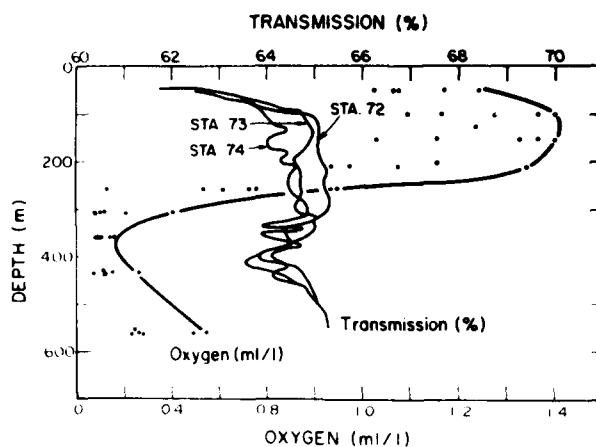
Fig. 5.   A profile of oxygen determined by the envelope of the data from all of the stations in the 'P' line (near 4 S) and light transmission profiles from three stations in the section near 4 S. A few oxygen concentration values larger than 1.4 ml l⁻¹ near 200 m are not included in the figure because the intermediate oxygen maximum is defined without them.

(Fig. 6(a)
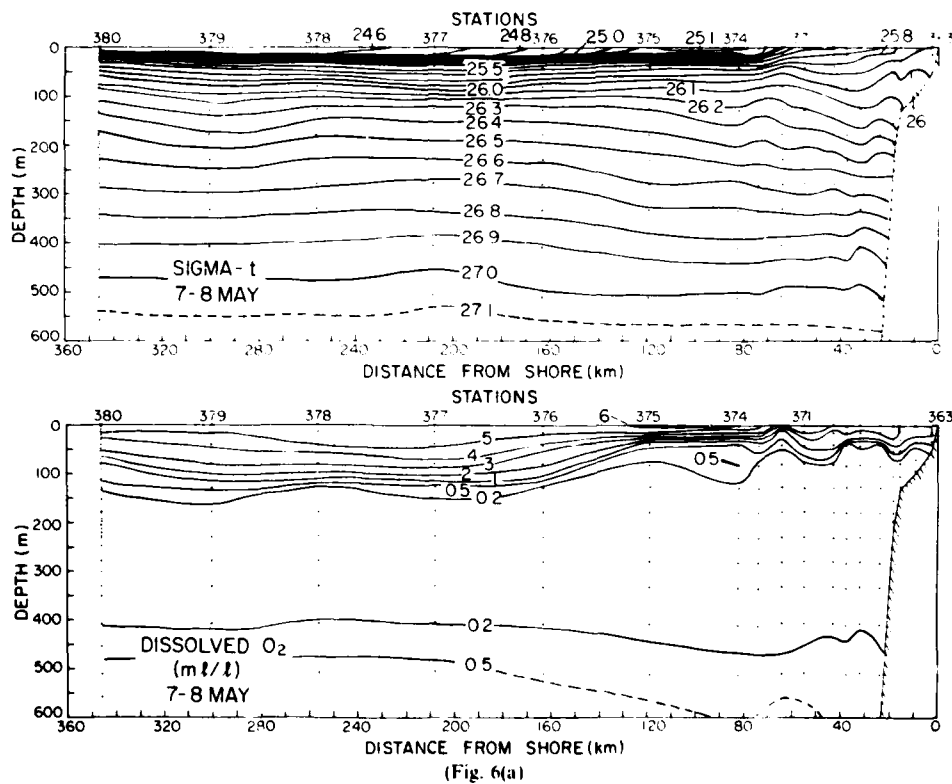
Fig. 6.   Distribution of (a) sigma-t and dissolved oxygen and (b) nitrite and nitrate in the 'C' line.

scattering observations on the 'C' line during R.V. *Melville* Leg IV (Fig. 8) and kindly provided us with his light scattering data. They are particularly valuable because the nitrite maximum is best defined at the 'C' line, where we were unable to make light transmission measurements. Vertical profiles of light scattering around 20°S from the direction of the forward light beam in the red, β_{20}-red, shows a well-defined particle maximum at 200 to 250 m with a layer thickness of about 200 m (Fig. 8). The presence of a particle maximum at the cores of low oxygen, nitrite maximum, and nitrate minimum water on the 'C' line is thus verified.

A comparison between the 'C' line near 15°S and the 'H' line near 10 S reveals significant meridional variations in the chemical distributions while little meridional variation in the particle maximum occurs. The nitrite maximum and nitrate minimum, well-defined at the 'C' line near 200 m, tended to dissipate toward the north. The maximum intensity of the nitrite maximum at the 'H' line, for example, was less than 20% of that at the 'C' line (Fig. 4), and it was not discernible at the 'P' line (no figure is presented). On the 'P' line there was a weak offshore nitrite maximum (CODISPOTI and PACKARD, 1980), which was more or less coincident with the well-developed 400-m particle maximum (Fig. 3). South of the 'P' line no significant vertical structure of nitrite and nitrate was found to correspond to the weak particle maximum near 400 m.

Fig. 6 (b)

Fig. 7.   Profiles of light transmission observed at 23 S latitude and at Stas 11 and 34. The station locations are shown in Fig. 1. The light transmission profile from Sta. 50 is added for comparison.

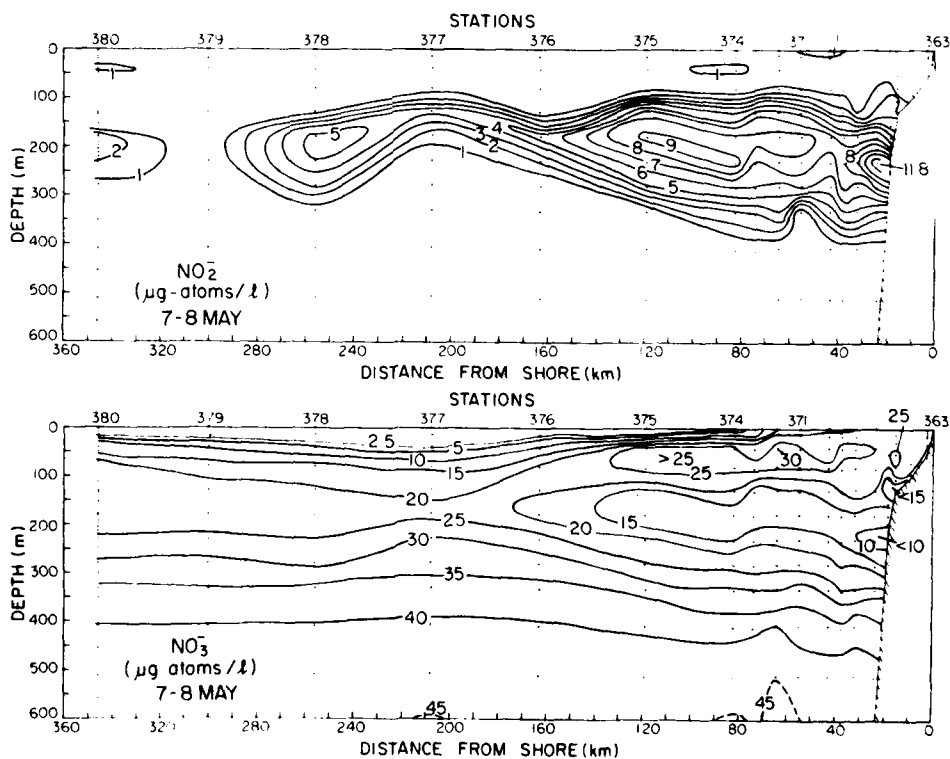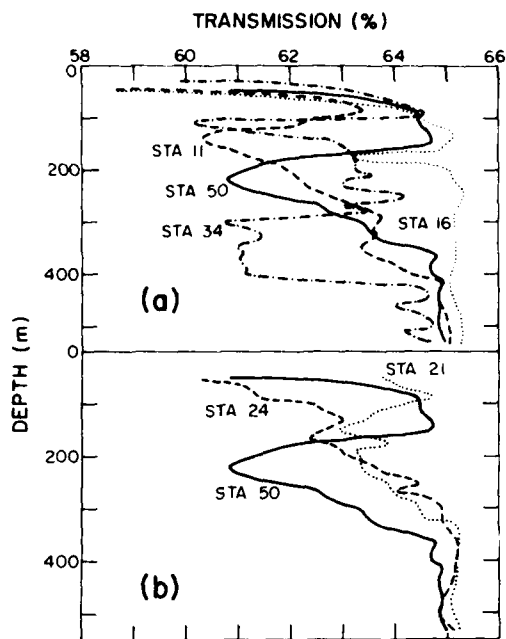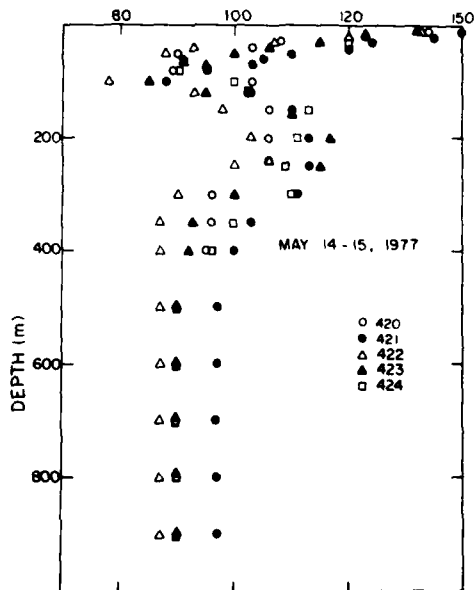Fig. 8.   Profiles of $\beta(20)$-red measured at the 'C' line during R.V. Melville Leg IV (provided by Dr. G. Kullenberg).

While the meridional variations in chemical variables can be at least roughly determined from changes among the three sections, a similar discussion of the suspended particle distribution is not possible because a quantitative comparison between β_{20}-red on the 'C' line and light transmission on the 'H' and 'P' lines is not possible. Nevertheless, we looked for meridional variations in the ~ 200-m particle maximum among a few stations scattered over the wide area shown in Fig. 1. The particle maximum was present at every station between ~ 9 and 23 S over the continental margin at depths varying from 140 to 220 m (Fig. 7). Kullenberg's data (Fig. 8) also show the particle maximum on the 'C' line. Thus, we are inclined to believe that the particle maximum has a greater longshore extent than the secondary nitrite maximum. However, the particle maximum is weak near the Peru Chile border (Stas 16, 21, and 24).

<center>DISCUSSION</center>

The intermediate particle maximum in relation to biological processes

An indirect indication that the 200-m particle maximum contains relatively large amounts of organic matter is found in the distribution of protein, observed during the *Melville* Leg IV 77 cruise: a protein maximum was observed to coincide with the nitrite (GARFIELD, PACKARD and CODISPOTI, 1979) and particle maxima. The few available data suggest that there may also be a respiration rate maximum associated with the maxima (T. T. PACKARD, personal communication), and if such a feature does exist it would help to confirm our suggestion that there is a significant organic component in the maximum.

The association of both the 200- and 400-m particle maxima with oxygen-deficient waters where much of the breakdown of organic matter might be expected to occur through the activities of bacteria raises an interesting question. Does the reduced zooplankton activity one would expect in the oxygen-deficient zones contribute to the maintenance of the particle maxima by preventing the 'repackaging' of small particles into rapidly sinking fecal pellets?

Particle transport

South of about 9 S the suspended particulate matter and nitrite maxima have tongue-shaped patterns with their bases over the outer shelf and upper slope (Figs 2 and 6b). The nitrate minimum shows a similar pattern (Fig. 6b). The oxygen minimum layer shows little or no tendency to be tongue-shaped, but this should be expected, because oxygen concentrations are zero or nearly zero over a relatively thick layer in which further respiration must be manifested in nitrate and nitrite changes rather than changes in oxygen content. The distributions demonstrate that several characteristic properties of the bottom water over the outer shelf and upper slope are found in the tongue-shaped intermediate particle maximum south of 9 S; furthermore, the intermediate particle layer is shown to be connected to the bottom water (Fig. 2). The characteristic properties include high concentrations of suspended particulate matter and nitrite and low concentrations of oxygen and nitrate. The distributions of the properties therefore suggest that the water and its properties could be transported offshore from the shelf edge along a quasi-horizontal path (Fig. 9).

In addition to the connection between the shelf waters and the intermediate layer shown in the distributions of properties (Figs 2 and 6), there is other evidence for a horizontal
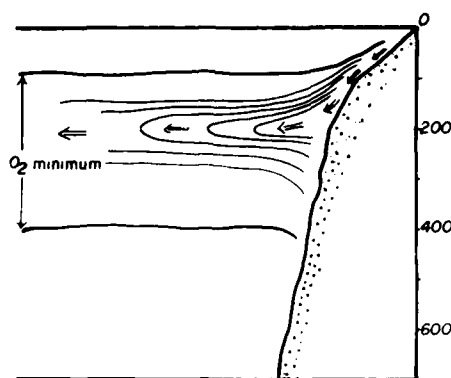
Fig. 9.   Diagram of the offshore particle transport based on the characteristic distributions of suspended particles and chemical parameters within the oxygen minimum layer.

offshore transport of the bottom water over the outer shelf. For example, measurements by means of a vertical profiling current meter along the 'C' line during April 1976 (van Leer, personal communication) indicate a net offshore flow in the bottom water over the shelf and upper slope. In addition, poleward subsurface currents have been observed by moored current meters over the shelf and upper slope near the 'C' line during 11 May to 30 June 1976 (Brink, Allen and Smith, 1978) and near 5 S latitude during 3 April to 18 May 1977 (Brockman, Fahrback and Urquizo, 1978). Isopycnals bending downwards toward the coast (Fig. 6) also suggest poleward subsurface currents (Brink et al., 1978), and the bottom Ekman transport that should arise from this subsurface poleward flow would produce an offshore transport of bottom water over the shelf and upper slope. An offshore flow is, of course, consistent with the offshore transport of suspended particles. Intermediate nepheloid layers similar to those off Peru have been observed over the continental shelf off Oregon, and they were also interpreted to arise from offshore advection of bottom nepheloid layers on the shelf (Pak and Zaneveld, 1978).

Based on the above arguments, the generation of the 200-m particle maximum can be at least partially explained by a horizontal offshore transport from the shelf edge. The horizontal spreading of particles could arise from turbulent transport or advection or both. As horizontal scales of diffusion are much larger than vertical scales, and as a large particle source exists at the shelf edge, turbulent transports alone could account for the 200-m particle maximum.

Suspended particles in the ocean also settle through the water column. Thus, we have to consider the process of particle settling from the surface water as an alternative mode of intermediate particle maxima formation. Vertical settling is often assumed to be the major process of particle transport in the ocean (Rex and Goldberg, 1958; McCave, 1975), but vertical settling alone cannot readily account for many of our observations. The waters above and below particle maxima are relatively clear, indicating that direct settling of particles has a minimal effect on their formation. If a maximum is to be formed by settling alone, settling velocities of most of the particles would have to be reduced at the same depth after they quickly settle through the clean water above the maximum, an unlikely possibility, particularly in the 200-m maximum where the stability is relatively low (Barber

and HUYER, 1979). Furthermore, because the entire water column is stratified, settling velocities below the maxima should be even less than within these features. An increase in turbulence below the particle maxima cannot reduce particle concentration in the turbulent layer because turbulence merely makes the layer homogeneous by mixing. Thus, it is difficult to envision how settling alone could produce the clean water found below the maxima. Because zooplankton and fish populations may increase below the oxygen-deficient zones that are coincident with the maxima under discussion, it is possible that aggregation (e.g. fecal pellets) of particles below the particle maxima would create an increase in mean sinking rates and thereby contribute to a situation in which increases in settling rates by aggregation could produce a particle maximum. However, the mechanism should produce a maximum centered near the bottom (~ 350 m) of the oxygen-poor ($O_2 < 0.2$ ml l^{-1}, Figs 4 and 6a) zone, and south of 9 S the main particle maximum is above this depth.

Direct settling to the bottom over the shelf and upper slope may play an important role in the formation of particle maxima. Characteristic properties of particles in the bottom sediments are often well correlated with those in the surface water over the sediments. To overcome the difficulty of slow settling by individual particles in explaining the correlation between bottom sediments and suspended particles, McCAVE (1975) proposed rapid settling of particles as fecal pellets. Thus, fecal pellets may play an important role in carrying organic matter from the surface water to the bottom water over the shelf. Bottom nepheloid layers are ubiquitous on the continental shelf off Oregon (PAK and ZANEVELD, 1977) and our observations over the Peruvian shelf also indicate extensive bottom nepheloid layers. One exception was found in the region near 23 S (Stas 16, 21, and 24), where the bottom nepheloid layers were conspicuously weak. We speculate that fecal pellets are broken into small individual particles after they reach to or near the bottom over the shelf and upper slope, and then the small particles enter the bottom nepheloid layer by turbulence of the bottom water.

Meridional variations

The decrease in the nitrite maximum and nitrate minimum from the 'C' line to the 'H' line may be accounted for by an increase in oxygen supply in the upper 160 m. Oxygen distributions in the 'H' line show that oxygen concentrations in the bottom water over the shelf edge are often more than 0.2 ml l^{-1}. As dissolved oxygen is still available in the bottom water over the shelf edge, extensive denitrification should not occur (RICHARDS, 1965). In contrast, the upper boundary of the oxygen-deficient water for the 'C' line is often at about 50 m (Fig. 4). In the 'P' line (Fig. 5), the thickness of the oxygen minimum layer is reduced by approximately 50"$_0$ and its core depth deepens by approximately 200 m compared to that in the 'C' line (Fig. 4a). The increase in oxygen concentrations in the upper 200 m at the 'H' and the 'P' lines are probably due to intrusions of the Equatorial Undercurrent (PAK and ZANEVELD, 1974; LOVE, 1972), the South Equatorial Subsurface Countercurrent (TSUCHIYA, 1975), or both. Neither the Equatorial Undercurrent nor the South Equatorial Subsurface Countercurrent is precisely defined over the continental margin off Peru, but intrusions of water with relatively high oxygen concentrations should be anticipated from these two eastward currents which have been defined to the west of 86 W. As the two currents transport water with relatively high oxygen concentrations

eastward at depths of 100 to 200 m, feedings of such water into the shelf bottom water would explain the northward increase of oxygen concentration over the shelf.*

According to WOOSTER *et al.* (1965), the secondary nitrite maximum between 10 and 25 S is associated with a water mass of narrow range in temperature, salinity, and specific volume. Based on the relation between secondary nitrite maximum and water mass characteristics, they suggested a prevailing southward subsurface flow within the feature. This would explain the nitrite maximum as an accumulation of the chemical element on the downstream side of 10 S. The temperature and salinity values of the particle maximum at ~4 S are 9.5 C and 34.50‰ (about 400-m depth), and at 13 S they are 12.62 C and 34.68‰ (about 200-m depth). The two regions are thus not directly related hydrographically and the features at 200 and 400 m are probably in separate flow regimes.

While we have explained the meridional variations in the secondary nitrite maximum between about 10 and 15 S by the meridional oxygen variations, we tacitly assumed that the offshore transport described in the previous section does not vary meridionally. This is because the variation of the 200-m particle maximum between Stas 11 and 50 (Fig. 7) appears to be rather small in spite of the variations in chemical properties.

The different meridional variations in chemical properties and particle concentration associated with the oxygen minimum water are not incompatible. Offshore transport of water is conceivable at the 'H' line as well as at the 'C' line, based on the presence of the intermediate particle maximum. Consequently, the particle concentration in the maximum could be relatively homogeneous meridionally. Chemical properties of the water associated with the maximum vary however, because the bottom water over the shelf edge cannot be associated with increased nitrite concentrations until oxygen is depleted. As a result, oxygen concentrations in the 200-m maximum decrease and nitrite concentrations increase as one proceeds south from about 10 S (downstream), even though there may be little change in suspended particle concentrations.

The particle maximum near 400-m depth

In the section near the 'P' line, the vertical distribution of suspended particles (Fig. 3) is quite different from that in the section near the 'H' line (Fig. 2): near the 'P' line the particle maximum was spread between depths of about 150 to 500 m within 200 km of the shelf edge (out to Sta. 75), and further west a well-defined particle maximum was only found near 400 m. Maximum values of the particle concentrations were generally lower than those in the intermediate maximum further south and a weak nitrite maximum was only found in the offshore portion of the particle maximum (CODISPOTI and PACKARD, 1980). Besides the difference in depth, the 400-m particle maximum differed from the 200-m maximum in its horizontal distribution: the 400-m maximum was well developed only in our 4 S section. It was weak in the other regions (Figs 3 and 7), but despite its weakness away from 4 S, the 400-m maximum may be more extensive than the 200-m maximum.

The spatial variations, found in the horizontal distributions of the 400 and the 200-m maxima, might be related to the large scale circulation. For example, moored current meter observations over the upper slope regions show a long-term mean current directed toward the south in the upper 50 to 300 m below the thin surface drift, and this flow tended to

---

* Because the feeding points of the two waters may be separated by a few degrees, it is not clear that the increase to the north is monotonic as our data suggest. There could be, for example, a decrease in oxygen concentrations between about 5 and 10 S.
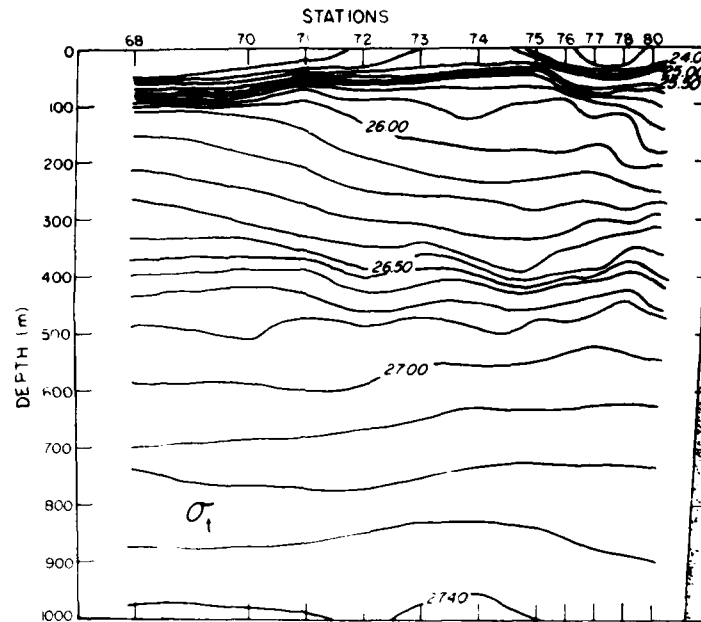
Fig. 10. Distribution of sigma-t observed during the *Weloc* 77 cruise in a section at approximately 4 S.

decrease with depth to become a zero or northward flow near 250 to 400 m (BRINK *et al.*, 1978; BROCKMAN *et al.*, 1978). If the mean current is toward the north at 400 m, the westward extension of the 400-m maximum near the equator can be interpreted as the westward transport of suspended particles by counterclockwise turning of the northward deep current near the equator. Such a current could explain the westward transport but not the source of the particulate matter. The source of the 400-m maximum remains to be identified. The particle distribution near 9 S (Fig. 2) which is upstream of the maximum at 4 S, shows no indication of a particle source near 400 m. In addition, the equatorward bottom current, at 400-m depth, will cause the bottom Ekman transport to be directed toward the shore rather than offshore. Because of these factors and because the stations near 4 S are not close enough to shore to establish the connection between the 400-m maximum and the bottom nepheloid layer over the shelf, we cannot establish the initial source of the particles in the maximum.

The 400-m maximum was approximately at the bottom of a relatively strong density gradient (Fig. 10). The gradient layer was well defined on the offshore side of the section, but it weakened considerably at the nearshore station (Sta. 80). Within about 300 km of the coast, the concentration of suspended particles was relatively high in the wate ∿ above 400 m. Beyond 300 km the 400-m particle maximum became clearly defined. Becav..e we cannot identify a likely nearshore particle source for the 400-m particle maximum and because it is associated with a stability maximum, we cannot exclude the possibility that it arises largely from vertical processes.

REID (1965) described the large-scale westward extension of oxygen-poor water ($O_2 < 0.25$ ml l^{-1}) in the eastern tropical North Pacific as a 'dead area' bypassed by the

27

California and North Equatorial currents, and he emphasized that the lobe pattern of the oxygen minimum does not require a flow in a similar pattern. If horizontal processes are important in producing the offshore extensions of the 400-m maximum, the oxygen-depleted water extending westward in the eastern equatorial South Pacific probably cannot be described in the same way. Instead it may be associated with the westward transport of suspended particles. In other words, the suspended particle maximum near 4 S was in the oxygen minimum water, and their concurrent existence suggests offshore flow of the oxygen-poor water. Because the particle maximum at the westernmost station (Sta. 68) was well developed, and because the horizontal distribution of oxygen-poor water in the area shows a branch extending over 3000 km westward (REID, 1965; TSUCHIYA, 1968), the particle maximum may also extend further west.

As already described, the 400-m particle maximum occurred in a layer of water with a maximum density gradient. No such density gradient was associated with the 200-m maximum. Such a large density gradient was limited to near 4 S during the *Weloc* 77 cruise, but it was observed more extensively during 23 July to 16 August 1976 (HUYER, GILBERT, SCHRAMM and BARSTOW, 1978a) and during 4 March to 22 May 1977 and 5 April to 19 May 1977 (HUYER *et al.*, 1978b). However, it was not observed at every station, suggesting spatial and temporal variations.

The incidence of the particle maximum and the maximum density gradient at the same depth suggests they are interrelated. In particular, the fact that the 400-m particle maximum is well developed only in the equatorial regions where the density gradient maximum is strong, may be significant.

We are leaving two unsolved problems concerning the 400-m particle maximum, (1) the mode of generation of the maximum and (2) the exact relation between it and the maximum vertical gradients in hydrographic parameters and biological processes, for future studies. Both problems appear to be important considering the spatial and temporal scales of the particle maximum.

CONCLUSIONS

1. A well-defined 200-m particle maximum observed off western South America may be formed largely by quasi-horizontal transport (advective, diffusive, or both) of a bottom nepheloid layer.

2. The 200-m particle maximum is associated with vertical extremes in dissolved oxygen, nitrate, nitrite and protein.

3. The 400-m particle maximum that is best defined in the equatorial region is associated with a maximum in vertical temperature and density gradients and is sometimes associated with oxygen minima and nitrite maxima.

4. Due to the apparent lack of a nearshore particle source, the 400-m particle maximum cannot easily be explained by the same quasi-horizontal process that appears to explain the 200-m maximum.

REFERENCES

BARBER R. T. and A. HUYER (1979) Nitrite and static stability in the coastal waters off Peru. *Geophysical Research Letters*, **6**, 409 412.

BARTZ R., J. R. V. ZANEVELD and H. PAK (1978) A transmissometer for profiling and moored observations in water. *Society of Photo-optical Instrument Engineers*, **160**, 102 108.

BRINK K. H., J. S. ALLEN and R. L. SMITH (1978) A study of low-frequency fluctuations near the Peru coast. *Journal of Physical Oceanography*, **8**, 1025 1041.

BROCKMAN C., E. FAHRBACK and W. URQUIZO (1978) *Escan Data Report 51*. Institut für Meerskunde an der Christian-Albrechts-Universität, Kiel, 42 pp.

CODISPOTI L. A. and T. T. PACKARD (1980) On the denitrification rate in the eastern tropical Pacific. *Journal of Marine Research*.

GARFIELD P. C., T. T. PACKARD and L. A. CODISPOTI (1979) Particulate protein in the Peru upwelling system. *Deep-Sea Research*, **26**, 623 639.

HAFFERTY A. J., L. A. CODISPOTI and A. HUYER (1978) JOINT II R.V. *Melville* cruise, Leg I, II and IV. R.V. *Iselin* Leg II, bottle data, March to May 1977. *Coastal Upwelling Ecosystems Analysis Data Report*, **45**, 779 pp.

HAFFERTY A. J., D. LOWMAN and L. A. CODISPOTI (1979) JOINT II *Melville* and *Iselin* bottle data sections, March to May 1977. *Coastal Upwelling Ecosystem Analysis Data Report*, **38**, 129 pp.

HUYER A., W. E. GILBERT, R. SCHRAMM and D. BARSTOW (1978a) Temperature and salinity observations off the coast of Peru, R V *Eastward*, July 23 to August 16, 1976. *Coastal Upwelling Ecosystems Analysis Data Report*, **47**, 183 pp.

HUYER A., W. E. GILBERT, R. SCHRAMM and D. BARSTOW (1978b) CTD observations off the coast of Peru, R V *Melville*, March 4 to May 22, 1977, and R V *Columbus Iselin*, April 5 to May 19, 1977. *Coastal Upwelling Ecosystems Analysis Data Report*, **55**, 409 pp.

LOVE C. M. (1972) *Eastropac atlas*, Vol. 1, Phys. Oceanogr. Metero. data from principal participating ships, first survey cruise, February to March 1967. U.S. Dept. Commerce Circ. 330.

McCAVE I. N. (1975) Vertical flux of particles in the ocean. *Deep-Sea Research*, **22**, 491 502.

PAK H. and J. R. V. ZANEVELD (1974) The Cromwell Current on the east side of the Galapagos Islands. *Journal of Geophysical Research*, **78**, 7845 7859.

PAK H. and J. R. V. ZANEVELD (1977) Bottom nepheloid layers and bottom mixed layers observed on the continental shelf off Oregon. *Journal of Geophysical Research*, **82**, 3921 3931.

PAK H. and J. R. V. ZANEVELD (1978) Intermediate nepheloid layers observed on the continental margin off Oregon. *Society of Photo-optical Instrument Engineers*, **160**, 9 17.

PETERSON R. (1977) A study of suspended particulate matter: Arctic Ocean and northern Oregon continental shelf. Ph.D. Thesis, Oregon State University, Corvallis, Oregon, 122 pp.

REX R. W. and E. D. GOLDBERG (1958) Quartz contents of pelagic sediments of the Pacific Ocean. *Tellus*, **10**, 153 159.

REID J. L., Jr. (1965) *Intermediate waters of the Pacific Ocean*. The Johns Hopkins Press, Baltimore, Maryland, 85 pp.

RICHARDS F. A. (1965) Anoxic basins and fjords. In *Chemical oceanography*, J. 1 RILEY and G. SKIRROW, editors. Academic Press, New York, pp. 611 645.

TSUCHIYA M. (1968) *Upper waters of the intertropical Pacific Ocean*. The Johns Hopkins Press, Baltimore, Maryland, 50 pp.

TSUCHIYA M. (1975) Subsurface counter currents in the eastern equatorial Pacific Ocean. *Journal of Marine Research*, **33**, 145 175.

WOOSTER W. S., T. J. CHOW and J. BARRETT (1965) Nitrite distribution in Peru current waters. *Journal of Marine Research*, **23**, 210 221.

Description and occurrence of macrourid larvae and juveniles in the northeast Pacific Ocean off Oregon, U.S.A.

DAVID L. STEIN*

Abstract—Although there are over 100 species of North Pacific macrourids, few of their larvae have previously been identified to species. Descriptions of postlarvae and juveniles of *Coryphaenoides acrolepis, C. filifer,* and *C. leptolepis* are given, with a provisional key to the identification of most species known from off Oregon. Vertical distribution of the larvae and juveniles of *C. acrolepis* apparently changes with ontogenetic development, the smallest individuals occurring shallowest. Macrourid eggs have not yet been identified from Oregon waters.

INTRODUCTION

LARVAE and juveniles of a few species of North Atlantic macrourids have been described, most recently by MERRETT (1978). Despite the presence of over 100 macrourid species in the North Pacific, apparently there have been no descriptions of macrourid eggs, only two descriptions of prejuveniles, and few references to identified larvae and juveniles. GILBERT and BURKE (1912) described a new genus and species *Ateleobrachium pterotum* based on a postlarval macrourid from off Kamchatka. HUBBS and IWAMOTO (1977) described postlarvae and juveniles of a new species of pelagic macrourid, *Mesobius berryi*, from off southern California and north of Hawaii. SAVVATIMSKII (1969) discussed the relationship of depths of occurrence to length of *Coryphaenoides acrolepis* (Bean) 1884 and seasonality of spawning of *C. acrolepsis* and *Coryphaenoides pectoralis* (Gilbert) 1892. NOVIKOV (1970) discussed the early life history of *C. pectoralis*. Neither SAVVATIMSKII nor NOVIKOV (*op. cit.*) described the larvae or supplied a reference to such descriptions. Judging by the lack of information, MARSHALL's (1965) comment about the lack of collected specimens of larval macrourids applies particularly to the situation in the North Pacific Ocean.

This paper describes the macrourid postlarvae and juveniles collected by the School of Oceanography, Oregon State University (OSU), off the Oregon coast since 1961. The collections, made with a variety of net types during all seasons, contain 106 specimens of young macrourids. The captures have been so infrequent that only recently has sufficient material become available to allow identifications.

METHODS AND MATERIALS

Specimens from midwater were collected with 3.0-m and 1.8-m Isaacs-Kidd Midwater Trawls (IKMT), 2.4-m IKMT-EMPS trawls with serial opening-closing cod ends

---

* School of Oceanography, Oregon State University, Corvallis, OR 97331, U.S.A.

(PEARCY, KRYGIER, MESECAR and RAMSEY, 1977), modified Cobb trawl with EMPS cod ends (PEARCY, 1980), and 0.7-m bongo nets. Almost all the pelagic specimens were captured between 80 and 145 km off Newport, Oregon. Juveniles and adults from bottom trawls were from the collections described by IWAMOTO and STEIN (1974). Samples were preserved at sea in 10% buffered formalin–seawater solution and later transferred to 45% isopropanol for storage.

Head length was measured as the distance from the tip of the mandible in postlarvae and the tip of the snout in juveniles to the posterior tip of the opercular flap. Other measurements used are explained below.

Specimens were measured to the nearest 0.1 mm using an ocular micrometer or dial calipers. Counts follow IWAMOTO (1970). Terminology for life history stages follows HUBBS (1943).

All larvae and juveniles examined and specimens of adults used for comparative purposes are on deposit at the School of Oceanography, OSU.

Characters and terminology used for identification and description

Characters most useful in the study were premaxillary and dentary tooth patterns (useful in juveniles but not in larvae), number of rays in the first dorsal and pelvic fins, number of gas glands and retia, and pigmentation (Table 1). Pigmentation patterns proved most useful in determining conspecificity of larvae.

The study was facilitated by the relatively low number of macrourid species known from the study area (eight) and the availability of a recent review of those species (IWAMOTO and STEIN, 1974). The area considered by IWAMOTO and STEIN (1974) included the eastern North Pacific from the Bering Sea to central California. Although it is possible that larvae of species not occurring in the study area are carried into it by the prevailing currents, I consider it unlikely. Consequently, I initially assumed that larvae and juveniles captured off Oregon were conspecific with species known to occur in the same area. Because of differences in patterns of teeth in the jaws, number of swimbladder gas glands and retia, and numbers of first dorsal fin rays and pelvic fin rays, some species are easily identifiable. A complete developmental series was available for the least distinct species, *C. acrolepis*, which otherwise could have been identified only tentatively.

Macrourid larvae may be pigmented externally (on the skin surface) or internally (within myomeres, on myomeres, on the stomach or peritoneum, etc.). Internal pigment can be diffuse or composed of distinct melanophores. The distinction between internal and external melanophores may be difficult to make, as in ventral pigmentation of the stomach and peritoneum; the body wall is very thin and transparent ventrally; as a result, internal pigment appears to be external. Preservation may change intensity of pigmentation, although it does not appear to change pigment patterns. For instance, fresh specimens of juvenile *C. acrolepis* are silvery, but after preservation, they become dull.

Differences in the ratio of head length (HL) to total length (TL) are difficult to express because macrourids often lose some part of their tail when captured; the convention ordinarily used to avoid using total length is to use head length as its analog. To quantify the differences in relative body lengths among the three species described here, the horizontal diameter of the pigmented eyeball was measured, then the distance from the snout tip to the point on the tail where depth (exclusive of fin height) equalled eye diameter was measured. This distance was then expressed as number of head lengths.

Numbers of gas glands and retia are useful in identification. It is possible to identify one

Table 1. *Morphological characters most useful in identifying macrourid larvae occurring or likely to occur off the coast of Oregon, U.S.A.*

	C. armatus	C. leptolepis	C. acrolepis	C. filifer	C. pectoralis	C. cinereus
Body pigment	*Unknown	*Melanophores on trunk and head, closely spaced, not posterior to anal fin ~10th ray	*Melanophores on dorsum and venter, absent on last 20% of tail and on midline	*Melanophores widely scattered on dorsum around dorsal fin only	*Unknown	*Unknown
D_1 fin rays	8-10	8-10	9-11	11-15?	7-9	10-12
P_2 fin rays	10-11	9-10	8-9	9-10	6-8	8-10
Pyloric caeca	10-13	~11	12-14	8-12	12-16?	5-7
Rostral scutes	Absent	Absent	Strong†	Strong†	Absent	Strong†
Size at which pectorals normalize	<18.2 mm HL	6.2-15.0 mm HL	9.4-9.8 mm HL	14.1-14.6 mm HL	—	—
Precaudal vertebrae	13-15	12	14-15	—	13-14	13-14
Gas glands	5-6	6	4	4	2	4
Retia	5-6	6	4	4	2	4

* Larval character.   † Adult/juvenile character.

species (*C. pectoralis*) solely by its possession of two gas glands. The swimbladder is present and apparently functional at 1.5 mm HL in at least one species, *C. rupestris* (Gunnerus), 1765 (MERRETT, 1978). All specimens examined in the study were larger than 1.8 mm HL. The swimbladder in postlarvae and juveniles is easily reached through an incision in the side of the abdominal cavity, and its careful examination or excision results in little damage to the specimen.

For purposes of description here, the transition from larva to juvenile is called metamorphosis; it seems to be rapid, and there is only a small difference in head lengths between premetamorphic and postmetamorphic individuals of both *C. acrolepis* and *C. filifer* (Table 1). The most important morphological change at this time is the loss of the pectoral fin peduncle and appearance of the adult pectoral fin form. Simultaneously, the mouth, formerly at a distinct angle, becomes horizontal, the snout becomes distinct, and the stomach is reduced in prominence, decreasing the depth of the posterior part of the trunk. Stomach prominence may be a function of feeding habits. Larvae are commonly found with the stomach crammed with food, but juveniles are not. The phenomenon may be a partial cause of the very different appearances of larvae and juveniles.

RESULTS AND DISCUSSION

Larval diagnosis and development

Coryphaenoides acrolepis (*Fig.* 1). This is the only species examined of which a complete developmental specimen series was available. The characters most important in identification were number of first dorsal fin and pelvic fin rays, number of gas glands, and presence of rostral scutes in juveniles greater than about 16 mm HL (Table 1). Pigment pattern enabled definite determination of conspecificity of small individuals lacking rostral scutes with larger specimens having them. All 78 individuals examined have a distinctive pigment pattern in which the entire body is internally or externally pigmented except the last part of the tail, which abruptly becomes internally unpigmented. The fraction of the body that is pigmented is quite consistent; HL represents 27.8 to 34.2% of the pigmented length (PL). The fraction does not vary with size of individual. A linear regression of HL versus PL is highly significant (HL $= 0.08 + 0.30$ PL; $r^2 = 0.97$). The distinct character, seen in juveniles and in the smallest individual studied (1.8 mm HL), is unaffected by period of preservation and is clearly not a preservation artifact.

As in all known macrourine larvae, a peduncular pectoral fin is present and well developed. It disappears between 9.4 and 9.8 mm HL, at which time the 'normal' adult pectoral appears. All other fins have their full complement of rays by 3.8 mm HL.

1.8 mm HL (*Fig.* 1A)

Individuals of this size may be recently hatched; ripe eggs of *C. acrolepis* are at least 2.0 mm in diameter (observations of STEIN and PEARCY). The dorsal and anal fins are not developed; the pelvic fins are well developed. Stellate chromatophores form a bilaterally symmetrical patch on the frontal region of the head; the lower jaw is completely but sparsely pigmented. Very small, scattered melanophores occur along the bases of the dorsal and anal finfolds; they are especially noticeable on the posterior part of the caudal region. Extensive internal pigmentation is present within the myomeres and on the peritoneum. Myomeric pigment is absent from the posterior part of the tail.
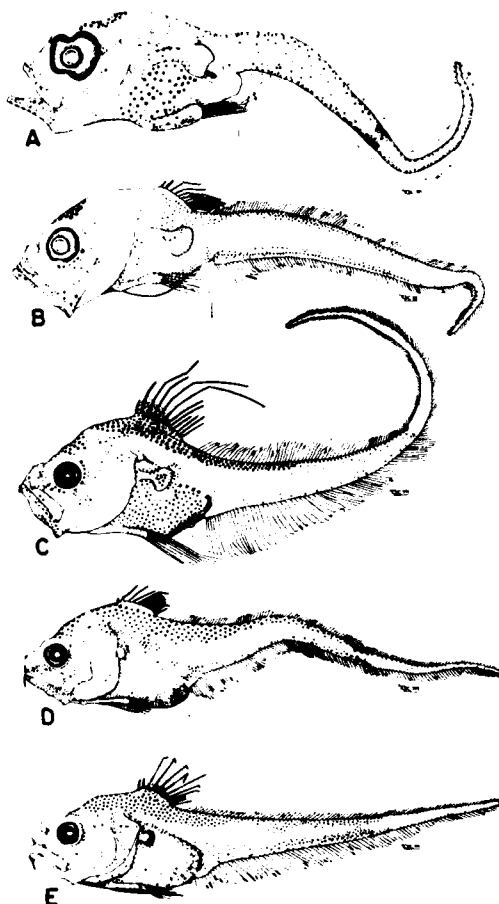
Fig. 1. *Coryphaenoides acrolepis.* A : 1.8 mm HL; B : 3.8 mm HL; C : 6.7 mm HL; D : 9.8 mm HL;
E : 12.5 mm HL.

3.8 mm *HL* (*Fig.* 1B)

Frontal pigment has increased and become divided into two similar oval patches, one on each side of the head. The lower jaw is pigmented except for the anterior part of the gular region. Pigment along the bases of the median fins is still present, but it is not so prominent posteriorly. Internal pigmentation is as above.

4.7 mm *HL*

The anterior dorsal melanophores have become larger and denser, forming a longitudinal dorsal patch reaching from the first dorsal fin spine posteriorly to about half the length of the fish. The anterior part of the gular region remains unpigmented.

6.7 mm HL (Fig. 1C)

Pigmentation has become much more extensive. The dorsal pigment extends from the nuchal region to the caudal end of the myomeric pigment and onto the first dorsal fin. Ventral melanophores are present but sparse on the caudal region. Peritoneal melanophores are evenly distributed; external pigment is sparse on and around the bases of the pelvic fin rays and is quite dense around the anus. Pigment is scattered on the suborbital and postorbital regions. The anterior part of the gular region remains unpigmented. The mandibular barbel is present as a small, broad-based flap or bump.

7.4 mm HL

Dorsal and ventral pigmentation is extensive, composed of large and small pigment spots coalescing in the trunk area below the first dorsal fin. The basipterygia are completely pigmented, and the pigment around the anus is not so dense as at 6.7 mm HL. The anterior part of the gular area remains unpigmented; a broad band following the lateral line down the sides of the tail is externally unpigmented but is evenly pigmented internally.

9.4 mm HL

The area along the lateral line is sparsely pigmented externally, and trunk pigment is more extensive; internal myomeric pigment is more prominent in the previously unpigmented caudal region. The dorsal pigment now extends to the frontal region, and the previously unpigmented part of the gular region of the lower jaw is smaller, although its anteriormost third remains pigment free. The pectoral fins are still peduncular, and the barbel, although distinct, is quite short.

9.8 mm HL (Fig. 1D)

Metamorphosis has occurred, although the stomach is still relatively larger and more swollen than in later juveniles. The unpigmented caudal region has some internal pigmentation consisting of distinct melanophores and diffuse myomeric pigment, is very lightly pigmented along the fin bases, and remains distinct. The lower jaw is completely pigmented. The pectorals are adult in form, although their bases form small lobes. The barbel is slender, short, and lightly pigmented.

12.5 mm HL (Fig. 1E)

The body is covered with small punctate melanophores evenly distributed except along the lateral line, where they are relatively sparse. The transition between internally pigmented and unpigmented caudal regions is less abrupt. The peritoneum, which can be seen through the body wall, is uniformly darkened. The barbel is fully developed.

15.3 mm HL

The adult body form is clearly present; the stomach is not swollen as it was previously At this size, the distinctive pigment-free caudal region cannot be clearly distinguished from the remainder of the tail.

16.6 mm HL

The rostral scutes and scales begin to form.

Coryphaenoides leptolepis (Günther) 1877 (Fig. 2D, E). Although the eight specimens
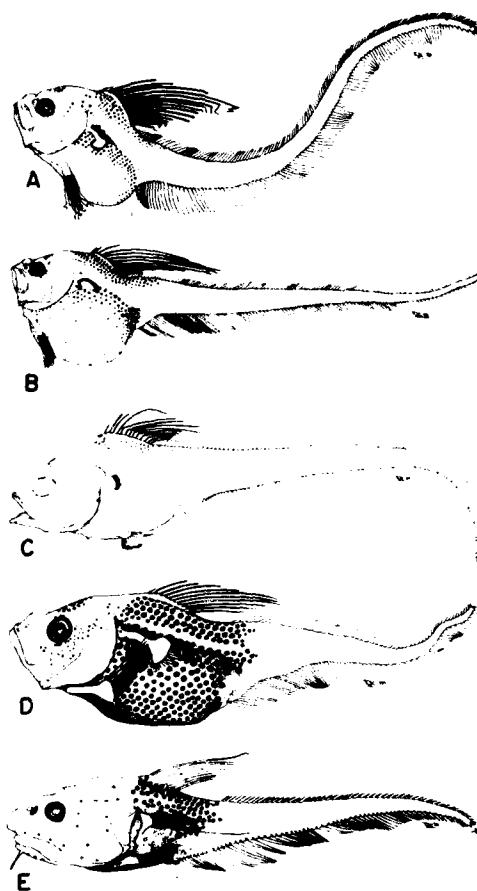
Fig. 2.   *Coryphaenoides filifer.* A: 6.4 mm HL; B: 10.5 mm HL; C: ~14.6 mm HL (a composite from two damaged specimens). *Coryphaenoides leptolepis.* D: 6.2 mm HL; E: 15.2 mm HL. Posterior of caudal not drawn, although present, in E.

available do not form a complete series, they are clearly conspecific and allow description of important characters and of several growth stages. The characters most important in identification were pigment pattern, number of gas glands, and number of first dorsal and anal fin rays (Table 1). The pigment pattern is present even in relatively large juveniles; it provided the connection between juveniles identifiable using adult characters and smaller individuals not so identifiable. In all specimens up to at least 19.6 mm HL (>84 mm TL), evenly scattered pigment spots occur on the trunk from just anterior to the dorsal fin posterior to about the 10th anal fin ray. The pigment spots are visible even in specimens darkened by preservation. Posterior to the 10th anal ray no comparable pigment is present. The pigmented area is sharply distinct from the rest of the tail.

All fins other than the pectorals are fully developed by 5.9 mm HL. The pectorals are peduncular and paddle-like distally. The peduncular fin is lost between 6.2 and 13.6 mm HL, at which size a fully developed adult form of pectoral fin is present.

5.9 mm HL

Clearly separated melanophores are dense on the trunk and stomach. Some melanophores are evenly distributed over the frontal region of the head, and a few are present on the ascending processes of the premaxillae. Pigment is present around the basipterygia and under them on the stomach, visible through the body wall. A wide notch between the anteriormost teeth is present at the tip of the premaxillaries.

6.2 mm HL (Fig. 2D)

Trunk pigmentation is less dense than at 5.9 mm HL; it is composed of evenly distributed stellate melanophores. Peritoneal pigmentation is denser anteroventrally and posterodorsally. The large and small punctate frontal melanophores form a bilaterally symmetrical heart-shaped pattern with the apex pointing posteriorly. A narrow band of internal melanophores on the head extends in an arc from the suborbital region to above the opercle. Dense black punctate melanophores are present on the peritoneum under the unpigmented basipterygia.

15.2 mm HL (Fig. 2E)

Metamorphosis has occurred. The trunk melanophores are relatively larger, blotchier, and more widely separated than in the postlarval stages. The adult form of pectoral fin is present. The light brown body is fully scaled. The trunk melanophores make the body anterior to about the 10th anal fin ray appear blackish.

19.6 mm HL

Trunk melanophores are still present although they have become large, blackish, widely separated spots. Fish at this size are easily identifiable by using keys to adults.

Coryphaenoides filifer (Gilbert) 1895 (Fig. 2A, B, C). The 10 available specimens do not form a complete series but are clearly conspecific. Characters most useful in identification of C. filifer were number of first dorsal fin rays, pelvic fin rays, gas glands, and pigment pattern (Table 1). The species can be distinguished from all others likely to be captured off Oregon by the abundance of the rays in the first dorsal fin. One larval individual, identical in other respects to the other specimens identified as C. filifer, had 15 first dorsal fin rays. The highest previously reported ray number was 14 (Iwamoto and Stein, 1974). The pigment pattern allowed identification of individuals with 11 or 12 first dorsal fin rays. The specimens might otherwise have been confused with C. acrolepis or C. cinereus (Gilbert) 1895. The distinct pigment pattern in all postlarvae and juveniles examined consists of a 'dorsal oval' of melanophores surrounding the first dorsal fin; its long axis parallels the length of the fish. The dorsal oval generally extends anterior to the first dorsal fin, posteriorly to about the 12th ray of the second dorsal fin, and ventrolaterally as far as the lateral line. The peritoneum is distinctly pigmented dorso-laterally. There are scattered small melanophores along the lateral line and on the gular and suborbital regions of the head.

All fins except the pectorals have their full complement of rays in the smallest specimen examined (6.4 mm HL). Metamorphosis occurs at a greater HL (between 14.1 mm and 14.6 mm) than in either C. acrolepis or C. leptolepis.

The species is distinctly longer at any given head length than are either of the other two species; total lengths of the two specimens that had lost the least amount of caudal were 6.7 times HL (at 6.4 mm HL) and 6.9 times HL (at 11 mm HL). The distance from the snout to

where the caudal fin is equal in depth to the horizontal diameter of the pigmented eyeball ranges between 3.5 and 4.6 times head length, whereas for *C. leptolepis* the range is 2.4 to 2.7 and for *C. acrolepis* it is 1.8 to 2.4.

6.4 mm *HL* (*Fig.* 2A)

The melanophores forming the dorsal oval are small, punctate, dense black or dark brown, and closely spaced. Pigment is abundant on the dorsolateral surface of the peritoneum but not on the ventral surface, possibly because the stomach of the specimen is greatly swollen with food. There are a few tiny melanophores on the ventral surfaces of the lower jaw. On each frontal is an oval patch of small, widely separated stellate melanophores.

10.5 mm *HL* (*Fig.* 2B)

The melanophores forming the dorsal oval and stomach pigmentation are much larger and less dense, forming relatively large spots that tend to coalesce. A few small pigment spots are present on the isthmus and the ventral margin of the opercular opening, along the lateral line, and on the posteriormost part of the caudal. Apparently neither number nor size of pigment spots increases on the frontal surfaces of the head or ventral surfaces of the lower jaw or the stomach.

~14.1 mm *HL* (*damaged*)

Metamorphosis starts to occur at about 14 mm. Relative to smaller specimens, the angle of the mouth is nearer the horizontal, the stomach is smaller, the posterior part of the trunk is not so deep and is about equal in depth to the anterior part of the tail. The peduncular pectoral fin is still present and well developed.

~14.6 mm *HL* (*damaged*) (*Fig.* 2C)

Metamorphosis is almost complete. The dorsal oval is still distinct. Both available specimens near this size are in poor condition, precluding further descriptions of pigment patterns. The pedunculate pectoral fin has disappeared and the fully developed adult form of pectoral fin is present.

~16 mm *HL* (*damaged*)

Similar to 14.6 mm specimens. Pigmentation differs in the presence of small dark brown pigment dots over the entire body, especially on the tail, forming diffuse lengthwise bands above, below, and along the lateral line.

Coryphaenoides armatus (*Hector*) 1875. No larvae or postlarvae of this species, the most abundant macrourid occurring off Oregon (observations of PEARCY, STEIN and CARNEY), were identified. One juvenile (18.2 mm HL) was collected by IKMT between the surface and 2520 m in 3909 m of water. The specimen was clearly of adult form and was easily identified. Metamorphosis thus occurs in *C. armatus* by this size, and judging by the complete squamation of the specimen, it probably occurs at some significantly smaller size.

Provisional key to postlarvae and juveniles of Coryphaenoides *occurring off Oregon*

A.   Pyloric caeca 5–7 (first dorsal fin rays 10–12, pelvic fin rays 8–10) .   *C. cinereus*
AA. More than 9 pyloric caeca   .   .   .   . **B**
B.   Gas glands and retia 2; 6–8 pelvic fin rays   .   .   .   .   *C. pectoralis*

BB.	Gas glands and retia 4–6; 8–10 pelvic fin rays C
C.	Gas glands and retia 4 . . . . D
CC.	Gas glands and retia 5–6 . . . . E

D.   Pyloric caeca fewer than 11; first dorsal fin rays 11–15; pelvic fin
rays 9–10. Pigment generally confined to dorsum, forming an oval
surrounding dorsal fin base; melanophores sparse, well separated .   . *C. filifer*

DD.   Pyloric caeca 12–14; first dorsal fin rays 9–11; pelvic fin rays 8–9.
Body and tail pigmented except for last part of tail; pigmented
length 2.9–3.6 times HL. . . . . *C. acrolepis*

E.   Trunk with large dark pigment spots posteriorly to about 10th anal
fin ray, up to at least 20 mm HL; 12 precaudal vertebrae; gas glands
and retia 6. Premaxillary teeth forming a wide inner band of small
teeth with an outer enlarged series . . . . *C. leptolepis*

EE.   Trunk pigment not as above; 13–15 precaudal vertebrae; gas glands
and retia 5–6. Premaxillary teeth biserial or irregularly biserial   .   *C. armatus*

The key is based upon available specimens and should be considered provisional. Two rare species [*C. yaquinae* (IWAMOTO and STEIN, 1974) and *Nezumia stelgidolepis* (Gilbert) 1891] have been omitted. Although postlarvae of only three of the six species included have been identified and described, it seems reasonable to use the adult characters that proved useful in identification of larvae of the three species for all seven species. Such a key may be useful to future studies by distinguishing other larvae found in the same waters from the three species described here. Hopefully, it will also stimulate examination of previously unexamined macrourid larvae in other collections.

Abundance and vertical distribution

To see whether juveniles avoid small nets, I compared relative abundances of all *C. acrolepis* juveniles captured in midwater in the OSU collections; they were captured with two kinds of nets (IKMT and Cobb trawl). The effects of factors such as seasonal abundance, distance offshore, and depth of capture on relative abundances and distribution could not be determined. Captures of larvae and juveniles were too rare, even after pooling, to allow separate analyses on these bases. Net size affected catch rates; a small (50 m²) opening–closing Cobb trawl (PEARCY, 1980) yielded almost 50 juvenile *C. acrolepis* in four hauls at 500 to 600-m depth during one cruise. However, the number of individuals $(10^6 \text{ m}^3)^{-1}$ was even lower than for individuals captured by 1.8-, 2.4-, and 3-m IKMT's. Values for IKMT captures average 18.8 individuals $(10^6 \text{ m}^3)^{-1}$, and for Cobb trawl captures average 8.9 individuals $(10^6 \text{ m}^3)^{-1}$. The larger (18 vs 6 mm) mesh size of the Cobb trawl may explain the relatively lower catches.

The rarity of macrourid larvae, postlarvae, and juveniles is a puzzle that has been often discussed but remains unresolved (e.g. JOHNSEN, 1927; MARSHALL, 1965, 1973; MERRETT, 1978). The collections for this study were from over 2700 midwater trawl hauls, many of which (∼900) were with multiple opening–closing nets, and thus are the equivalent of 5000 to 6000 separate tows. Yet relatively few specimens in any of the three developmental stages were captured. Of these, none was a prolarva, some were postlarvae, and most were juveniles.

Vertical distribution of early growth stages of two of the three species studied here is generally unknown. Most of our specimens of *C. filifer* and *C. leptolepis* were captured

before we began to use opening–closing midwater trawls and thus the depth of their capture cannot be stated definitely. SAVVATIMSKII (1969) reported *C. acrolepis* 10 to 15 mm TL occurred at 100 to 200 m. The specimens of *C. acrolepis* show a pattern of vertical distribution (Fig. 3) that supports the general pattern postulated by MARSHALL (1965) and apparently given, but not cited, by SAVVATIMSKII (1969) and recently supported by MERRETT (1978). The four smallest specimens of *C. acrolepis* ($\leqslant 6.7$ mm HL) were captured between the surface and 200 m. All but one of the remaining specimens (73) were captured in tows reaching 500 m or deeper. In a series of day and night horizontal tows from 2 to 5 September 1978, at depths of 500, 650, 800 and 1000 m, with a 50 m^2 opening closing Cobb trawl net, juvenile *C. acrolepis* were captured only in nets fished at 650 to 800 m; postlarvae were collected at 500 m. In general, of all specimens examined for this study, those less than 6.7 mm HL occurred at 200 m or less, those of about 7.3 to 15.6 mm HL at 600 m or less, those 9.8 to 18.0 mm HL between 500 and 800 m; only individuals greater than 13 mm HL occurred below 800 m. This the sparse data generally support the hypothesis of ontogenetic migration of subadult macrourids off Oregon.
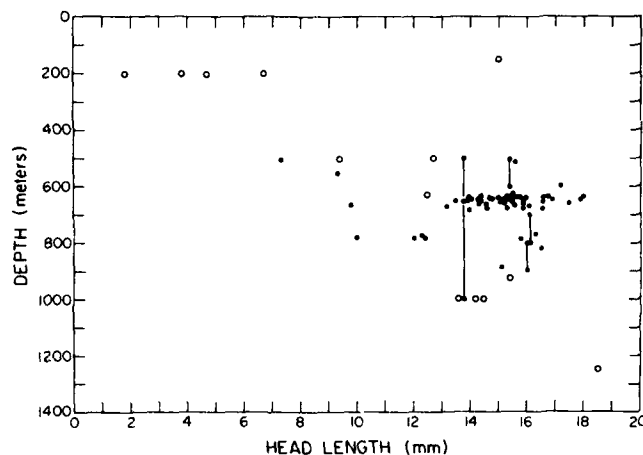
Fig. 3. Depth of capture vs head length for *C. acrolepis*. ○ : maximum depth of capture by non-closing net; ● : depth of capture by opening–closing net. Vertical lines represent depths of single captures in oblique hauls by opening–closing nets. where change in depth was $\geqslant 100$ m.

The results complement the work of MULCAHY, KILLINGLEY, PHLEGER and BERGER (1979), who analyzed ratios of oxygen and carbon isotopes in otoliths of *C. acrolepis*. They concluded that *C. acrolepis* undergoes an ontogenic migration "of at least 1400 m" "early in the life cycle", based on decreasing estimated temperatures of 6 to 2°C at times of otolith deposition. The temperatures of the water in which the specimens examined in this study were captured ranged from 1.7 to 8.1°C. Specimens less than 6.7 mm HL collected at 200 m or less were all in water of 6.6°C or warmer (unpublished OSU data report and *in situ* temperature sensor on trawls).

specimens with great skill and patience. He and BETSY WASHINGTON freely supplied advice and criticism
throughout this study. Temperature data were supplied in part by JANE HUYER from an unpublished data report.
The study was supported by Office of Naval Research Contract No. N00014 79 C 0004

REFERENCES

GILBERT C. H. and C. V. BURKE (1912) Fishes from Bering Sea and Kamchatka. *Bulletin of the United States Bureau of Fisheries*, **30**, 31-96.
HUBBS C. L. (1943) Terminology of early stages of fishes. *Copeia*, 260.
HUBBS C. L. and T. IWAMOTO (1977) A new genus (*Mesobius*), and three new bathypelagic species of Macrouridae (Pisces, Gadiformes) from the Pacific Ocean. *Proceedings of the California Academy of Sciences*, series 4, **41**, 223-251.
IWAMOTO T. (1970) The R.V. *Pillsbury* deep-sea biological expedition to the Gulf of Guinea, 1964-65. 19. The macrourid fishes of the Gulf of Guinea. *Studies in Tropical Oceanography*, University of Miami (4), part 2, 316-431.
IWAMOTO T. and D. L. STEIN (1974) A systematic review of the rattail fishes (Macrouridae: Gadiformes) from Oregon and adjacent waters. *Occasional Papers of the California Academy of Sciences*, **111**, 1-79.
JOHNSEN S. (1927) On some bathypelagic stages of macrourid fishes. *Nytt Magasin for Naturvidenskaberne*, Oslo, **65**, 221-241.
MARSHALL N. B. (1965) Systematic and biological studies of the macrourid fishes (Anacanthini-Teleostii). *Deep-Sea Research*, **12**, 299-322.
MARSHALL N. B. (1973) Family Macrouridae. In: *Fishes of the Western North Atlantic*, D. M. COHEN, editor-in-chief. *Memoir, Sears Foundation for Marine Research*, **1**, part 6, pp. 496-537.
MERRETT N. R. (1978) On the identity and pelagic occurrence of larval and juvenile stages of rattail fishes (Family Macrouridae) from 60°N, 20°W and 53°N, 20°W. *Deep-Sea Research*, **25**, 147-160.
MULCAHEY S. A., J. S. KILLINGLEY, C. F. PHLEGER and W. H. BERGER (1979) Isotopic composition of otoliths from a benthopelagic fish, *Coryphaenoides acrolepis*, Macrouridae: Gadiformes. *Oceanologica Acta*, **2**, 423-427.
NOVIKOV N. P. (1970) Biology of *Chalinura pectoralis* in the North Pacific. In: Soviet fisheries investigations in the Northeastern Pacific, P. A. MOISEEV, editor. *Proceedings of the All-Union Scientific Research Institute of Marine Fisheries and Oceanography (VNIRO)*, **70**. Jerusalem: Israel Program for Scientific Translations, 1972, pp. 304-331.
PEARCY W. G. (1980) A large opening-closing midwater trawl for sampling oceanic nekton, and comparison of catches with an Isaacs-Kidd midwater trawl. *Fishery Bulletin*, **78**. In press.
PEARCY W. G., E. E. KRYGIER, R. MESECAR and F. RAMSEY (1977) Vertical distribution and migration of oceanic micronekton off Oregon. *Deep-Sea Research*, **24**, 223-245.
SAVVATIMSKII P. I. (1969) Makrurus Severnoi Atlantiki. *Trudy PINRO*, 3-72. (The grenadier of the North Atlantic.) Fisheries Research Board of Canada Translation, Serial No. 2879, 1-86.

Note added in proof—Since this paper went to press, examination of additional specimens of *C. armatus* has shown
that some small benthic juveniles, but not all, have trunk pigmentation similar to that of *C. leptolepis* postlarvae.
As noted above, the only pelagic juvenile captured of *C. armatus* lacks such pigment. Consequently, identifications
of larvae as *C. leptolepis* should stand as described for the present, but must be considered as provisional pending
availability of more material.

Reply

JAMES J. SIMPSON

Scripps Institution of Oceanography, La Jolla, CA 92093

CLAYTON A. PAULSON

Oregon State University, Corvallis 97331

25 July 1980

McLeish's comments on our paper (Simpson and Paulson, 1980) are welcome. His remarks deal with the interpretation of our observations of sea surface temperature spectra. The spectral features he discusses are 1) the high-frequency cutoff, 2) the low-frequency slope and 3) the mid-frequency plateau.

McLeish suggests that the decrease in spectral density at frequencies above 0.5 Hz may be caused by spatial averaging by the instrument in the presence of advection. We feel that alternate interpretations cannot be excluded. In particular, the effect of advection by the orbital motions of waves probably should be considered in addition to mean advection. Typical amplitudes and periods of the surface gravity waves were ~1 m and 10 s, respectively. This results in sinuous horizontal advection having an amplitude of 0.6 m s^{-1}. The corresponding rms velocity is 0.4 m s^{-1} which, when added to the mean advection, yields an effective advection of ~0.5 m s^{-1}. The interpretation of frequency spectra as wavenumber spectra by means of an assumed mean advection is not affected by the oscillating flow for wavelengths large compared to the wave ampli-

tude. However, the effect of the oscillatory flow is quite complicated when wavelengths of the same order as the wave amplitude are considered. Qualitatively, the effect of the oscillations is to smear energy at a particular wavelength into a frequency band. For example, consider a wavelength of 0.25 m (the smallest that can be resolved by the instrument). The center of the frequency band in which the energy appears will be about 0.5 m s^{-1}(0.25 m)$^{-1}$ = 2 Hz. The spectral density at this frequency (Simpson and Paulson, 1980, Fig. 4) is about a factor of 10 less than that in the plateau. One must conclude, therefore, that the decrease in spectral density at frequencies > 0.5 Hz may be associated with a decrease in energy at wavelengths < 0.5 m s^{-1} (0.5 Hz)$^{-1}$ = 1 m. A definitive interpretation must await further investigation beyond the scope of this reply.

We agree with McLeish's view that the low-frequency portion of the spectra, given a constant advection rate, is consistent with previous observations of wavenumber spectral densities (McLeish, 1970; Saunders, 1972) that decrease with a log-log

slope of about -2. Taking 10 cm s^{-1} as the mean advection during our observations implies that wavelengths between 10 and 100 m obey the -2 power law. We did not include this interpretation in the paper because of uncertainty about the magnitude of errors caused by reflected downward long-wave radiation. Recently we have analyzed additional observations and have concluded that these errors do not affect the general shape of our frequency spectra. A paper including these results is in preparation.

McLeish has correctly noted that slicks may account for temperature variations in the intermediate frequency band between 0.05 and 0.5 Hz. As pointed out by Katsaros (1980), slicks can affect the surface brightness temperature in several ways: "(a) The emissivity of oils is typically less than that of water so the correction for sky reflection will be greater and the surface will appear cooler; (b) some organic materials, but not all, decrease evaporation; (c) since capillary waves will not form on a slick and since waves reduce ΔT (the temperature difference across the layer just below the surface),

other factors being constant one would expect a greater ΔT in the area of a slick; (d) if the oil film is fairly thick, but not so thick that convection occurs within it, its effect is to provide an additional layer through which heat is conducted primarily at the molecular rate, thereby augmenting ΔT in the water." Additional research is required to better understand and quantify the effects of slicks on surface brightness temperature under various atmospheric and oceanic conditions.

REFERENCES

Katsaros, K., 1980: Infrared surface temperature and gradients. *Air-Sea Interactions: Instruments and Methods*, Chap. 16, pp. 293–317, Dobson, F., L. Hasse and R. Davis, Eds., Plenum 801 pp.

McLeish, W., 1970: Spatial spectra of ocean surface temperature. *J. Geophys. Res.*, 75, 6872–6877.

Saunders, P. M., 1972: Space and time variability of temperature in the upper ocean. *Deep-Sea Res.*, 19, 467–480.

Simpson, J. J., and C. A. Paulson, 1980: Small-scale sea surface temperature structure. *J. Phys. Oceanogr.*, 10, 399–410.

Particulate organic carbon flux in the oceans—surface productivity and oxygen utilization

Erwin Suess

School of Oceanography, Oregon State University, Corvallis, Oregon 97331

Organic detritus passing from the sea surface through the water column to the sea floor controls nutrient regeneration, fuels benthic life and affects burial of organic carbon in the sediment record[1-3]. Particle trap systems have enabled the first quantification of this important process. The results suggest that the dominant mechanism of vertical transport is by rapid settling of rare large particles, most likely of faecal pellets or marine snow of the order of >200 μm in diameter, whereas the more frequent small particles have an insignificant role in vertical mass flux[4-6]. The ultimate source of organic detritus is biological production in surface waters of the oceans. I determine here an empirical relationship that predicts organic carbon flux at any depth in the oceans below the base of the euphotic zone as a function of the mean net primary production rate at the surface and depth-dependent consumption. Such a relationship aids in estimating rates of decay of organic matter in the water column, benthic and water column respiration of oxygen in the deep sea and burial of organic carbon in the sediment record.

The relationship is based on flux data compiled from particle traps installed throughout the world's oceans[7-19] by many investigators and from annual mean organic carbon production rates of the respective surface waters[20-29] (Table 1). In a few cases biological production rates were determined at the time of installing the sediment trap[12-16], the remaining data were compiled from other sources, often using annual mean rates from the general area of investigation. The predicted flux may overestimate the proportion of surface production intercepted at any given depth, when traps were installed during times of peak productivity (which was mostly the case) but then were normalized to lower mean annual production rates. Accordingly, equation (1) gives an upper limit of the net vertical carbon flux, if the production is known:

$$C_{flux(z)} = \frac{C_{prod}}{0.0238z + 0.212};$$

$$n = 33, \quad r^2 = 0.79, \quad z \geq 50 \qquad (1)$$

C_{prod} is the primary production rate of carbon at the surface, C_{flux} is the organic carbon flux at depth measured by the sediment traps, both in units of (g m^{-2} yr^{-1}), $z (\geq 50)$ is the water depth (m) at which the traps were moored, n is the number of observations, and r^2 the coefficient of correlation. Only flux data from below the euphotic zone (>50 m) are used in defining equation (1). This limitation also causes the non-zero intercept for $b = 0.212$. Moreover carbon fluxes in shallow waters, as in the western Baltic Sea[12-13] and along cross-shelf transects of the Peru coastal upwelling regime[16-18], are consistently less than predicted by extrapolating equation (1) to such depths (Fig. 1). These low yields are probably due to non-vertical motions of particles caused by advection, horizontal currents and locomotion of live plankton, thus exporting particulate matter from the site of sediment trap deployments.

Effects of ±15% uncertainty in primary production estimates are also shown in Fig. 1. This uncertainty is of the same magnitude as the variations and ranges of repeated flux measurements obtained using several traps at the same location. For example, particle flux measurements below the California Current[10] were repeated within the same season whereas the data from the Peru coastal upwelling system[17,18] are averaged

over several seasons, as indicated in Table 1. The collection and closure efficiency of certain trap designs, the problems of *in situ* decay of non-poisoned collectors, horizontal and resuspended flux probably contribute even more significantly to the scatter of the data[10,11].

However large the present uncertainties may be for the relationship of vertical fluxes of particulate carbon in the oceans, they have interesting implications. First, if depth can be adequately transformed into time, the slope of equation (1) implies some sort of rate constant. Actual measurements of large particle size spectra with depth are not available. For small particles ($d < 100$ μm) many theoretical models and empirical distribution patterns have been presented which suggested that particle populations get smaller in diameter with increasing depth[4,32]. The decrease in particle diameter with depth is thought to be a function of various chemical dissolution or oxidation processes[33-35]. Thus one would expect a gradual decrease in particle settling rates with depth. However, recent investigations suggest that biological repacking by successive feeding actually produces larger particles at the expense of smaller ones and that settling rates are extremely rapid[36]. A relationship of carbon-flux to surface-production from which minimum sinking rates can be inferred was recently also observed by Deuser and Ross[14] who showed that seasonality in surface production is reflected in like changes of the carbon flux in the deep Sargasso Sea. The coupling between production at the surface and deep flux—here at a depth of 3,200 m—within a period of a month or less, requires sinking rates of particles in excess of 100 m day^{-1}. Also Shanks and Trent[6] measured sinking rates of ~50-100 m day^{-1} for other large aggregates (marine snow) primarily involved in vertical mass transfer.

As a first approximation, then, depth and residence time may be linearly related and for simplicity a settling velocity of $w_s = 100$ m day^{-1} may be assumed in transforming depth (z) of equation (1) into time. This then enables the definition of an
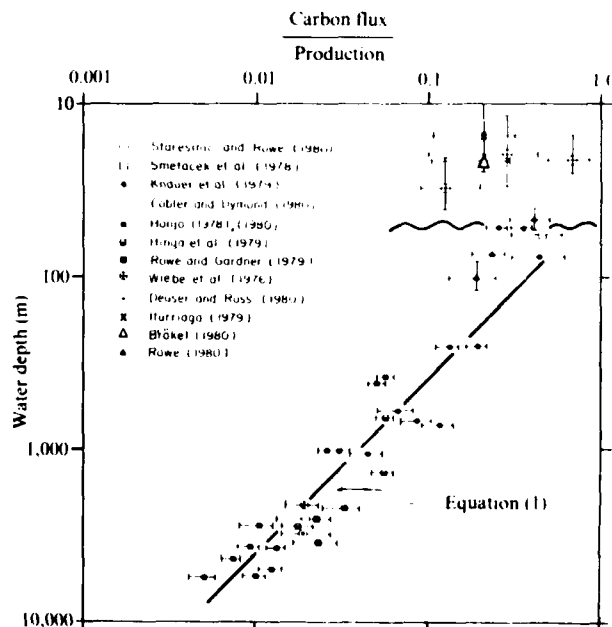
Fig. 1 Organic carbon fluxes with depth in the water column normalized to mean annual primary production rates at the sites of sediment trap deployment. The undulating line indicates the base of the euphotic zone, the horizontal error bars reflect variations in mean annual productivity as well as in replicate flux measurements during the same season or over several seasons; vertical error bars are depth ranges of several sediment trap deployments and uncertainties in the exact depth location. The data points by Rowe (1980) represent selected averages of 2-5 single sites at ~10 m above the bottom, where resuspension was assumed to be minimal

2

Table 1 Organic carbon fluxes in the water column and mean primary production rates

Latitude	Longitude	Water depth (m)	Carbon flux (g m⁻² yr⁻¹)	Production (g m⁻² yr⁻¹)	Refs
31 32 5′N	55 55 4′W	976	0.89	40	8, 29
		3,694	0.32		
		5,206	0.026[*]		
31 32 0 N	55 00.8′N	5,367	0.45	45	8, 29
13 30 2′N	54 00.1′W	389	2.46	50	8, 26
		988	1.44		
		3,755	0.63		
		5,068	0.62		
15 21.1′N	151 28 5′W	378	1.30	40	8, 26
		978	0.20[*]		
		2,778	0.40		
		4,280	0.32		
		5,582	0.24		
25 nm SE Bermuda		3,200	0.77	40	14, 23
0 36 N	86 6. W	2,570	2.0	100	15, 22
27 42. N	78 54. W	660	5.3	100	9, 24, 26
33 30. N	76 15. W	1,350	10.9	200	
38 23. N	69 45. W	3,520	5.6	250	
24 51. N	77 39. W	2,100	2.0 ± 0.3	100	7
36 42. N	122 13′W	50	158 ± 5	500	10, 20, 21
		250	92 ± 5		
		700	42 ± 2		
36 42. N	122 13′W	50	33 ± 7	150	
		250	19 ± 2		
		700	17 ± 2		
32 47. N	144 26′W	75	25 ± 10	100	
		575	5.3 ± 1		
		1,050	4.4 ± 2		
38 50. N	72 31. W	2,160	6.4 ± 0.2	200	11, 26, 28
38 28.5′N	72 02.3 W	2,800	3.5 ± 0.7	200	
38 19 N	69 37. W	3,500	5.4 ± 1.0	250	
55 38.6 N	15 22.9 E	55	65	4608, 150	12
7 39.5 S	79 31.9′W	22	378[‡]	650	17, 25
10 04.2 S	78 11.2′W	19	370[‡]	450	
11 58.5 S	77 11.0′W	20	253[‡]	300	
13 40.4 S	76 17.3′W	13	167[‡]	350	
15 04.5 S	75 26.6′W	50 ± 10	240 ± 100[‡]	1,200 ± 600	16, 17, 25
15 05 4 S	75 28.1′W	70	130 ± 20[‡]	600	17, 25
15 06 3 S	75 29.7′W	100 ± 10	110 ± 30[‡]	600	
53 30 N	10 02. E	20	30 ± 10	150	13, 19, 27

[*] Plotted as one datum point.
[‡] Flux measured during one season only.
[‡] Flux measured during two or more seasons.
§ Productivity determined during the same season when sediment traps deployed.

Table 2 Organic carbon utilization by benthic processes at two sites of the coastal upwelling regime off Peru

	Station 7706-39	Station 7706-36
Latitude	11 15.1′S	13 37.3′S
Longitude	77 57.4′W	76 50 5′W
Water depth (m)	186	370
	C-org (g m⁻² yr⁻¹)	
Production annual mean	500	400
Flux to seafloor using equation (1)	108	44
Burial rate from sediment accumulation[†]	40	17
Benthic utilization as carbon difference[‡]	68 38[*] 142	27
	O₂ (l m⁻² yr⁻¹)	
Oxygen demand	160 93-345[‡]	63

[*] Equivalent oxygen consumption rates are based on 2.43 ml O₂ consumed = 1.0 mg C utilized[41].
[†] Ref. 38.

time it is effectively removed from decomposition through burial is related to benthic respiration. In many cases the burial rate of organic carbon can be independently determined from linear bulk sedimentation rates, sediment densities, porosities and organic carbon contents. Consequently, the benthic respiration is the difference between the net vertical flux as predicted by equation (1) and the burial rate. The burial rate of organic matter, in turn, seems to be primarily controlled by the linear rate of sedimentation, as discussed elsewhere[37]. Results in Table 2 at two stations from the coastal upwelling regime off Peru illustrate how to estimate benthic respiration from vertical carbon flux minus carbon burial rate. The carbon utilization rates and the inferred bottom oxygen demand are well within the ranges reported from other coastal upwelling areas. Based on benthic production and faunal analyses, Christensen and
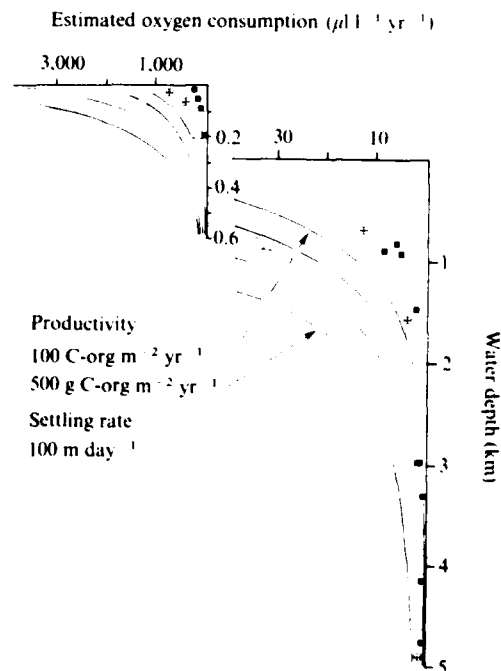
apparent rate constant for organic carbon decomposition from equation (2):

$$\frac{1}{\dfrac{C_{flux}}{C_{prod}}} - 0.212 = 2.38t \qquad (2)$$

where C_{prod} = production at $t = 0$, and the constant $k = 2.38$, [that is $z(0.0238)$], has the dimension day⁻¹ and the properties of a second-order rate constant. This is inferred because equation (2) is analogous to the expression for second-order rates in chemical kinetics: $1/C_t - 1/C_0 = kt$. In testing experimental data to ascertain second-order rate kinetics, $1/C_t$ plotted against t should yield a straight line relationship whose slope is equal to the rate constant k and the intercept equal to $1/C_0$. Accordingly, a fit for the carbon flux data in relation to depth (z), to settling velocity (w_s) and to primary production C_{prod} defines the equation above.

As a second implication, the extrapolation of the predicted carbon flux from equation (1) to the interception with the sea floor at any site yields the net carbon sedimentation before burial. This is independent of the actual rate laws and mechanisms that control organic matter consumption at depth or the variation in sinking rates of particulate matter. Net carbon sedimentation is an important parameter because it gives the upper limits of organic carbon accumulation in the sediment column. The preserved rate of burial can only be smaller than this flux. The magnitude of continued consumption of organic matter from the time it arrives at the sediment surface to the

Estimated oxygen consumption (μl l⁻¹ yr⁻¹)

Fig. 2 Vertical distribution of oxygen consumption rates in the ocean derived from changes of particulate carbon fluxes. The profiles are generated from equation (3) for mean primary productivities of between 100 and 500 g C-org m⁻² yr⁻¹, respectively. Vertical transfer of particles is at constant sinking rate of 100 m day⁻¹. Maximum potential oxygen consumption rates are shown for comparison from electron transport activities (□) and the corresponding estimated actual oxygen utilization (■). ∓, Oxygen consumption from bacterial utilization rates. The data points represent a composite profile from the eastern Pacific Ocean[42, 43]; note scale changes.

Packard[18] estimated benthic oxygen utilization rates at water depths ranging from 20 to 200 m for coastal upwelling areas off north-west Africa and Baja California to be between 93 and 345 (l m^{-2} yr^{-1}). Also, oxygen utilization rates of 60–550 (l m^{-2} yr^{-1}), with strong seasonal fluctuations, are reported from the first direct measurements of O_2-distribution profiles *in situ* and from incubation experiments of near-shore anoxic sediments from the western Baltic Sea[39,40].

The most far-reaching, yet tentative implication, is coupling oxygen consumption in the water column to the observed changes in vertical flux of particulate organic carbon. If for every 106 mol organic carbon consumed, 138 mol oxygen are utilized[41] and if the residence time of the particles within a parcel of seawater can be ascertained, rates of oxygen utilization at any depth can be predicted. Again for simplicity, assuming a mean sinking rate for particles $w_s = 100$ m day^{-1} yields the distribution of the total cumulative oxygen utilization with depth as:

$$\Delta O_2 = C_{prod}(6.66 \times 10^{-5})\left[1 - \frac{1}{0.0238(z) + 0.2.212}\right] \quad (3)$$

where the constant 6.66×10^{-5} converts carbon consumption to oxygen utilization in units of (ml l^{-1} day^{-1}); that is $\frac{1}{365}$ g C-org m^{-2} day^{-1} utilizes $2.43 \times \frac{1 O_2}{100}$ m^3 when assuming settling velocity of particles $w_s = 100$ m day^{-1}; therefore, $\frac{2.43}{365} \times 10^{-5} \times 10^{3} = 6.66 \times 10^{-5}$ ml l^{-1} day^{-1}. The proportion of organic carbon consumed is given by the expression $1 - \frac{1}{0.0238(z) + 0.212}$ and again, z is limited to depths $\geqslant 50$ m. To illustrate the usefulness of equation (3), vertical distribution profiles of oxygen consumption rates are generated for a water-column profile where the input of oxidizable particulate organic matter from the euphotic zone is between 100 and 500 g C m^{-2} yr^{-1} and the vertical mass transfer is assumed to be primarily through large particles at sinking rates of 100 m day^{-1}. Comparable oxygen consumption rates in water-column profiles deduced from electron transport activities, bacterial utilization rates and respirometer measurements are in general agreement with these predicted values, although ETS O_2-consumption rates appear higher by an order of magnitude at greater water depths (Fig. 2)[42-45]. Equation (3) also assumes O_2-consumption to be only by the utilization of particulate organic matter, whereas actually, dissolved organic carbon is also utilized[46].

The oxygen distribution resulting from the predicted consumption rates of equation (3) largely follows that of the classical circulation model by Wyrtki[47], the basic difference being that his model utilizes an exponential oxygen consumption term with depth following first-order rate kinetics, that is $C_z = C_0 e^{-kz}$, whereas the carbon flux measurements presented here are better approximated by a second-order fit. The only way that the carbon flux data would follow a first-order rate expression is in the case of accelerated settling of particles; that is, if sinking rates were actually to increase with depth in the water column.

These early results from particle traps apparently tie together successfully processes of organic carbon cycling in the oceans that previously have been treated separately by marine biologists, chemists and sedimentologists. Sizes and shapes of particles involved in vertical mass flux and seasonally adjusted surface productivity and deep carbon fluxes hold the key to understanding fully organic carbon cycling in the ocean and related oxygen and nutrient distributions.

1. Redfield, A. C., Ketchum, B. H. & Richards, F. A. in *The Sea*, Vol. 2 (ed. Hill, M. N.) 26-77 (Wiley, New York, 1963).
2. Smith, K. L. *Mar. Biol.* **47**, 337-347 (1978).
3. Müller, P. J. & Suess, E. *Deep-Sea Res.* **26**, 1347-1362 (1979).
4. McCave, I. N. *Deep-Sea Res.* **22**, 491-502 (1975).
5. Schrader, H.-J. *Science* **174**, 55-57 (1971).
6. Shanks, A. L. & Trent, D. *Deep-Sea Res.* **27**, 137-143 (1980).
7. Wiebe, P. H., Boyd, S. H. & Winget, C. *J. mar. Res.* **34**, 341-354 (1976).
8. Honjo, S. *J. mar. Res.* **36**, 469-492 (1978); **38**, 53-97 (1980).
9. Hinga, K. R., Sieburth, J. & Heath, G. R. *J. mar. Res.* **37**, 557-579 (1979).
10. Knauer, G. A., Martin, J. H. & Bruland, K. W. *Deep-Sea Res.* **26**, 97-108, 1979.
11. Rowe, G. T. & Gardner, W. D. *J. mar. Res.* **37**, 581-600 (1979).
12. Smetacek, V., von Brokel, K. & Zeitschel, Zenk, W. *Mar. Biol.* **47**, 211-226 (1978).
13. Iturriaga, R. *Mar. Biol.* **55**, 157-169 (1979).
14. Deuser, W. G. & Ross, E. H. *Nature* **283**, 364-365 (1980).
15. Cobler, R. & Dymond, J. *Science* **209**, 801-802 (1980).
16. von Brokel, K. *Abstr. IDOE int. Symp. on Coastal Upwelling*, Los Angeles, 1980.
17. Rowe, G. T. *Symp. on Bio-productivity of Upwelling Ecosystems*, Moscow, 1979.
18. Staresinic, N. & Rowe, G. T. *Abstr. IDOE int. Symp. on Coastal Upwelling*, Los Angeles (1980).
19. Zeitschel, B. *Kieler Meeresforsch.* **21**, 55-80, 1965.
20. Owen, R. W. *California Cooperative Oceanic Fisheries Investigations, Atlas* No. 20, 98-104 (State of California, Marine Research Committee, 1974).
21. Ryther, J. H. *Science* **166**, 72-76 (1969).
22. Love, C. M. & Allen, R. M. (eds) *Eastropac Atlas 10* (US Government Printing Office, Circ. 330, 1973).
23. Menzel, D. W. & Ryther, J. H. *Deep-Sea Res.* **6**, 351-367 (1960).
24. Ryther, J. H. in *The Sea*, Vol. 2 (ed. Hill, M. N.) 347-380 (Wiley, New York, 1963).
25. Guillen, O., de Mendiola, B. R. & de Rondan, R. I. *Oceanography of the South Pacific* (New Zealand National Committee for UNESCO, Publ. 405-418, 1973).
26. Koblentz-Mishke, O. J., Volkovinsky, V. V. & Kabanova, J. G. *Scientific Exploration of the South Pacific* (ed. Wooster, W.) 183-193 (National Academy of Sciences, Washington, 1970).
27. von Bodungen, B. thesis, Univ. Kiel (1975).
28. Ryther, J. H. & Yentsch, C. S. *Limnol. Oceanogr.* **3**, 327-335, 1958.
29. Ryther, J. H. & Menzel, D. W. *Deep-Sea Res.* **6**, 235-238 (1960).
30. Dymond, J. *et al. Earth planet. Sci. Lett.* (in the press).
31. Kirchner, W. B. *Limnol. Oceanogr.* **20**, 657-660 (1975).
32. Brun-Cottan, J. C. *J. geophys. Res.* **81**, 1601-1606, 1976.
33. Lal, D. & Lerman, A. *J. geophys. Res.* **80**, 423-430, 1975.
34. Wollast, R. *The Sea* Vol. 5 (ed. Goldberg, E. D.) 369-392 (Wiley, New York, 1974).
35. Lal, D. *Science* **198**, 997-1008 (1977).
36. Honjo, S. & Roman, M. R. *J. mar. Res.* **36**, 45-75 1978.
37. Müller, P. J. & Suess, E. *Deep-Sea Res.* **26**, 1347-1362 (1979); *Colloq. int. du CNRS* No. 293, 17-26 (1980).
38. Christensen, J. P. & Packard, T. T. *Deep-Sea Res.* **24**, 331-343 1977.
39. Revsbech, N. P., Jorgensen, B. B. & Blackburn, T. H. *Science* **207**, 1355-1356 1980.
40. Revsbech, N. P., Sorensen, J., Blackburn, T. H. & Lomholt, J. P. *Limnol. Oceanogr.* **25**, 403-411 (1980).
41. Richards, F. A. *Chem. Oceanogr.* **1**, 611-645 1965.
42. Packard, T. T., Healy, M. L. & Richards, F. A. *Limnol. Oceanogr.* **16**, 67-70 1971.
43. Knoppnick, P. *Deep-Sea Res.* **21**, 211-227 (1974).
44. Craig, H. *J. geophys. Res.* **76**, 5078-5086 (1971).
45. Carlucci, A. F. & Williams, P. M. *Naturwissenschaften* **65**, 541-542, 1978.
46. Williams, P. M. & Carlucci, A. F. *Nature* **262**, 810-811 1976.
47. Wyrtki, K. *Deep-Sea Res.* **9**, 11-23 (1962).

PRODUCTIVITY, SEDIMENTATION RATE
AND SEDIMENTARY ORGANIC MATTER IN THE OCEANS
II. – ELEMENTAL FRACTIONATION

Erwin SUESS and Peter J. MÜLLER *
School of Oceanography, Oregon State University, Corvallis, Oregon 97331

RÉSUMÉ. – Le flux vertical des substances organiques d'origine biogénique à la surface des sédiments est fonction de la profondeur d'eau et de la productivité primaire : ceci peut s'exprimer par la relation empirique :

(1) Flux $C_{org} = 5,9 \cdot$ profondeur d'eau $^{-0.616} \cdot$ productivité

En descendant la colonne d'eau et avant d'être enterré, le détritus organique biogénique subit un fractionnement des éléments par la soustraction préférentielle de composés organiques azotés et phosphoriques. A l'interface eau-sédiment une partie du détritus est convertie en biomasse par des organismes benthiques concentrant ainsi l'azote et le phosphore par rapport au carbone. Ces deux processus se reflètent dans la composition élémentaire des matières sédimentaires d'origine organique. Un troisième processus concentre la matière organique dans les sédiments, par adsorption sur les argiles. Cette matière adsorbée a un haut contenu en azote organique et est dépourvue de phosphore organique ; elle a un rôle important seulement pour les argiles pélagiques. Les quantités respectives de chacune des trois formes de matière organique, c'est-à-dire – détritique, en biomasse, et adsorbée – peuvent être calculées en employant les formules suivantes :

(2) $C_{adsorbe}$-org. $= 0.005 \ Al_2O_3$

(3) $C_{detritus}$-org. $= \dfrac{C_{total}\text{-org.} - C_{adsorbe}\text{-org.} - e \ N_{total}\text{-org.}}{(1 - e/f)}$

(4) $C_{biomasse}$-org. $= C_{total}$-org. $- C_{detritus}$-org. $- C_{adsorbe}$-org.

Dans ces expressions e et f sont respectivement les proportions de C/N élémentaire de la biomasse et du détritus.

ABSTRACT. – The vertical flux of biogenous organic matter to the sediment surface is a function of water depth and primary productivity ; this relationship can be expressed empirically as :

(1) org-$C_{flux} = 5.9 \cdot$ depth $^{-0.616} \cdot$ productivity

Upon descent through the water column and prior to burial, biogenous *detrital organic matter* undergoes strong elemental fractionation by preferential removal of nitrogenous and P-containing organic compounds. At the water-sediment interface, a portion of the detritus is converted into *biomass* by benthic organisms, which concentrate nitrogen and phosphorus relative to carbon. These two processes are reflected in the elemental composition of sedimentary organic matter. A third process concentrates organic matter in sediments by sorption onto clays. This *sorbed material* is high in organic-N and devoid of organic-P ; its relative abundance is high only in pelagic clays. The concentrations of each of the three forms of organic matter – detrital, biomass, and sorbed – can be calculated from the following expressions :

(2) org-$C_{sorb} = 0.005 \cdot Al_2O_3$

(3) org-$C_{det} = \dfrac{\text{org-}C_{total} - \text{org-}C_{sorb} - e \cdot \text{org-}N_{total}}{(1 - e/f)}$

(4) org-$C_{biom} = $ org-$C_{total} - $ org-$C_{det} - $ org-C_{sorb}

where e and f are the C/N elemental weight ratios of biomass and detritus respectively.

INTRODUCTION

Biogenous organic matter is the most complex and the least chemically stable mixture of all constituents in the oceans. Biochemical processes begin to fractionate this mixture extensively as soon as it leaves the euphotic zone. Fractionation persists throughout the subsequent history of settling, decomposition, dissolution, ingestion, resuspension and eventual burial as part of the sediment record. The significance of chemical fractionation here is

that the elemental assemblage contains information about the nature of the biochemical processes and allows estimates to be made of the magnitude and sources of organic matter reservoirs.

In this study, we examine the fractionation of org-C, org-N and org-P in biogenous matter in the oceans, and develop a preliminary model that partitions the total sedimentary organic matter into marine plus terrestrial detritus, benthic biomass, and clay-sorbed material. In three of the following sections we develop arguments

* Geologisches Institut, Olshausenstrasse 40-60, 2300 Kiel, Fed. Rep. Germany.

and present data which yield the major elemental compositions of the three end-members used in this model. These different forms of organic matter when mixed in varying proportions, make up the total sedimentary organic matter inventory and are also responsible for its characteristic org-C:org-N:org-P ratios.

Major advances are presently being made in related fields which serve to emphasize the importance of understanding elemental fractionation. Attempts are underway to directly measure vertical mass fluxes in the oceans, thus contributing to the quantification of factors controlling organic matter accumulation.

Relevant to the discussion here are data on the composition and fluxes of biogenous matter as reported by Bishop et al. (1977), Cobler and Dymond (1980), Hinga et al. (1979), Honjo (1978), Knauer et al. (1979), Smetacek et al. (1978), Spencer et al. (1978), and Staresinic (1978). Also, the mechanisms of fractionation have been studied extensively and models have been proposed for microbial decomposition under oxic, suboxic and anoxic conditions. These models are based primarily on pore-water chemical data and nutrient distributions near the water-sediment interface (Berner, 1974; Bender et al., 1977; Froelich et al., 1979; Murray et al., 1978; Suess, 1976, 1979). Finally, external factors controlling organic matter preservation and composition in marine environments have been receiving increasingly more attention. Important factors are rate of burial, oxygenation of bottom waters, primary production, terrigenous organic matter input, role of benthic biomass and stabilization by clay interaction (Demaison and Moore, 1980; Dow, 1978; Heath et al., 1977; Kepkay et al., 1979; Müller, 1975, 1977; Müller and Suess, 1979; Suess et al., 1980).

ORGANIC MATTER FLUX

Ever since McCave (1975) pointed out that the rare, large particles (> 100 μm) in the oceans potentially dominate the vertical mass transport, direct vertical flux measurements have greatly proliferated. The first generation of particle trap experiments dealt with sampling efficiency, general design, deployment and sample handling; the present generation of instruments have provided the first data that can be used to estimate fairly reliable fluxes. By no means are all of the problems of such direct measurements entirely solved, however.

In Figure 1 the depth dependent vertical organic carbon flux – as measured by various particle trap systems – has been compiled and normalized to the rate of primary carbon fixation. This empirical relationship allows the organic carbon flux at any depth in the water column to be estimated from the primary carbon fixation at the surface, multiplied by $5.9 \cdot x^{-0.616}$, where x = water depth.

Both the kinetics of organic matter decomposition and particle settling probably contribute to this observed relationship (Suess, 1980a). For the purpose of the dis-

cussion here, however, only one point appears important; i.e., that the vertical organic carbon flux in deep waters – although greatly reduced – still reflects surface productivity in a predictable fashion. Figure 1 allows the net organic carbon flux to the sediment surface prior to burial (in the following called carbon sedimentation) to be estimated at any point in the deep sea. Comparison of this net flux to the rate of carbon burial (in the following called carbon accumulation) reveals additional complications. It is at this stage that the bulk sedimentation rate plays a crucial role in organic carbon preservation (e.g., Müller and Suess, 1979; Figure 2).

Slow rates of sedimentation allow enhanced decomposition of organic matter prior to burial, whereas rapid rates reduce decomposition since the exposure time and loss of organic matter due to remineralization are reduced. This interrelationship between organic matter production and consumption in the water column and at the water-sediment interface is reflected in the elemental fractionation of organic carbon, organic nitrogen and organic phosphorus.

FRACTIONATION

During settling of organic matter through the water column and exposure prior to burial the major biogenous elements C, N and P are differentially mobilized. Table I shows mass fluxes, elemental compositions and accumulation rates of organic matter from four marine environments compiled from published sources and from our own investigations. In each section, the production numbers represent integrated, mean annual carbon productivity rates from which, where no direct analysis was available, organic-N and organic-P have been calculated using the well-known Redfield ratios.

The elemental flux and compositional data for the water column are direct measurements reported by the authors referenced. Available accumulation rate data are from near-surface sediments in the general areas of sediment trap deployment (refs. : see footnote Table I). We selected for this compilation only radiometrically dated sediments with undisturbed surfaces – generally collected with box cores – and with direct measurements available for bulk density and porosity.

The changes in elemental ratios normalized to atomic carbon = 106 indicate preferential organic-N and organic-P losses from particulates settling through the water column, but relative enrichments of theses elements in near-surface sediments. The fractionation between carbon, nitrogen and phosphorus in the water column is in accordance with what we know about and expect from nutrient regeneration (Redfield et al., 1963; Richards, 1965; Berner, 1977, 1974; Almgren et al., 1975; Billen, 1977).

The changes of elemental composition in near-surface sediments we attribute to differing benthic popula-

TABLE I

Biogenous element fluxes in the water column and accumulation in the sediment record

OPEN OCEAN (1)

	Biogenous Element Fluxes (g m^{-2} year^{-1})			Elemental Ratios (Redfield)		
	C	N	P	C	N	P
Production	50	8.8	1.2	106	16	1.0
Particle flux						
Euphotic zone	25	2.1	0.16	106	7.9	0.25
Water column	0.80	0.030	0.0022	106	3.5	0.11
Accumulation	0.0031	0.00069	0.000069	106	20	0.91

CALIFORNIA MARGIN (2)

	Biogenous Element Fluxes (g m^{-2} year^{-1})			Elemental Ratios (Redfield)		
	C	N	P	C	N	P
Production	250	44	6.1	106	16	1.0
Particle flux						
Euphotic zone	158	21	2.15	106	12	0.56
Water column	42	4.6	0.58	106	10	0.56
Accumulation	2.2	0.23	0.032	106	10	0.60

PERU MARGIN (3)

	Biogenous Element Fluxes (g m^{-2} year^{-1})			Elemental Ratios (Redfield)		
	C	N	P	C	N	P
Production	350	62	8.5	106	16	1.0
Particle flux						
Euphotic zone	195	31		106	14	
Water column	87	8.8		106	9.2	
Accumulation	38	4.7	0.47	106	11.0	0.23

BALTIC SEA (4)

	Biogenous Element Fluxes (g m^{-2} year^{-1})			Elemental Ratios (Redfield)		
	C	N	P	C	N	P
Production	160	28	3.9	106	16	1.0
Particle flux						
Euphotic zone	24	3.1		106	11.7	
Water column	65	6.5	0.42	106	9.1	0.27
Accumulation	28	3.8	0.55	106	12.4	0.34

(1) Composite data from : Knauer *et al.* (1979), Cobler and Dymond (1980).
(2) Composite data from : Knauer *et al.* (1979), Sholkovitz (1973),
    Bruland *et al.* (1974).
(3) Composite data from : Staresinic (1978), Müller ans Suess (1979).
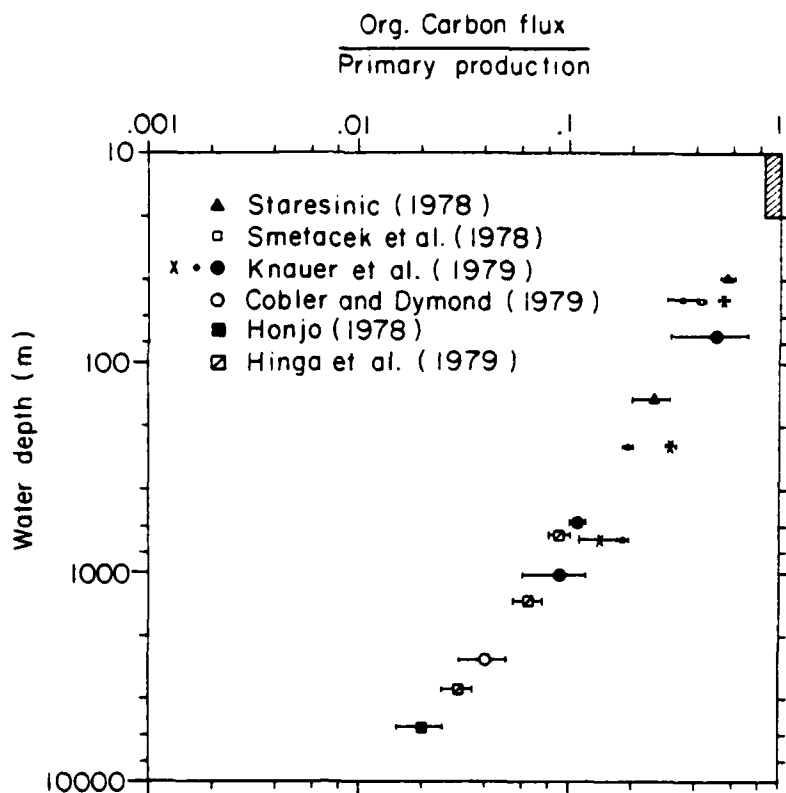(4) Composite data from : Smetacek *et al.* (1978), Suess and Erlenkeuser (1975).

$$\frac{\text{Org. Carbon flux}}{\text{Primary production}}$$

FIG. 1. – Vertical flux of org-C through the water column as a function of primary productivity and water depth; compiled from the sediment trap data of many investigators.

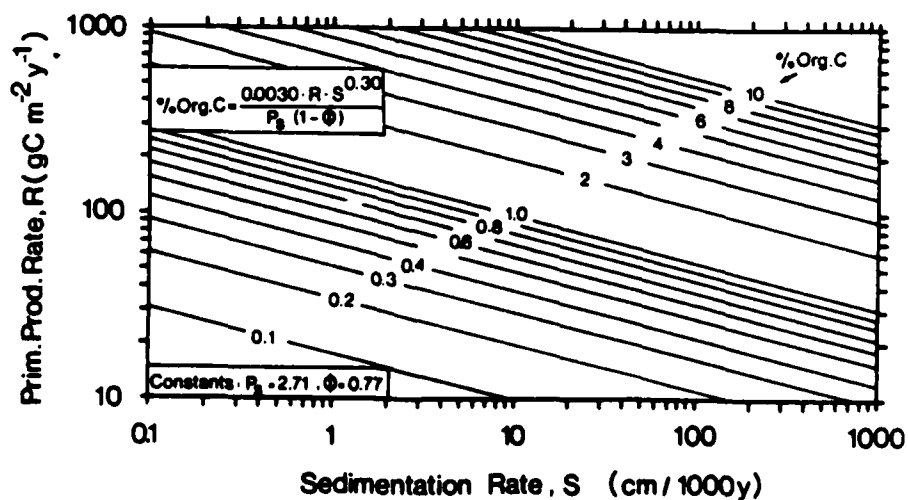% org-C remaining = $5.9 \cdot x^{-0.616}$

x = water depth, n = 17, $r^2 = 0.93$.

FIG. 2. – Dependence of sedimentary organic carbon contents on primary productivity rates (R) and sedimentation rates (S) for constant physical properties (p_s = dry density of solids, φ = porosity). At constant primary production rates the org-C content approximately doubles with each 10-fold increase in sedimentation rate. Muller and Suess (1979).

tions and to the role of clay-sorbed organic matter. A comparison of C/N atomic ratios of particulates and bottom sediments from the Peru margin and the Baltic Sea (Table I) shows that 80 ± 5 % of the organic-N is remineralized but only 65 ± 5 % of the org-C is consumed during the first ~ 100 m of descent through the water column at these sites. In the organic matter of the respective surface sediments, however, the sequence is reversed and org-C appears more strongly depleted than organic-N and organic-P. This change we attribute to the synthesis of new benthic biomass from settling detritus and to the increased respiration of org-C.

Knauer et al.'s data and the only existing organic-P value from the Balctic Sea particulate flux measurements show that the fate of organic-P is quite similar to that or organic-N. In fact, it appears that org-C:org-P ratio changes might be more sensitive fractionation indicators than org-C:org-N rations, and might, in waters shallower than 200 m, even be related to the magnitude of primary organic matter production rather than to water depth alone. For the purpose of this discussion, however, we shall characterize organic detritus, the first component of our model, by :

org-C:org-N:org-P = 106:9:0.3.

This is typical of detritus produced in highly fertile waters, provided its descent through oxygenated waters does not exceed 200 m, as is the case for the examples from the Peru margin and the Baltic Sea. For less fertile waters and greater transit depths stronger fractionation affects the organic detritus such that is composition is given by :

org-C:org-N:org-P = 106:6:0.1.

As more sediment-trap data become available, it should be possible to derive an expression for the detrital organic input to the sediment surface (= *organic matter sedimentation*) as a function of primary produc-

tion, water depth and degree of elemental fractionation. Such an expression would not, however, differentiate between terrigenous and authigenic marine organic matter.

⸫ ᴋBED MATTER

In pelagic sediments, where detrital marine and terrestrial organic matter input are greatly reduced, Müller (1975, 1977) found a unique nitrogen-rich organic matter fraction that is attributable to clay-sorbed material. Detection was possible by differentiating analytically between inorganically-bound N – largely as fixed NH_4 of illitic clays – and organically-bound N. The chemical nature and origin of the sorbed organic matter fraction have not been determined as yet but Hedges (1979) suggests that melanoidians might form from amino acids and sugars catalyzed by clay surfaces and Müller (1977) speculates that amino acids may be preferentially sorbed from sea-water by clays. Whatever the nature and mechanisms of formation may be, sorbed organic matter appearts difficult to metabolize, it is devoid of organic-P, and its quantity in pelagic sediments is related to the Al_2O_3 content (Figure 3).

In a recent paper Müller and Mangini (1979) have partitioned the organic carbon reservoir of pelagic sediments into a metabolizable and a residual fraction. These data are here supplemented by organic-P values (Suess, 1980b) for two central Pacific near-surface sediment cores to define the mean composition of the sorbed organic matter fraction and also give a limit for the composition of the benthic biomass (Table II).

Clearly the quantity of sorbed organic matter is insignificant within a total carbon inventory of surface sediments since it is limited by the clay mineral content. The high organic-N concentration and the absence of
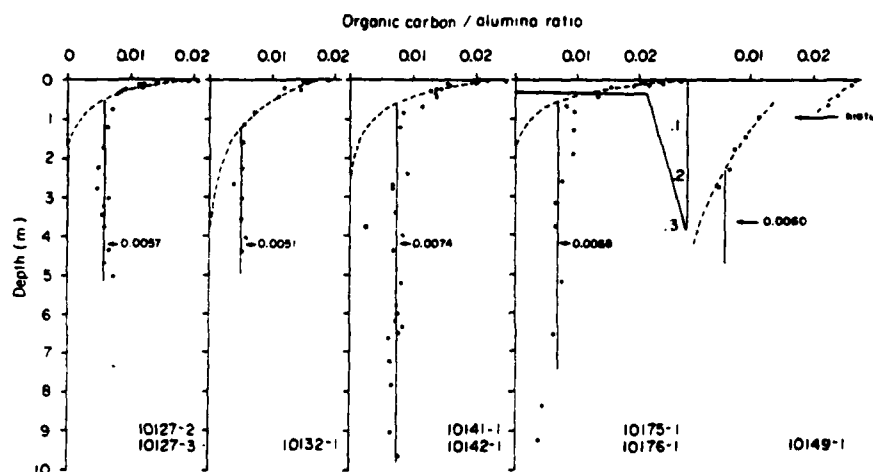

FIG. 3. – Depth distribution of org-C/Al_2O_3 in sediments from the central North Pacific. Constant values below about 1 m depth indicate clay-sorbed residual organic carbon. Above this depth metabolizable organic carbon, consisting of biomass and detritus, is gradually depleted. Core 10149-1 shows a $\sim$70,000 year hiatus. Modified from Müller and Mangini (1979).

organic-P do strongly affect the ratios of the major elements of sedimentary organic matter when they are used as indicators for typical reservoirs in sediments containing less than 1.0 wt.-% org-C; but in sediments with more than 1 wt.-% org-C, sorbed organic matter and its elemental chemistry may safely be ignored. We conclude that sorbed organic matter, as the second constituent of our model, is characterized by org-C/$Al_2O_3 = 0.0028$.

BENTHIC BIOMASS

Where rates of sedimentation are extremely slow, such as beneath the centers of the oceanic gyres, hardly any of the sedimented carbon is buried. Instead it appears to be entirely utilized by benthic organisms which produce a strong elemental fractionation. Organic-C is respired and org-N and org-P are enriched in the newly synthesized organic matter under such conditions. This process can best be evaluated by observing org-C/org-P ration changes as a function of the percentage of organic carbon preserved in the sediment (Figure 4). The

relative high org-P contents of central Pacific sediments described earlier (Table II) seem to us indicative of a significant proportion of benthic biomass there. If the metabolizable organic carbon in cores 10132-1 and 10149-1, as listed in this table, consists dominantly of benthic biomass carbon and small amount of detrital carbon, the biomass fraction must have org-C/org-P wt.-ratios of less than 20-40. This range is not unlike that of microbial biomass (Gunsalus and Stanier, 1960). Since, however, a small amount of org-P is tied up in detrital organic matter, the biomass fraction must have an even lower value for the elemental wt.-ratio. We take the ratio org-C_{biom}/org-P_{biom} to be about 16. This then characterizes the composition of the third component of our organic partition model, the benthic biomass.

PARTITIONING MODEL

Attempts at partitioning elements of sedimentary components among several sources are not new. Mackenzie and Garrels (1966) have shown how distributing

TABLE II

Down-core distribution of alumina and biogenous elements in central Pacific sediments.

The near-surface sections show evidence for the presence of *benthic biomass* and *detrital* organic matter, whereas the deeper sections contain only *claysorbed* organic matter.

VA 10149-1

Depth	Al_2O_3	org-C_{total}	org-N_{total}	N_{fixed}	org-P_{total}
0-2	14.0	0.354	0.131	0.027	0.008
2-4	13.7	0.329	0.077	0.025	0.004
4-6	13.4	0.309	0.077	0.026	0.005
6-9	14.1	0.156	0.062	0.013	0.000
9-12	13.7	0.127	0.050	0.011	0.001
12-16	12.5	0.091	0.036	0.009	0.000
16-20	10.9	0.069	0.033	0.007	0.000
20-24	11.9	0.060	0.021	0.008	0.000

VA 10132-1

Depth	Al_2O_3	org-C_{total}	org-N_{total}	N_{fixed}	org-P_{total}
0-4	11.7	0.219	0.049	0.017	0.006
4-8	11.0	0.163	0.038	0.015	0.005
8-12	8.2	0.128	0.031	0.014	0.007
18-24	8.2	0.096	0.021	0.013	0.003
24-30	7.4	0.107	0.022	0.014	0.002
38-52	9.8	0.110	0.034	0.017	0.000
78-92	12.6	0.090	0.040	0.012	0.000
111-124	14.4	0.081	0.040	0.013	0.000

Data from : Müller and Mangini (1979) and Müller (1975).
Depth in cm below interface.
Concentrations in wt.-% of dry sediment.

elements among mineral phases on a quasi-normative basis is a useful tool for gaining a first understanding of the sedimentary mass balance in the oceans. Heath and Dymond (1977). Dymond *et al.* (1977) and Boström *et al.* (1973, 1978) used chemical models based on interelement relations to partition certain major and minor elements of surface sediments of the Pacific Ocean into detrital, hydrothermal, hydrogenous and biogenous sources. More recently, linear programming has been utilized to optimize the algebraic solutions (Dymond *et al.*, 1979). Here, we use a simple model to partition organic matter between detrital, biomass, and sorbed sources. Partitioning is governed by the following relations :

(1) $\text{org-C}_{total} = \text{org-C}_{sorb} + \text{org-C}_{biom} + \text{org-C}_{detr}$

(2) $\text{org-N}_{total} = N_{total} - N_{fixed}$

(3) $\text{org-N}_{total} = \text{org-N}_{sorb} + \text{org-N}_{detr} + \text{org-N}_{biom}$

(4) $\text{org-P}_{total} = \text{org-P}_{biom} + \text{org-P}_{detr}$

These relations require that there are no organic reservoirs other than sorbed material, biomass and detritus; that each reservoir has a characteristic elemental composition; and that Al_2O_3, N_{fixed}, N_{total}, org-C, and org-P for the bulk sediment can be determined analytically. Listed below are our estimates of the chemical characteristics of the three organic matter reservoirs (values refer to surface sediments only) :

(5) $\text{org-C}_{sorb} = a \cdot Al_2O_3$

(6) $\text{org-N}_{sorb} = 1/b \cdot \text{org-C}_{sorb}$

(7) $\text{org-P}_{sorb} = 0$

where a = 0.005

b = org-C_{sorb} /org-N_{sorb} wt.-ratio = 1.8

(8) $\text{org-C}_{detr} = \dfrac{\text{org-C}_{total} - \text{org-C}_{sorb} - c \cdot \text{org-P}_{total}}{(1-c/d)}$

where c = org-C_{biom} /org-P_{biom} wt.-ratio = 16

d = org-C_{detr} /org-P_{detr} wt.-ratio = 400

Alternatively, org-C detritus can also be calculated from the nitrogen-to-carbon relationships. Accordingly,

(9) $\text{org-C}_{detr} = \dfrac{\text{org-C}_{total} - \text{org-C}_{sorb} - e \, (N_{total} - N_{fix})}{(1-e/f)}$

where e = org-C_{biom} /org-N_{biom} wt.-ratio = 4

f = org-C_{detr} /org-N_{detr} wt.-ratio = 15

Finally, then, the remainder of the elemental proportions are found by using the detrital organic carbon contents and the respective elemental ratios of detritus and biomass to yield :

(10) $\text{org-N}_{detr} = N_{total} - N_{fixed} - \text{org-N}_{sorb} - \text{org-N}_{biom}$

(11) $\text{org-P}_{detr} = \text{org-P}_{total} - \text{org-P}_{biom}$

In the following examples these equations and the characteristic elemental ratios are used to partition the total organic carbon of 8 surface sediments from widely differing environments into their respective fractions of sorbed, detrital and biomass material. The results are illustrated in Fig. 5. The areas of each circle reflect the amounts of different organic carbon reservoirs in each sample. The sorbed fraction amounts to ~1/4 of the total organic carbon in pelagic sediments, whereas in
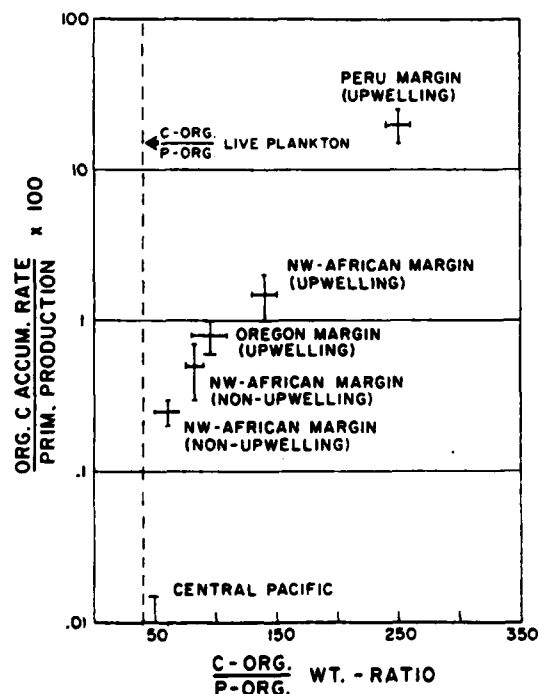

FIG. 4. – Decomposition of sedimentary organic matter (org-C/org-P wt.-ratios) as a function of the percentage preserved in the sediment. For low percentages (< 0.1 %) preserved, the organic matter composition approaches that of the benthic biomass and for high percentages (> 1.0 %), it is dominated by detrital organic matter.
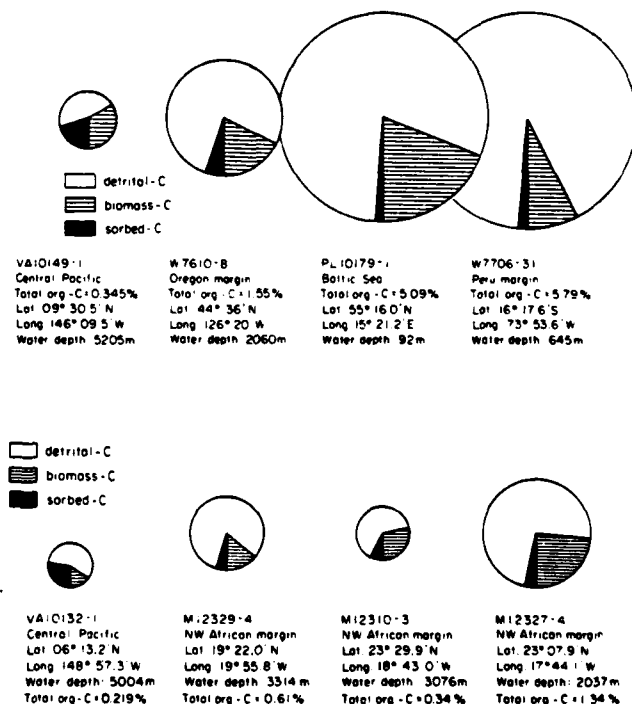
FIG. 5. – Proposed partitioning of sedimentary organic carbon into detritus, biomass and sorbed material. Sorbed and biomass carbon are important only in pelagic sediments; continental margin sediments are dominated by organic detritus. Absolute amounts of biomass and relative amounts of detritus decrease steadily with increasing water depth.

continental margin sediments it is negligible. Benthic biomass and marine plus terrestrial detritus dominate the organic carbon content in pelagic sediments. It is interesting that the absolute amount of biomass carbon steadily decreases with increasing water depths regardless of the proportions of detritus and the absolute amounts of org-C_{total}. Also, it is striking that the proportions – and absolute amounts – of detrital carbon decrease with distance from the coast, in response to decreasing fertility, terrestrial organic matter input and bulk sedimentation rate, or some combination of these factors. In environments where the sedimentation of organic matter is dominated by only one source, the elemental ratios may be interpreted directly without partitioning to identify approximately the controlling source. Two such examples in the regional distribution patterns of org-C/org-P and org-C/org-N wt.-rations of surface sediments from the eastern South Pacific are shown below (Figs. 6, 7). The possible regional extent (Fig. 6) of detrital organic matter and clay-sorbed material in these sediments is suggested by the elemental ratios. Values of org-C/org-P below 50 indicate the presence of some org-P depleted detritus, whereas values of more than 200 identify the sites where organic detrital sedimentation is dominant. In this example from the Peru margin the organic detritus which dominates sedimentation in the areas of present-day coastal upwelling is likely to be of marine origin.

The second example (Fig. 7) illustrates the regional extent of clay-sorbed, nitrogen-rich organic matter. Patterns of org-C/org-N wt-ratios show values of less than

5 in the Peru and Chile Basins. The portion of the Chile Basin with values below 3 is located beneath the northeast margin of the South Pacific gyre and below the calcite compensation depth. Accordingly, detrital organic matter and benthic biomass are low, so that nitrogen-rich sorbed material dominates the organic matter in the sediments.

Clearly, the partitioning model for organic matter in surface sediments and the resultant interpretation of elemental ration patterns are of a preliminary nature. Nevertheless we believe that this model provides an alternative to existing techniques for interpreting organic analyses of sediments in terms of sources and transformation reactions. Improvements are necessary in the areas listed below before applying this model more extensively :

(a) Better knowledge of the general variability in elemental composition of the three proposed sources;

(b) Independent verification of our estimates of benthic biomass, particularly that produced by microbes;

(c) Improvements in analytical techniques for the determination of organic-P in the presence of large amounts of inorganic phosphate;

(d) Determination of the chemical nature and association mechanisms of clay-sorbed matter;

(e) Expansion of the fractionation scheme to include organic oxygen and hydrogen as major biogenous elements so that the model can utilize organic matter classifications based on van Krevelen's interpretation (Tissot and Welte, 1978);

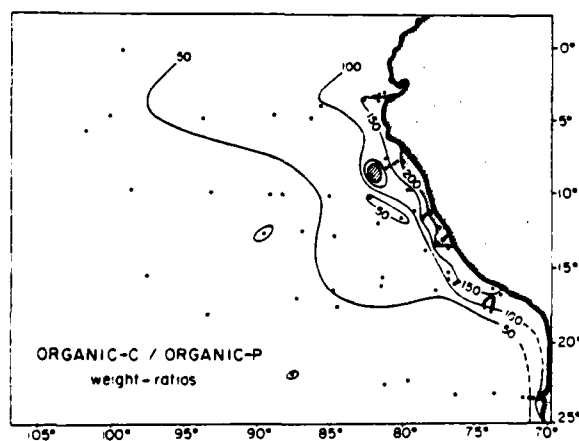(f) Further attempts to differentiate between organic detrital components of marine and terrestrial origin.

FIG. 6. – Regional pattern of org-C/org-P wt. ratios in surface sediments of the eastern South Pacific. High ratios (> 200) in continental margin sediments indicate the dominant input of detrital organic matter from coastal upwelling productivity off Peru. Low ratios (< 50) delineate the extent of benthic biomass as a significant constituent of sedimentary organic matter.
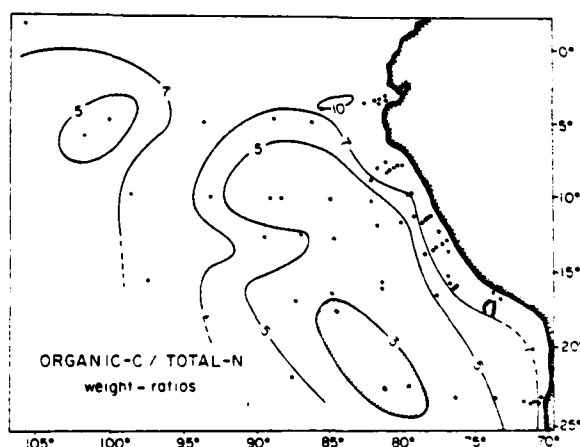
FIG. 7. – Regional pattern of org-C/org-N_{total} wt. ratios in surface sediments of the eastern South Pacific. Low ratios (< 5) in the Peru, Chile and Bauer Basins delineate the extent of nitrogen-rich, clay-sorbed organic matter. These ratios are not corrected for fixed N.

ACKNOWLEDGEMENTS

REFERENCES

ALMGREN T., L.-G. DANIELSSON, D. DYRRSEN, T. JO-HANSSON, and G. NYQUIST (1975). − Release of inorganic matter from sediments in a stagnant basin. *Thalassia Yugoslav, 11*, p. 19-29.

BENDER M.L., K.A. FANNING, P.N. FROELICH, G.R. HEATH, V. MAYNARD (1977). − Interstitial nitrate profiles and oxidation of sedimentary organic matter in the eastern equatorial Atlantic. *Science, 198*, p. 605-608.

BERNER R.A. (1974). − Kinetic models for the early diagenesis of nitrogen, sulfur, phosphorus and silicon in anoxic marine sediments. *In : E.D. Goldberg, (ed.), The Sea, Marine Chemistry, Wiley and Sons, 5*, p. 427-450.

BERNER R.A. (1977). − Stoichiometric models for nutrient regeneration in anoxic sediments. *Limnol. Oceanogr., 22*, p. 781-786.

BILLEN G. (1977). − Etude écologique des transformations de l'azote dans les sédiments marins. Ph. D. thesis, Université Libre de Bruxelles Laboratoire d'environnement, 266 p.

BISHOP J.K., J.M. EDMOND, D.R. LETTEN, M.P. BACON, W.B. SILKERS (1977). − The chemistry biology, and vertical flux of particulate matter from the upper 400 m of the equatorial Atlantic Ocean. *Deep-sea Res., 24*, p. 511-548.

BOSTRÖM K., T. KRAEMER, and S. GARTNER (1973). − Provenance and accumulation rates of opaline silica, Al, Ti, Fe, Mn, Cu, Ni, and Co in Pacific pelagic sediments. *Chem. Geol., 11*, p. 123-148.

BOSTRÖM K., L. LYSEN, and C. MOORE (1978). − Biological matter as a source of authigenic matter in pelagic sediments *Chem. Geol., 23*, p. 11-20.

BRULAND K.W., K. BERTINE. M. KOIDE, and E.D. GOLDBERG (1974). − History of metal pollution in Southern California coastal zone *Environ. Science and Techn., 8*, p 425-432.

COBLER R. and J DYMOND (1980). − Sediment trap experiment on the Galapagos Spreading Center. *Equatorial Pacific. Science* (in press).

DEMAISON G.J and G.T. MOORE (1980). − Anoxic environments and oil source bed genesis *Org. Geochem. 2*, p. 9-31.

DOW W.G. (1978). − Petroleum source beds on continental slopes and rises. *Amer. Assoc. Petrol. Geol. Bull., 62*, n. 9, p. 1584-1606.

DYMOND J., J. CORLISS, R. COBLER, C. MEREDITH, C. CHOU, and R. CONARD (1979). − Composition and origin of sediments recovered by deep sea drilling of sediment mounds. *In : R. Hekinian, B.R. Rosendahl et al., (eds.), Initial Reports of Deep Sea Drilling Project, Leg 54*, in press.

DYMOND J., J.B. CORLISS, and G.R. HEATH (1977). − History of metalliferous sedimentation at Deep Sea Drilling Site 319, in the southeastern Pacific. *Geochim. Cosmochim. Acta, 41*, p. 741-753.

FROELICH P.N., G.P. KLINKHAMMER, M.L. BENDER, N.A. LUEDTKE, G.R. HEATH, D. CULLEN, P. DAUPHIN, D. HAMMOND, B. HARTMAN, and V. MAYNARD (1979). − Early oxidation of organic matter in pelagic sediments of the eastern Equatorial Atlantic : suboxic diagenesis. *Geochim. Cosmochim. Acta, 43*, 1075-1090.

GUNSALUS I.C., and R.Y. STANIER (eds.) (1960). − The Bacteria, vol. I, chapt. 7, Academic Press, New York.

HEATH G.R., and J. DYMOND (1977). − Genesis and transformation of metalliferous sediments from the East Pacific Rise, Bauer Deep, and Central Basin, northwest Nazca Plate. *Geol. Soc. Amer. Bull., 88*, p. 723-733.

HEATH G.R., T.C. MOORE, Jr., J.P. DAUPHIN (1977). − Organic carbon in deep-sea sediments. *In : N.R. Andersen and A. Malahoff eds., The Fate of Fossil CO_2 in the Oceans, Plenum Press, New York.

HEDGES J. (1979). − Relationship between humic acid and inorganic matter in marine surface sediments (this volume).

HINGA K.R., J. Mc N. SIEBURTH, G.R. HEATH (1979). − The supply and use of organic material at the deep-sea floor. *J. Mar. Res., 37*, p. 557-579.

HONJO S. (1978). − Sedimentation of materials in the Sargasso Sea at a 5,367 m deep station. *J. Mar. Res., 36*, n. 3, p. 469-492.

KEPKAY P.E., R.C. COOKE and J.A. NOVITSKY (1979). − Microbial autotrophy : A primary source of organic carbon in marine sediments. *Science, 204*, p. 68-69.

KNAUER G.A., J.H. MARTIN and K.W. BRULAND (1979). − Fluxes of particulate carbon, nitrogen, and phosphorus in the upper water column of the northeast Pacific. *Deep-sea Res., 26A*, p. 97-108.

MACKENZIE F.T., and R.M. GARRELS (1966). − Chemical mass balance between rivers and oceans. *Amer. J. Science, 264*, p. 507-525.

McCAVE I.N. (1975). − Vertical flux of particles in the ocean. *Deep-sea Res., 22*, p. 491-502.

MÜLLER P.J. (1975). − Diagenese stickstoffhaltiger organischer Substanzen in oxischen und anoxischen marinen Sedimenten. *« Meteor » Forsch.-Ergebnisse C*, n. 22, p. 1-60.

MÜLLER P.J. (1977). − C/N ratios in Pacific deep-sea sediments : Effect of inorganic ammonium and organic nitrogen compounds sorbed by clays. *Geochim. Cosmochim. Acta, 41*, p. 765-776.

MÜLLER P.J. and A. MANGINI (1979). − Organic carbon decomposition rates in sediments of the Pacific manganese nodule belt dated by [230]Th and [231]Pa. Submitted to *Earth & Planet. Sci. Letters*.

MÜLLER P.J. and E. SUESS (1979). – Productivity, sedimentation rate and sedimentary organic matter in the oceans. I. – Organic carbon preservation. *Deep-sea Res.,* *26,* p. 1347-1362.

MURRAY J.W., V. GRUNDMANIS, and W. SMETHIE (1978). – Interstitial water chemistry in the sediments of Saanich Inlet. *Geochim. Cosmochim. Acta, 42,* p. 1011-1026.

REDFIELD A.C., B.H. KETCHUM and F.A. RICHARDS (1963). – The influence of organisms on the composition of seawater. *In :* M.N. Hill, (ed.), The Sea, v. 2, p. 26-77, Wiley & Sons, New York.

RICHARDS F.A. (1965). – Anoxic basins and fjords. *In :* J.P. Riley and G. Skirrow, (eds.), Chemical Oceanography, Academic Press, p. 611-645.

SHOLKOVITZ E. (1973). – Interstitial water chemistry of the Santa Barbara Basin sediments. *Geochim. Cosmochim. Acta, 37,* p. 2043-73.

SMETACEK V., K. Von BRÖCKEL, B. ZEITZSCHEL, and W. ZENK (1978). – Sedimentation of particulate matter during a phytoplankton spring bloom in relation to the hydro graphical regime. *Mar. Biol., 47,* p. 211-226.

SPENCER D.W., P.G. BREWER, A. FLEER, S. HONJO, S. KRISHNASWAMI, and Y. NOZAKI (1978). – Chemical fluxes from a sediment trap experiment in the deep Sargasso Sea. *J. Mar. Res., 36,* p. 493-523.

STARESINIC N. (1978). – Ph. D. Dissertation WHOI-MIT. Joint Program in Oceanography (abstract).

SUESS E. (1976). – Porenlosungen mariner Sedimente – Ihre chemische Zusammensetzung als Ausdruck fruhdiagenetischer Vorgange. Habilitationsschrift, Universitat Kiel, 193 p.

SUESS E. (1979). – Mineral phases formed in anoxic sediments by microbial decomposition of organic matter. *Geochim. Cosmochim. Acta, 43,* p. 339-352.

SUESS E. (1980a). – Phosphate regeneration from sediments of the Peru continental margin by dissolution of fish debris. Subm. *Geochim. Cosmochim. Acta.*

SUESS E. (1980b). – Productivity, sedimentation rate and sedimentary organic matter in the oceans. VI Vertical carbon Flux. Subm. *Nature* (London).

SUESS E. and H. ERLENKEUSER (1975). – History of metal pollution and carbon input in Baltic Sea sediments. *Meyniana, 27,* p. 63-75.

SUESS E., P.J. MÜLLER, H.S. POWELL, and C.E. REIMERS (1980). – A closer look at nitrification in pelagic sediments. Subm. to *J. Geochem.*

TISSOT B.P. and D.H. WELTE (1978). – Petroleum Formation and Occurrence. A new Approach to Oil and Gas Exploration. Springer-Verlag, 538 p.

DISCUSSION

R. Dawson : Do you not think that the apparent increase in N in your C:N ratios of sediments may in fact be explained by a decrease in organic carbon ?

Handa showed carbohydrate to be preferentially preserved in particulate material in the water column when compared with proteins. In the sediment upper layers however the benthic community may well only be interested in the carbohydrate fraction of the sediments for their energy requirement since they can use the abundant available inorganic nitrogen forms for their nitrogen requirements.

E. Suess : I think that this would not affect the rate of change of the C:N ratio in the sediment, but why should the processes with the particulate matter be different for the sediment ?

R. Dawson : Because the flora and fauna are totally different in the two phases.